# Post-transcriptional regulation of adult central nervous system axonal regeneration by Cpeb1

**Dissertation**

submitted to the

Combined Faculties for the Natural Sciences and for Mathematics of the Ruperto-Carola University of Heidelberg, Germany

for the degree of

Doctor of Natural Sciences

Presented by

Pak Kin Lou

# Post-transcriptional regulation of adult central nervous system axonal regeneration by Cpeb1

**Dissertation**

submitted to the

Combined Faculties for the Natural Sciences and for Mathematics of the Ruperto-Carola University of Heidelberg, Germany

for the degree of

Doctor of Natural Sciences

Presented by

Pak Kin Lou

**Dissertation**

submitted to the

Combined Faculties for the Natural Sciences and for Mathematics of the Ruperto-Carola University of Heidelberg, Germany

for the degree of

Doctor of Natural Sciences

Presented by

M.Phil. Anatomical and Cellular Pathology

Pak Kin Lou

born in Hong Kong

Oral examination: 30th May, 2016

**Post-transcriptional regulation of adult central nervous system axonal regeneration by Cpeb1**

Referees:

Prof. Dr. Ana Martin-Villalba

Prof. Dr. Christine Clayton

# Abstract

Axons of the adult mammalian central nervous system (CNS) are unable to regenerate following axonal injury. Thus, spinal cord injury (SCI) leads to devastating and permanent functional impairments, the extent of which depends on the position of the lesion. At present, our understanding of the response to axonal injury and what underlies the failure of CNS axons to regenerate is far from complete. Therefore, despite various strategies proposed and tried, a robust method to improve axon regeneration after SCI is yet to be found. Due to growing evidence highlighting the role of post-transcriptional control towards protein expression and the importance of localised protein synthesis in axon physiology, we decided to investigate the post-transcriptional regulation mechanisms that could govern the regeneration of CNS neurons.

At a very early time window following SCI, axon regrowth still occurs, but is however limited in duration and extent. This however offers a rare opportunity of learning how nature initiates a regenerative response in the CNS. In order to study the difference between the total level of RNA and the subset that is actually translated, we profiled and compared total and polysome-bound RNAs from spinal cords early after injury and naïve ones, and revealed substantial uncoupling between mRNA abundance and ribosome loading. mRNAs of genes related to nervous system development were highly reduced following injury, while still being stably loaded onto ribosomes. By analysing motifs recognised by RNA-binding proteins, it was discovered that mRNAs harbouring the cytoplasmic polyadenylation element (CPE) exhibit increased transcript abundance upon SCI relative to those that do not, and were highly enriched in nervous system development genes in both mouse and *Drosophila* genomes. By manipulating the expression of Cpeb1, the binding protein of CPE, we found that Cpeb1 is a positive regulator of regeneration in both mouse and *Drosophila* CNS neurons. In an attempt to identify the targets of Cpeb1 mediated injury response, we analysed the transcriptome of naïve and injured processes from wild-type and Cpeb1 knockout cortical neurons with RNAseq. It was found that Cpeb1 knockout processes have a much attenuated transcriptional activation-response towards injury. In particular, the Jun and Fos family of transcription factors, which are highly up-regulated upon injury in wild-type processes, failed to do so in their Cpeb1 knockout counterparts. In addition, Cpeb1 knockout

was found to have an effect on alternative polyadenylation. However, the precise molecular mechanisms underlying observed changes remain a subject of future studies.

In conclusion, this study demonstrates widespread uncoupling between mRNA abundance and ribosome-loading in the injury response of CNS neurons, and identifies Cpeb1 as a conserved positive regulator of regeneration, as well as a mediator of this uncoupling effect.

# Zusammenfassung

Axone im zentralen Nervensystem (ZNS) sind nach einer Verletzung nicht in der Lage zu regenerieren. Daher führt eine Rückenmarksverletzung zu einer schwerwiegenden und dauerhaften Beeinträchtigung, dessen Umfang von der Position der Schädigung abhängig ist. Unser Verständnis der Reaktion nach axonaler Verletzung und der assoziierten fehlenden Regeneration ist gegenwärtig unzureichend. Daher gibt es trotz zahlreicher Versuche immer noch keine verlässliche Methode um die axonale Regeneration nach Rückenmarksverletzung zu fördern. Unlängst wurde die hohe Bedeutung von posttranskriptioneller Regulation für Proteinexpression und die Rolle von lokalisierter Proteinsynthese für die Physiologie von Axonen hervorgehoben. Daher haben wir entschieden posttranskriptionelle Mechanismen, welche zur Regeneration von ZNS-Axonen beitragen könnten, zu studieren.

In einem kurzen Zeitfenster nach Verletzung wachsen Axone nach. Hier bietet sich die Möglichkeit diese in Zeit und Umfang begrenzte Regeneration zu studieren. Um die Level an gesamter messenger RNA (mRNA) und die Teilmenge welche tatsächlich in Proteine umgesetzt wird zu ermitteln, haben wir totale mRNA und polysom-gebundene mRNA in gesundem Rückenmark und kurze Zeit nach Verletzung analysiert. Dieser Vergleich ergab eine wesentliche Entkopplung zwischen gesamter mRNA-Menge und ribosomaler Beladung. mRNA von Genen welche mit der Entwicklung des ZNS assoziiert sind wurden nach Verletzung deutlich herunterreguliert, jedoch weiterhin stabil auf Ribosome geladen. Analyse von Motiven welche von RNA-bindenden Proteinen erkannt werden hat gezeigt dass mRNAs welche ein cytoplasmic polyadenylation element (CPE) aufweisen eine höhere Menge an Transkripten nach Verletzung aufweisen als mRNAs ohne CPE. Diese mRNAs sind zudem mit Genen angereichert welche sowohl in der Maus als auch in Drosophila mit der Entwicklung des ZNS assoziiert sind. Wir fanden durch Manipulation der Expression von Cpeb1, dem Bindeprotein von CPE, dass Cpeb1 ein positiver Regulator der Regeneration von Maus- und Drosophila-Neuronen des ZNS ist. Um die Zielgene von Cpeb1-mediierter Verletzungsreaktion zu identifizieren haben wir das Transkriptom von verletzten und unverletzten Prozessen von kortikalen Neuronen sowohl von Wildtyp-Mäusen als auch Cpeb1-Knockout-Mäusen per RNAseq untersucht. Die Ergebnisse haben gezeigt dass Prozesse mit Cpeb1-Knockout nach Verletzung eine abgemilderte Reaktion der

Transkriptionsaktivierung aufweisen. Besonders Gene der Jun- und Fos-Familie von Transkriptionsfaktoren, welche in Wildtyp-Prozessen nach Verletzung hochreguliert werden, zeigen eine fehlende Reaktion nach Cpeb1-Knockout. Zusätzlich wurde gezeigt dass Cpeb1-Knockout einen Effekt auf alternative Polyadenylierung hat. Die molekularen Mechanismen dahinter sind Gegenstand zukünftiger Studien.

Zusammengefasst zeigt diese Studie eine weit verbreitete Entkopplung zwischen gesamter mRNA-Menge und Ribosom-Beladung in der Verletzungsreaktion von ZNS-Neuronen und identifiziert Cpeb1 als einen konservierten positiven Regulator der Regeneration und Vermittler des Entkopplungseffekts.

# Acknowledgements

I could still remember the sense of uncertainty, curiosity and amazement five years ago, as I left my home in Hong Kong and came to this. I have to say it was truly a great experience, one that would undoubtedly have a great impact on my career as well as my life.

First I would like to express my deep gratitude to my supervisor Ana Martin-Villalba, for giving me this opportunity for coming here and learning a great deal from her lab. This has not been an easy project, and I am very grateful for you guidance and patience, and your enthusiasm which gave me the motivation to go on when times are tough.

I would also like to thank Christine Clayton and Georg Stöcklin, for your time spent being part of my thesis advisory committee and your valuable input, as well as my examiner Carmen Ruiz de Almodóvar.

I am immensely grateful to the people at the lab. Enric, thank you for your great suggestions and your infectious excitement in science and discovery. Discussions with you are always stimulating and broadens my mind, be it about our projects, science in general or every other thing. Also for being my partner in getting serious to learn new things like German or R, though I can't say we are entirely successful in either… Georgios, for being the fun bomb, doing all the things that tie the group together, and for caring when I am not in my best. I do appreciate that a lot. Andromachi, thank you for all the fun, the great food that feeds me, and more importantly for listening me out. It has become a comforting sight to walk into the office in ungodly hours to see the three of you being there. You guys are great company and make me feel at home here, for that I am very grateful. Avni, thank you for your questioning which has always been a good stimulation, reminding me not to take things for granted, and for keeping me motivated with your sarcastic comments. That was truly helpful. Steffi, I am grateful for all your help in the project, you are very dedicated and diligent. I still remember you came to pick me up the first day I arrived here. I also want to thank Damian, for your great passion to science which constantly reminds me of why we are doing this, and the talks during our runs when we discuss our ups and downs and future goals. Si, for being a great driver of activities that make us such a close group. Liang, for your great suggestions, for being the role model of a hardworking student, and for pushing me to improve my badminton

skills, though only with limited success. Robert, for all the smart comments and for motivating me to achieve the impossible feat of going running in the early morning. That never happened again after you left. I am truly grateful to you guys, who through these years have way exceeded being colleagues and became my best friends and family outside home. All the fun times we have together, the volleyball, the countless barbeques, the trips to Portugal, Crete, Barcelona. It is also incredible the way we blend work and fun together, talking about experiments after many drinks in a loud bar. It would be impossible to find such a great atmosphere anywhere else.

I also wish to thank Sascha, Maxim, Katrin, Marcin, Desiree, Sheng, Gülce, Klara, David, Carina, Melanie, Alvaro, Suse, Moritz, Julian, Jan and Alex, for your help over the years and for the great environment. I would also like to thank my friends outside the lab, Lihao, Yeung Yeung, Karin, Chiara, Marco, Benjamin, Ana, Calvin, and many others. You are all great friends and have given me a great Heidelberg experience, and a life outside the lab.

To my parents, I would like to express my deepest gratitude, for you have brought me up and educated me to be the person I am. You have showed me the world, and gave me the privilege to be able to pursue my dreams. None of this would have been possible without your guidance and patience through all these years.

Lastly, I would like to thank Suki, for coming into my life in the most extraordinary manner, for always being there, for being forgiving, and for believing in me. I cannot describe how comforting it is, knowing I can talk to you anytime about anything, and that has lifted me up from some of the lowest times. You gave me the confidence and drive to go on.

# Table of contents

# List of figures

# List of tables

# Abbreviations

| Abbreviation | Description |
|---|---|
| 4E-BP | eIF4E-binding protein |
| AAV | Adeno-associated virus |
| APA | Alternative polyadenylation |
| ARE | AU-rich element |
| ARE-BP | ARE-binding protein |
| AXIS | axis isolation devices |
| CNS | Central nervous system |
| CPE | Cytoplasmic polyadenylation element |
| CRE | cAMP responsive element |
| CST | Cortical spinal tract |
| DaPars | Dynamic analyses of Alternative PolyAdenylation from RNA-Seq |
| DIV | Days *in vitro* |
| DRG | Dorsal root ganglion |
| eIF | eukaryotic initiation factor |
| EJC | Exon junction complex |
| FDR | False discovery rate |
| FPKM | fragments per kilobase of transcript per million fragments mapped |
| GH | Growth hormone |
| GO | Gene ontology |
| KEGG | Kyoto Encyclopedia of Genes and Genomes |
| MBE | Musashi binding element |
| MOI | Moiety of infection |
| mTOR | Mammalian target of rapamycin |
| MWCO | Molecular weight cut-off |
| NLS | Nuclear localization signal |
| NP-40 | Nonidet P-40 |
| PAT | Poly(A) tail |
| PBE | Pumilio binding element |
| PCA | Principal component analysis |
| PFA | Paraformaldehyde |
| PNS | Peripheral nervous system |
| qPCR | Quantitative real-time PCR |
| RAG | Regeneration-associated gene |
| RBP | RNA-binding protein |
| RGC | Retinal ganglion cell |
| RI | Refractive index |
| RISC | RNA-induced silencing complex |

| | |
|---|---|
| RNP | Ribonucleoprotein |
| SCI | Spinal cord injury |
| SG | Stress granule |
| sLNv | Small lateral neuron ventral |
| TPM | Transcript per million |
| TSAA | Translation state array analysis |
| TUNEL | terminal dUTP nick end labelling |
| UTR | Untranslated region |

# 1. Introduction

## 1.1 Structure of a neuron

The neuron is the cell type within the nervous system that relays nerve signals. There are a number of different types of neurons, which differ in their morphology and function, but they all consist of a cell soma, axons, and dendrites. Axons and dendrites are collectively called processes.

The cell soma houses the nucleus and contains the majority of the organelles of the cell such as mitochondria, endoplasmic reticulum and Golgi apparatus. Most proteins of the neuron are synthesised within the cell soma. Most neurons contain one axon, which is a long process that can extend for great distances and connect to targets far away from the cell soma. Axons conduct nerve signals in the form of action potentials from the cell body towards the axon terminus. They are wrapped in a myelin shealth, which is an extended plasma membrane originating from oligodendrocytes or Schwann cells that enhances the speed of propagation of the action potential (Morell and Quarles, 1999). Axons connect to their targets via synapses. The axon terminal of the pre-synaptic cell releases neurotransmitters, which crosses the synaptic cleft and activate the post-synaptic cell (Lodish et al., 2000). Dendrites, in contrast to axons, transmit nerve signals towards the cell soma and are typically shorter. Most neurons contain multiple dendrites which allow them to receive signals from more than one neuron. Microtubules within axons and dendrites act as tracks for transport, for exchanging materials such as proteins, RNAs and organelles with the cell soma. This is termed anterograde and retrograde transport, depending on the direction of movement of the cargo molecules (Bramham and Wells, 2007; Setou et al., 2004).

The nervous system is divided into two major parts, the central nervous system (CNS) and the peripheral nervous system (PNS). The CNS consists of the brain, spinal cord, retina and optic nerves. One of the distinguishing factors between the two nervous system is that processes of the CNS has a very limited ability to regenerate following injury, in contrast to PNS (Huebner and Strittmatter, 2009).

## 1.2 Spinal Cord Injury

The spinal cord is a part of the CNS. It is responsible for relaying nerve signals between the brain and various organs of the body, as a conduit for sensory signals towards the brain and for motor signals originating from the brain. It also houses the neural circuits for certain reflexes. In a cross section, the spinal cord consists of white matter in the periphery, which mostly contains myelinated axons, and grey matter in the centre, which consists mainly of cell somas. Spinal nerves connect to the spinal cord along its length and relay signal between the spinal cord and the various organs connected.

Spinal cord injury (SCI) results in disruption of communication between the brain and the organs whose neural circuit enters the spinal cord below the lesion site. As a result, urinary, musculoskeletal, gastrointestinal and respiratory functions could be affected, depending on the site and extent of the injury. The spinal cord, being a part of the CNS, is largely unable to regenerate, often resulting in permanent disabilities for SCI patients (Silva et al., 2014). As of 2014 in the USA, acute spinal cord injury is affecting 276,000 persons, with approximately 12,500 new cases per year. The most common neurological outcome of the injury is incomplete tetraplegia (45%) (National Spinal Cord Injury Statistical Centre, 2014). Less than 1% of spinal cord injury patients experience complete neurological recovery, with most patients having to rely on long-term assistance in their daily lives for matters such as mobility and personal care, causing dramatic impact on patients' life and career. The long-term disability also leads to psychological problems such as depression and anxiety, and generates very high medical costs.

Damage to the spinal cord can be categorised into two types. The first is the acute mechanical injury which causes shearing of axons, haemorrhage and ischemia, and is restricted locally to the site of injury. The other type is secondary injury that follows days to weeks after the initial injury, in which a milieu of processes such as inflammation, disruption of the blood-spinal cord barrier, toxicity from free-radical and electrolyte disturbances cause further cell death among neurons and glia cells (Dumont et al.; Zhang et al., 2012). As Cajal y Ramon has observed almost a century ago, severed axons in the spinal cord do attempt to regrow, however the process is soon aborted (Cajal, 1928; Cajal et al., 1991; Kerschensteiner et al., 2005). Both cell intrinsic and extrinsic factors contribute to this failure to regrow. In spite of

decades of research, at present there still lacks a method to robustly induce axon regrowth following SCI.

## 1.3 Axonal regeneration in the CNS

Axotomy induces responses in different parts of the affected neuron. The distal part of the axon separated from the rest of the cell by axotomy undergoes gradual degeneration, called Wallerian degeneration, while the proximal part of the axon reseals the ruptured membrane. To regrow, a growth cone has to be developed from the damaged axon end. For axons of the adult mammalian CNS, which have a very limited regenerative capacity, the cut axon end often fails to transform into a growth cone, but develops into a retraction bulb instead (Hill et al., 2001; Li and Raisman, 1995). In SCI, damaged corticospinal tract (CST) axons make an initial attempt to regrow, but this regenerative phase is transient and abortive. During this phase, the axons form retraction bulbs and die back away from the lesion point (Bernstein and Stelzner, 1983; Cajal, 1928; Kerschensteiner et al., 2005; Li et al., 1997).

Axotomy also induces considerable changes to the cell soma. The acute response after injury includes displacement of the nucleus to cell periphery, swelling of cell soma, and loss or retraction of synaptic terminals, processes similar across CNS and PNS neurons (Liu et al., 2011). In the long-term, however, their responses show substantial differences. Cell somas of PNS neurons show signs of increased protein synthesis and metabolism. On the other hand, CNS neurons are atrophic and have reduced cell volume (Lieberman, 1971). Both neuron intrinsic and extrinsic factors have been discovered to influence the capability of axonal regeneration.

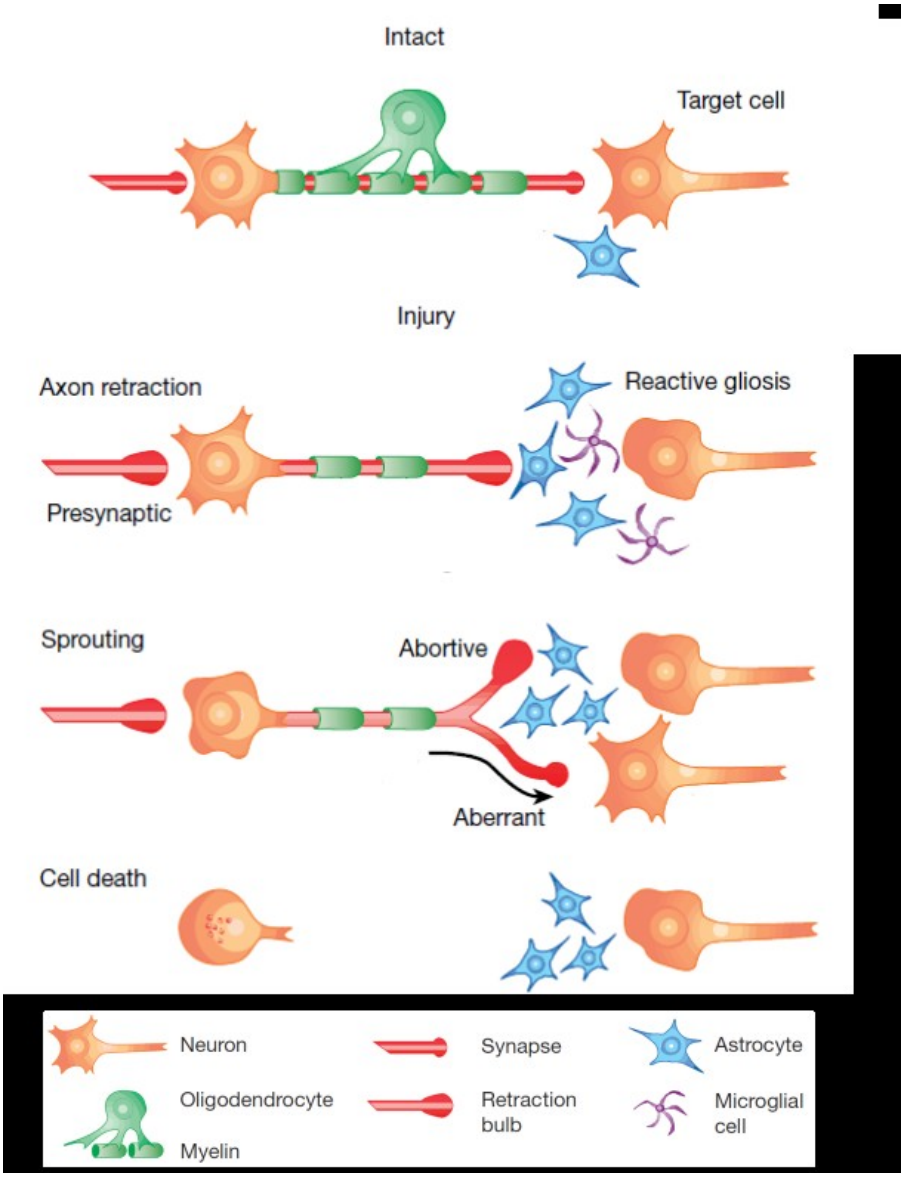


Figure 1: Response towards axonal injury in the CNS. Following injury, synaptic connection is lost, the axon end forms a retraction bulb and dies back. Astrocytes and microglia infiltrates the lesion zone as part of the inflammatory response. Axon sprouting occurs in certain cases, but is abortive, due to lack of a long-lasting intrinsic regenerative programme, an external environment hostile to axon growth from the inflammation, or a physical barrier from the glial scar. Sometimes aberrant sprouting occurs when the axon connects with an inappropriate target. In other cases, injured neurons could undergo cell death. Adapted from (Horner and Gage, 2000)

## 1.4 Factors influencing CNS axon regeneration

### 1.4.1 Inhibitory environment

Many studies have demonstrated that myelin in the CNS, but not in the PNS, contains inhibitory molecules to axonal regrowth. Several such inhibitors have been identified, including Nogo-A, myelin-associated glycoprotein (MAG), and the glycosylphosphatidylinositol-linkied oligodendrocyte myelin glycoprotein (OMgp) (Mingorance et al., 2004). These inhibitors share little structural similarities between each other, but they have all been found to have high binding affinity to Nogo receptor (NgR). NgR is part of a receptor complex that contains $p75^{NTR}$ and Lingo-1, which triggers a signalling cascade involving the activation of RhoA (Mi et al., 2004; Wang et al., 2002). Activation of RhoA changes the dynamics of actin and microtubules, leading to growth cone collapse and inhibition of neurite growth (Wu et al., 2005).

Molecules that inhibit various steps within this signalling cascade, for example C3 transferase and Cethrin, which inhibit Rho GTPase; and ATI-355, a humanised anti-Nogo antibody, have yielded encouraging results in enhancing axon regrowth and functional recovery, and some of these molecules have entered clinical trials (Muramatsu and Yamashita, 2014). However, inconsistent results have arisen from studies using a triple knockout of the three myelin inhibitors Nogo-A, MAG and OMgp, in which no enhanced regeneration was observed. This indicates that the source molecules of myelin inhibition remains unclear (Muramatsu and Yamashita, 2014).

In another approach, in which a permissive growth environment is provided for the severed CNS axons, for example by inserting grafts from a segment of peripheral nerve, have shown certain promises, allowing the CNS axons to extend for long distances and to guide the direction of regrowth (David and Aguayo, 1981). This demonstrates the importance of a permissive environment, with the effect possibly contributed by cytokines, inhibitory molecules, growth cues etc. However, the regenerative capacity conferred by a permissive graft only reaches so far as the graft itself, with the regeneration halting when the axon reaches the CNS environment (Côté et al., 2011). This limits the potential therapeutic use of the grafts, but illustrates the role played by extracellular environments.

### 1.4.2 Cell intrinsic factors

On the other hand, axon regeneration capability also depends on neuron intrinsic factors. One of the strongest evidence that exemplifies this comes from the effect of a conditioning lesion on dorsal root ganglion (DRG) sensory neurons. DRG neurons have a cell soma that resides in the PNS, but have a bifurcating axon that has two branches, one projecting into the PNS and the other into the CNS. As expected, the peripheral branch is able to regenerate, whereas the central branch cannot. However, if the peripheral branch is subjected to injury prior to the central branch, the central branch gains the ability to regenerate. This is not observed if the conditioning lesion is done on the central branch (Neumann and Woolf, 1999; Richardson and Verge, 1986). This suggests that injury to the PNS axon activates a regenerative programme in the neuron that is able to drive regeneration in the CNS axon.

#### 1.4.2.1 Regenerative signalling pathways and gene expression programmes

For some types of CNS neurons, it was demonstrated that there is a significant decline in ability for axon growth as they mature. For example, axons of embryonic retinal ganglion cells (RGCs), which is part of the CNS, extend about ten times faster than mature ones (Goldberg et al., 2002). Several molecules have been implicated to be the effectors behind this phenomenon, for example Bcl-2 and Kruppel-like factors (KLFs). Growth failure in optic nerves coincides with a developmentally correlated loss of Bcl-2 expression (Cho et al., 2005). KLFs are a set of zinc-finger transcription factors. KLF6 and KLF7, which are promoters of axon regrowth, are down-regulated in adult RGCs (Veldman et al., 2007). Conversely, KLF4, which is a strong inhibitor of axonal growth, is up-regulated in adult RGCs (Moore et al., 2009). These observations give rise to the hypothesis that as CNS neurons mature, their regenerative capability is shut off, and perhaps it could be reactivated. A few negative regulators of signalling pathways for growth have been discovered, the most prominent of which are Pten and Socs3.

Deletion of Pten was found to have a positive effect in regeneration, by preventing apoptosis and promoting axon extension in RGCs and CST neurons, as well as increasing compensatory sprouting from spared axons in the CST (Liu et al., 2010; Park et al., 2008). Pten is an antagonist of PI3K/Akt signalling, and thus a negative regulator of mammalian target of rapamycin (mTOR). Rapamycin treatment, which interrupts mTOR signalling, abolishes the regenerative effects of Pten deletion, indicating that Pten inhibits regeneration by suppressing mTOR (Park et al., 2008). mTOR is a regulator of cap-dependent translation, by controlling the activity of ribosomal S6 kinase and eukaryotic initiation factor 4E binding proteins (4E-BPs) (Guertin and Sabatini, 2007). The role of mTOR in regeneration is further implicated from the fact that mTOR levels decrease with development in RGCs and cortical neurons (Liu et al., 2010; Park et al., 2008). However, deletion of Tsc1, another inhibitor of mTOR, confers of a regenerative effect as deletion of Pten, indicating that the pro-regenerative effects of Pten deletion do not only come from mTOR (Park et al., 2008).

Socs3 is a negative feedback regulator of Jak/Stat signalling, being induced by this pathway while simultaneously suppressing it (Baker et al., 2009; Wunderlich et al., 2013). Expression of Socs3 is induced following injury in zebrafish optic nerves (Elsaeidi et al., 2014), and its deletion induces significant regeneration in mouse RGCs (Smith et al., 2009). Confirming the role of Jak/Stat signalling in promoting regeneration, activation of Stat3 is increased in regenerating axons in Socs3 deleted RGCs and optic nerves (Sun et al., 2011). In addition, expression of Stat3 was found to strongly increase sprouting from lesioned CST fibres, as well as collateral sprouting from unlesioned fibres, with improved functional recovery (Bareyre et al., 2011; Lang et al., 2013). Perhaps attributing to the negative feedback loop relationship with Socs3, expression of Stat3 only improves initiation of axonal regrowth (Bareyre et al., 2011). Co-deletion of both Pten and Socs3 produces a synergistic effect in promoting robust and sustained axon regeneration in RGCs (Sun et al., 2011). These findings point out the prominent role of upstream master negative regulators in restricting regeneration of adult CNS axons, and demonstrates the feasibility to coax regeneration by targeting these inhibitors.

Epigenetic regulation has also been implicated in controlling regeneration. Upon axon injury in DRG neurons, a calcium wave originating from the injury site propagates backwards towards the cell soma, leading to nuclear export of the histone deacetylase 5 (Hdac5) via PKCμ activation. This results in increased histone H3 acetylation and up-regulation of

several regeneration associated genes such as c-Jun, c-Fos and Gadd45a, and subsequent enhanced regeneration (Cho et al., 2013). Interestingly, this was not observed in RGCs, suggesting this is yet another process that differentiates the regeneration capability of PNS and CNS neurons.

#### 1.4.2.2 Cytoskeleton organisation

Regrowth of axons requires formation of a growth cone at the axon tip, and this is dependent on the dynamics of the microtubules and actin filaments. Upon rupture of the cell membrane from an injury, intra-axonal calcium is increased by diffusion. This leads to depolymerisation of microtubule and actin. Eventually the ruptured membrane is resealed by membrane collapse, and calcium removal mechanisms lower the intra-axonal calcium concentration, allowing repolymerisation of microtubule and actin. The actin filaments assemble at the leading edge of the lamellipodia to provide the mechanical force for the extension of the growth cone (Bradke et al., 2012; Hur et al., 2012). Stabilisation of microtubules, for example with taxol, a drug that stabilises the microtubule assembly, leads to formation of a growth cone at the site of axon lesion. On the other hand, disruption of microtubules with the drug nocodazole leads to formation of a retraction bulb (Ertürk et al., 2007). Part of this process has been shown to be regulated via Hdac5. Upon axon injury-induced nuclear export, Hdac5 is transported to axon tips, where it deacetylates tubulin and promotes growth cone dynamics and axon regeneration (Cho and Cavalli, 2012).

## 1.5 Post-transcriptional regulation of gene expression

Traditionally, and until today, RNA abundance is commonly used to infer the protein levels of a gene. However, numerous post-transcriptional mechanisms exist that control the fate of an RNA, and it has recently been suggested that uncoupling of transcription and translation is a widespread phenomenon (Schwanhäusser et al., 2011).

The numerous post-transcriptional control steps for RNA fate require mechanisms to direct RNAs to the specific processes needed. This role is often fulfilled by sequence specific motifs present on RNAs, in combination with their respective binding proteins. Many of such motifs are present in the untranslated region (UTR) of mRNAs, particularly the 3'UTR, which is also generally longer than the 5' UTR. For example, the average 3'UTR in the human transcriptome is more than 500nt long, in contrast to the 5'UTR, which is 150nt long (Mazumder et al., 2003; Pesole, 2002). So far a number of such motifs have been discovered situated in the 5' and 3' UTRs, exerting a variety of different functions, including subcellular localisation (Jansen, 2001), stability (Beelman and Parker, 1995) and translation efficiency (Sonenberg, 1994). The different levels of post-transcriptional regulation during the lifespan of an mRNA are introduced in the following sections.

### 1.5.1 Subcellular localisation of RNAs

Asymmetric subcellular RNA distribution is used by many cell systems to achieve polarity, and this is no exception in neurons. Different composition of the RNA pool in axons determines the availability for localised translation, and this is subject to changes in different contexts. For example, the repertoire of axonal mRNAs changes dynamically during development, indicating the different requirements for localised translation as neurons mature. Embryonic axons were found to have an mRNA pool enriched in cytoskeleton and axonal growth related genes, whereas adult axons are enriched in genes with a role in inflammation (Gumy et al., 2011). The mRNA for a number of transmembrane receptors, such as EphB4, were found in both growth cones and cell somas of mature RGC neurons, but only found in cell somas in young neurons, demonstrating developmentally controlled trafficking of RNA (Zivraj et al., 2010).

In an injury context, the repertoire of axonal mRNAs was also found to be different. mRNAs related to intracellular transport, mitochondrial function and cytoskeleton show a decrease in regenerating growth cones from injured cortical neurons, whereas mRNAs related to axonal targeting, synaptic functions show an increase (Taylor et al., 2009). Even within axons, the repertoire of mRNAs was found to have differences between axon shafts and growth cones. Although most of the growth cone transcripts are also present in axon shafts, a subset was

significantly enriched in growth cones, with functions related to cytoskeleton and protein synthesis (Zivraj et al., 2010).

### 1.5.2 Intracellular RNA trafficking

The presence of specialised mRNA pools in the axon shows that there are mechanisms which select and shuttle specific mRNAs to the axons (Gumy et al., 2013). In addition, the fact that only a few thousand transcripts from the entire mouse genome were found in axons and that the RNA pool differs between growth cones and axon shafts points out that the localisation of these mRNAs cannot be mere diffusion (Gumy et al., 2011; Zivraj et al., 2010).

mRNAs are transported via association with trans-acting factors in messenger ribonucleoprotein (mRNP) complexes. RNA-binding proteins (RBPs) in these complexes serve as adapters between motor proteins of microtubules and the mRNA to be transported. This role has been confirmed for Fmrp, a known component of RNA granules, which was found to bind the motor protein Kif3C. Neurons expressing a dominant-negative mutant of Kif3c has impaired transport of Fmrp containing RNA granules (Davidovic et al., 2007). Live imaging of mRNPs shows that movements of mRNPs along microtubules are bidirectional (Amrute-Nayak and Bullock, 2012; Zhang et al., 2001). Studies in Drosophila embryos revealed that a localisation signal on the mRNAs regulate the number of transport proteins recruited to the mRNP, through which a bias in the direction of movement is created in order for the mRNA to reach its destination. Mutant mRNAs lacking the localisation signal still associate with dynein and are transported, but exhibit a much attenuated bias of movement when compared to wild-type ones (Amrute-Nayak and Bullock, 2012; Bullock et al., 2006). Studies in mouse neurons and Drosophila embryos have also shown that mRNPs transport mRNAs in low copy numbers, often even in single copies (Amrute-Nayak and Bullock, 2012; Mikl et al., 2011). Carrying a single mRNA might not be energetically efficient, but does allow a high spatial and temporal control of gene expression.

Recognition of mRNAs to be packaged into mRNPs for transport is dependent on cis-elements on the mRNA. To date the best described element is a 54 nucleotide long sequence in its 3'UTR called the zip-code. The zip-code targets β-actin mRNA to the axons (Willis et

al., 2011). The zipcode-binding protein 1 (Zbp1) binds to the zip-code and transports the mRNA to the axon while suppressing translation during the transport process, by preventing the joining of 60S subunit to the translation pre-initiation complex (Hüttelmaier et al., 2005). Availability of Zbp1 was found to be a limiting factor in mRNA axonal localisation and a critical part of axonal regeneration, when introduction of β-actin 3'UTR competes with endogenous actin and Gap43 mRNA in binding to Zbp1, resulting in a reduction of axonal regrowth (Donnelly et al., 2011). The competition between β-actin and Gap-43 mRNAs for Zbp1 and shuttling towards axons was found to drive different modes of axonal growth. Increasing axonal synthesis of β-actin at the expense of Gap-43 leads to short and highly branched axons. In contrast, increasing axonal synthesis of Gap-43 at the expense of β-actin results in long axons with few branches (Donnelly et al., 2013).

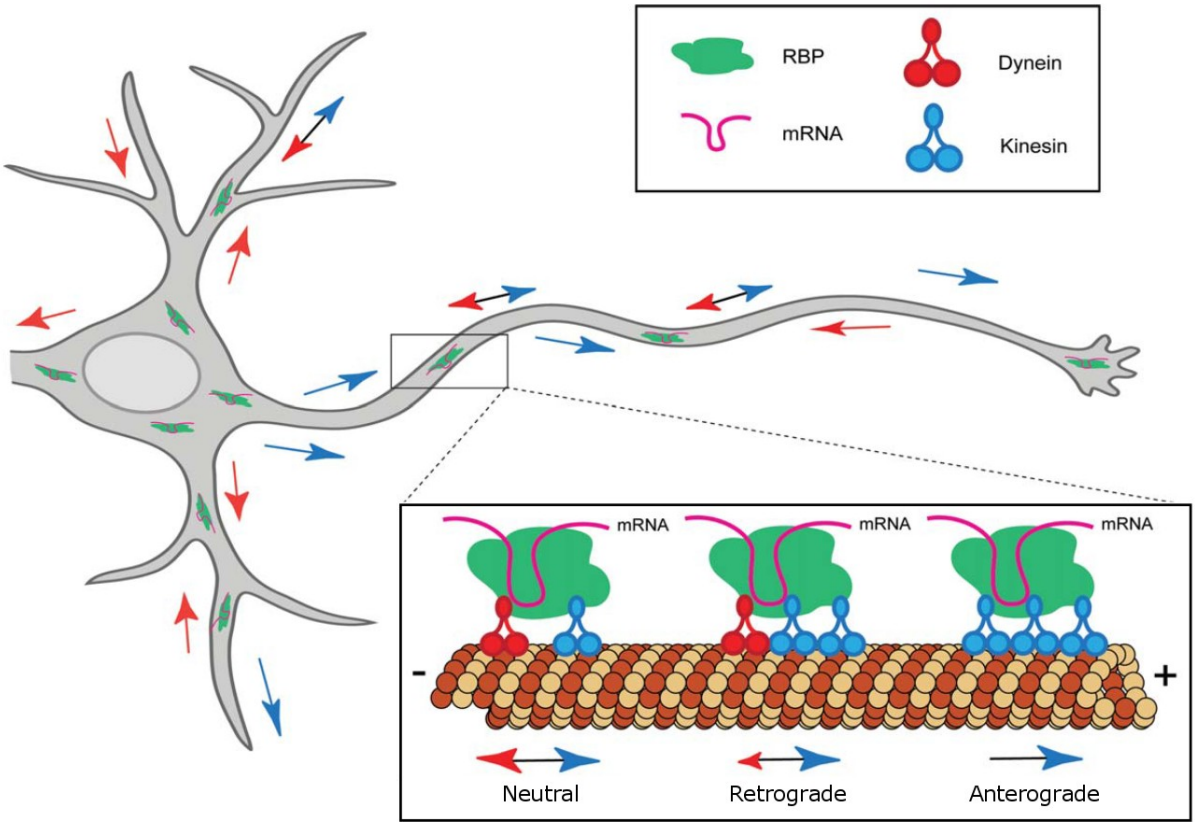


Figure 2: Schematic model showing mRNA localisation determined by the relative ratios of motor proteins with opposing actions. A higher ratio for kinesin leads to anterograde transport into axon tips, whereas a higher ratio for dynein leads to retrograde transport to the cell soma. Adapted from (Gumy et al., 2013).

### 1.5.3 RNA degradation: Regulation of mRNA turnover and quality control

An important part of RNA biology is its degradation, which serves the purpose of quality control, as well as complimenting other mechanisms to control gene expression by determining the lifespan of the mRNA available for translation. Control of mRNA quality occurs mainly via nonsense-mediated decay (NMD). After pre-mRNAs underwent splicing, the splicing mechanism deposits a protein complex called the exon junction complex (EJC) at the spliced site, which serves as a memory of the splicing event. After the mRNA is exported to the cytoplasm, distribution of EJCs would serve as an indication of mRNA quality and the basis for triggering NMD. One prevailing model is that EJCs are ejected by the ribosome as translation occurs. When a premature stop codon is created by faulty transcription or splicing, there could be EJCs still attached to the mRNA after the first round of translation, as the ribosome is released before it could reach the last EJCs. In this case NMD would be triggered and the mRNA would be targeted for degradation (Chang et al., 2007; Lejeune et al., 2003).

Besides quality control, RNAs have different lifespans, with the half lives of RNAs differing in several orders of magnitude. This allows fine temporal and spatial control of gene expression (Peltz et al., 1991). Together with transcription, the two processes determine the actual amount of mRNA available to ribosomes for translation. In systems where rapid changes of protein expression are needed, this is especially important as changes in transcription will take time to take effect. For example, hypoxia induced stress increases the stability of lactate dehydrogenase A (Ldh-A) mRNA, allowing more efficient energy production in anaerobic conditions from glycolysis (Short, 2000).

Over the last decades, many cis- and trans- factors have been discovered that influence the stability of given mRNA species. Of the most prominent ones are the AU-rich elements (AREs), a family of motifs with similar sequences located in the 3'UTR of mRNAs, regulating many mRNAs with fast turnover such as c-Fos, c-Myc and GM-CSF. So far the definition of an ARE is not concrete, but basically they all contain the pentamer AUUUA (Barreau et al., 2005). Initially thought to instil instability in the host RNA, AREs are now also known to promote stability. The heterogeneity of its action could be attributed to the diversity of sequences that constitute AREs and proteins that can bind to them. So far no binding specificity could be inferred between ARE binding proteins (ARE-BPs) and AREs,

with many ARE-BPs found to bind multiple AREs and some AREs found to interact with multiple ARE-BPs. The variety of possible interactions hints at a level of functional redundancy or antagonism for ARE-BPs in regulating RNA stability (Raineri et al., 2004), and it has been hypothesised that the fate of an ARE-containing RNA is dependent on the relative levels of stabilising and destabilising ARE-BPs recruited to it (Barreau et al., 2005). Intriguingly, AREs were also shown to have a role in regulating translation. AREs on the 3'UTR of IFN-β, c-Fos and GM-CSF mRNAs were found to have an inhibiting effect in translation that is independent from RNA degradation (Grafi et al., 1993; Grosset et al., 2004; Kruys et al., 1989).

The first identified ARE-BP to have an effect on RNA stability is Auf1, which directs RNA decay via a protein complex consisting of dimers of itself together with other factors such as eIF4G, Pabp and heat shock proteins hsc70-hsp70 (Laroia et al., 1999), although subsequent studies revealed that Auf1 could also increase RNA stability (Xu et al., 2001). Other well-studied ARE-BPs include the Hu family, which includes HuR/HuA, Hel-N1, HuC and HuD. Binding of HuR, Hel-N1 and HuD increases stability of their target mRNAs (Ford et al., 1999; Jain et al., 1997; Mobarak et al., 2000). As an example, hypoxia induced stability of VEGF mRNA occurs via HuR binding (Levy et al., 1998).

The main mechanisms in which mRNA is degraded in mammalian cells starts with 5' decapping or 3' deadenylation. Transcription of mRNAs from RNA polymerase II is followed by capping of the 5'end with modified nucleotides and prevents it from being accessed by 5' exonucleases. Decapping of the 5'end by the decapping enzymes Dcp1/2 precedes 5'-3' exonucleolytic decay by the 5'-3' exoribonuclease Xrn1. On the other hand, transcription is followed by polyadenylation of the 3' end of most mammalian mRNAs. The 3' ends are cleaved at specific polyadenylation sites, where then a long poly(A) tail is added by the poly(A) polymerase Pap1, and the tail is bound by poly(A)-binding protein (Pabp) (Görlach et al., 1994). The poly(A) tail confers a stabilising effect to the mRNA, likely via blocking the assembly of the exosome complex on the 3' end, which contains exonucleases (Ford et al., 1997; Wilson and Treisman, 1988). Evidence suggests that both degradation from both ends of an mRNA could occur simultaneously, with 3' deadenylation followed by 5' decapping (Couttet et al., 1997).

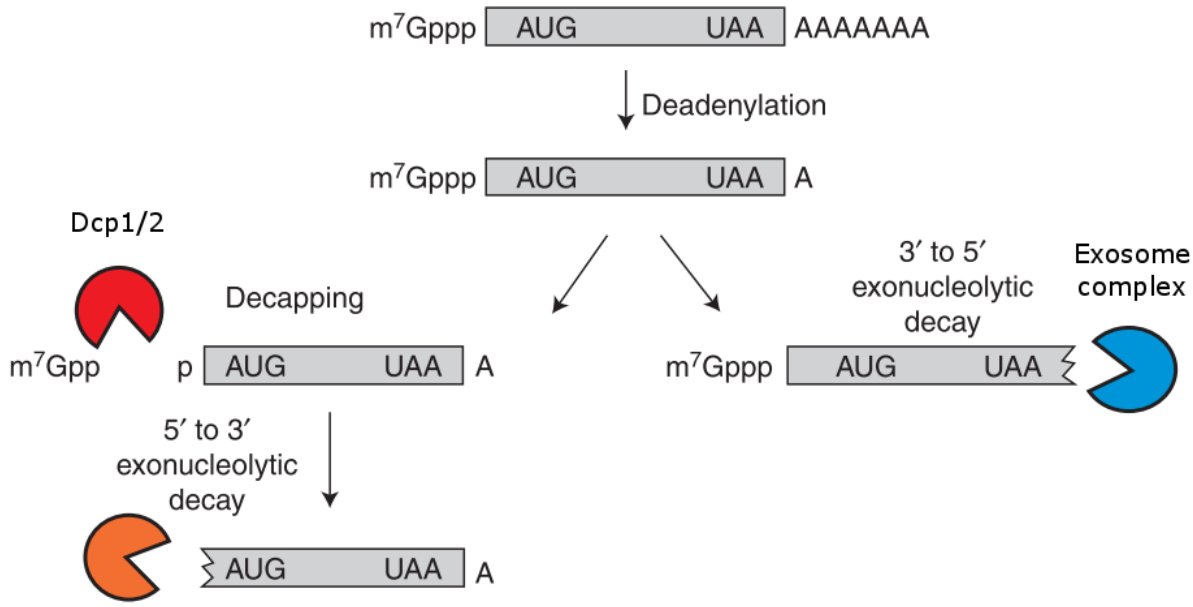


Figure 3: General mRNA degradation pathways. mRNAs to be degraded first undergo Deadenylation. This is followed by decapping by Dcp1/2 and 5' to 3' degradation by Xrn1, or recruitment of the exosome complex to the 3' end and 3' to 5' degradation. Adapted from (Decker and Parker, 2012).

### 1.5.4 RNA granules: Sites for RNA storage and degradation

Within the cell, mRNPs are sometimes assembled into very large protein-containing structures called RNA granules that are microscopically visible. Depending on their main protein constituents, RNA granules are classified into a few distinct types, some of the most studied being stress granules (SGs) and processing bodies (P-bodies), and they serve various purposes in RNA metabolism.

SGs, as their name suggests, are accumulated during cell stress, when mRNAs being translated are redirected from polysomes to these cytoplasmic foci (Kedersha and Anderson, 2007). Assembly of SGs are highly anti-correlated with translation and the assembly of ribosomes. It is initiated by phosphorylation of eukaryotic initiation factor 2α (eIF2α), which is also a step in blocking translation initiation (Kedersha et al., 1999). In addition, SG assembly is increased by puromycin induced disassembly of ribosomes, and reduced by emetine stabilisation of ribosomes (Kedersha et al., 2000). These findings, together with the

fact that SGs contain components of the translation initiation machinery, indicates that mRNAs could shuttle between translating ribosomes and SGs. mRNAs in SGs are not degraded (Laroia et al., 1999), thus they serve as a site for temporary storage of mRNAs.

While assembly of PBs is also driven by cell stress and they share certain proteins with SGs, they differ in that PBs do not contain translation initiation components but RNA degradation components, such as the decapping enzymes Dcp1/2 and the 5'-3' exoribonuclease Xrn1 (Kedersha et al., 2005), and are sites for RNA degradation (Parker and Sheth, 2007).

It has recently been shown that mRNAs could be transferred between these two (Kedersha et al., 2005; Wilczynska et al., 2005). It is thus hypothesised that SGs serve as a temporary storage point for mRNAs following translation arrest during cell stress, keeping its cargo mRNAs in a translationally repressed state. There the mRNAs wait for signals to either be redirected back to ribosomes for reinitiation of translation, or to PBs for degradation.

### 1.5.5 Cytoplasmic Polyadenylation

Before the discovery of cytoplasmic polyadenylation, it was thought that deadenylation of mRNAs would lead to its degradation. But since then, it was found that deadenylated mRNAs in the cytoplasm could persist for a long time in a translationally repressed state, and be re-adenylated for re-initiation of translation. Most of the biochemistry of this cytoplasmic polyadenylation was performed in Xenopus oocytes, where a repertoire of maternal mRNAs exists, in a deadenylated and "dormant" state, and are reactivated upon meiotic progression. Subsequent studies over the last decades have broadened the systems where cytoplasmic polyadenylation is known to occur to include mitotic cell cycle progression, senescence, tumourgenesis, synaptic plasticity (Richter, 2007; Villalba et al., 2011). As an example of cytoplasmic polyadenylation contributing towards temporal changes in protein expression, about 20% of proteins in the mouse liver that undergoes rhythmic protein expression from circadian control have a corresponding change in poly(A) tail length that precedes the change in expression (Kojima et al., 2012).

Cytoplasmic polyadenylation is mediated by the motif cytoplasmic polyadenylation element (CPE) located in the 3'UTR, its binding protein Cpeb1, and a hexanucleotide (hex) with the canonical sequence AAUAAA. Upon completion of transcription, a group of factors including the cleavage and polyadenylation specificity factor (Cpsf) mediate the cleavage of the pre-mRNA at 20-30 bases 3' of the hex motif, and add a long poly(A) tail of 200-250 bases to it (Mandel et al., 2006; Sachs and Wahle, 1993). Following nuclear export, mRNAs that contain CPE are recognised by Cpeb1, which recruits a protein complex consisting of the scaffold protein Simplekin, the deadenylase Parn and the poly(A) polymerase Gld2. Parn and Gld2 have antagonistic activities, but Parn is more active than Gld2, and when both are present the net effect is a shortening of poly(A) tail (Barnard et al., 2004; Kim and Richter, 2006). As a result this complex removes much of the poly(A) tail from CPE-containing mRNAs, and they remain in a translationally repressed state in the cytoplasm. It has even been proposed that Cpeb1 already binds to its target mRNAs before their nuclear export, to ensure tight translation repression (Lin et al., 2010).

Activation of these dormant mRNAs involves phosphorylation of Cpeb1 at Ser174 by the kinase Aurora A (Sarkissian et al., 2004). This expels PARN from the complex, allowing Gld2 to elongate the poly(A) tail (Kim and Richter, 2006). Upon poly(A) tail lengthening, poly(A) binding protein (Pabp) binds to the poly(A) tail, and recruits eIF4G to eIF4E on the 5' cap of the mRNA. This leads to circularisation of the mRNA, which is one of the processes during translation initiation (Wells et al., 1998).

In addition to Cpeb1, the RBP Pumilio (Pum) was also found to influence cytoplasmic polyadenylation and subsequent translation. Pumilio interacts with Cpeb1 in Xenopus oocytes and represses translation of cyclin B1 mRNA (Nakahata et al., 2001, 2003). This was found to be mediated in conjunction with Cpeb1, with a combinatorial code stemming from the arrangement of CPE, hex and the binding domain of Pum (PBE) on the 3'UTR of the mRNA determining polyadenylation and translation (Piqué et al., 2008).

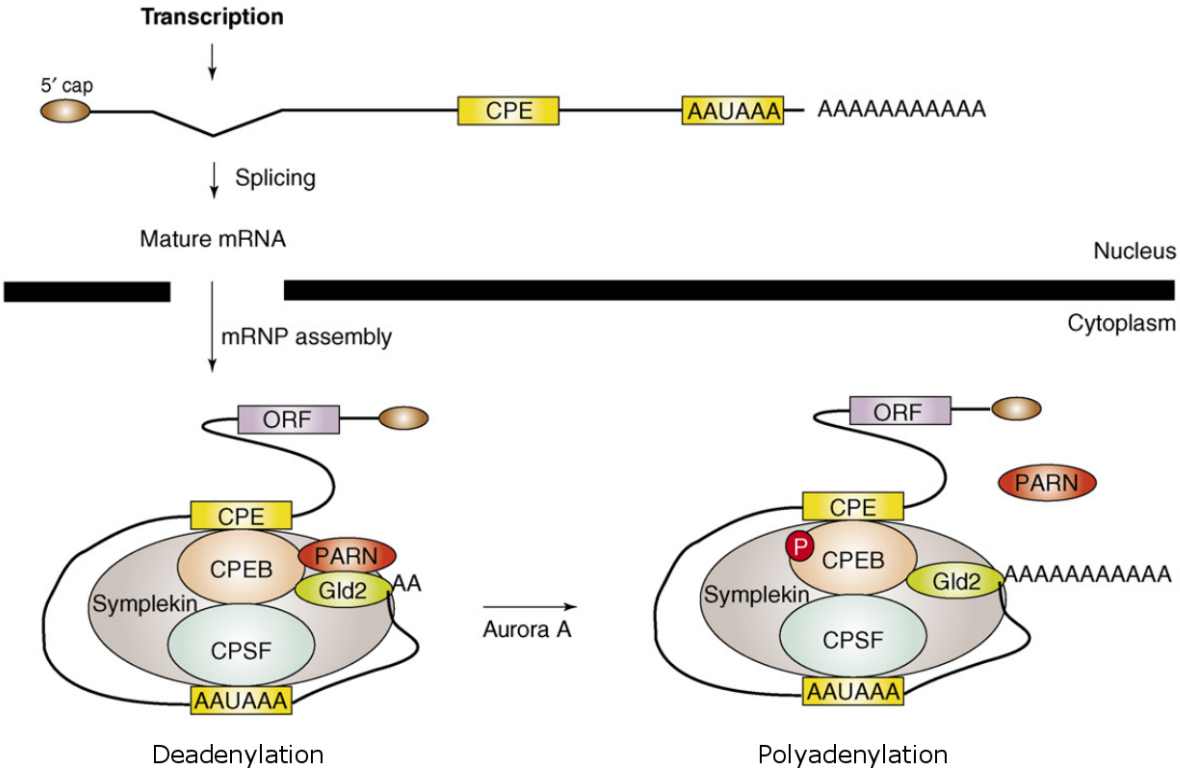


Figure 4: Regulation of cytoplasmic polyadenylation by Cpeb1. mRNAs are polyadenylated after transcription. Upon nuclear export, mRNAs with CPEs are targeted by a Cpeb1-containing protein complex. The opposing actions of the poly(A) polymerase Gld2 and the deadenylase Parn results in shortening of the poly(A) tail, as Parn has higher activity. Upon phosphorylation of Cpeb1 by the kinase Aurora A, Parn is expelled, leading to elongation of the poly(A) tail by Gld2. Adapted from (Richter, 2007).

### 1.5.6 Regulation of translation at initiation

Regulation of translation occurs principally at the initiation stage, rather than during elongation or termination (Jackson et al., 2010). For the majority of mRNAs, this occurs via a mechanism dependent on the 5' cap structure of the mRNA, and is referred to as cap-dependent translation (Merrick, 2004). At the onset of translation initiation, a ternary complex that consists of methionine-loaded initiator tRNA and GTP-coupled eIF2 is formed. This complex binds to the 40S small ribosomal subunit and other initiation factors to form the 43S pre-initiation complex. eIF4A unwinds secondary structures in the 5'UTR of the mRNA, and the 43S complex is recruited to the cap structure of the circularised mRNA via binding of

eIF3 to eIF4G, which then scans the mRNA in a 5' to 3' direction for the initiator AUG codon (Lamphear et al., 1995). Recognition of the initiator codon is assisted by eIF1 and eIF1A, and upon reaching it a stable 48S initiation complex is formed (Pestova et al., 1998). Subsequently, eIF5 and eIF5B promotes the hydrolysis of the eIF2-bound GTP, displacing the eIFs and recruiting the large 60S ribosomal subunit. Together the large and small subunit form the 80S initiation complex, and the Met-tRNA base pairs with the initiator codon (Gebauer and Hentze, 2004; Poulin and Sonenberg, 2013).

Regulation of initiation mainly occurs via impacting the eIFs. The best studied examples is changing the active states of eIF2α and eIF4E binding proteins (4E-BPs) via phosphorylation. Phosphorylation of the α subunit of eIF2 dissembles eIF2 from eIF2B and prevents GDP-GTP exchange, thus inhibiting translation. 4E-BPs is a group of 3 functionally equivalent proteins that normally bind to eIF4E, which prevents its association with eIF4G and thus the recruitment of the 43S pre-initiation complex to the mRNA. Upon phosphorylation of 4E-BPs, usually via mTOR signalling, they are released from eIF4E, allowing association of eIF4E with eIF4G and subsequent translation initiation (Gebauer and Hentze, 2004; Jackson et al., 2010).

### 1.5.7 Local protein translation and retrograde transport of axonally synthesised proteins

The temporal and spatial control over gene expression provided by cytoplasmic polyadenylation is important for localised translation, as mRNAs have to be translationally suppressed before they are transported to their destination and translation is required. The advantages offered by localised protein synthesis are especially important to neurons, whose axons and dendrites are far removed away from the cell soma. For proteins needed for a quick response, for example those needed in growth cones to respond to environmental cues to navigate the growth direction of the axon, to synthesise the protein in the cell soma and transport them to the axonal or dendritic tip would take too long. A similar case could be argued for functioning of synaptic connections (Jung et al., 2012).

Indeed, axons severed from the cell body are capable of growth and correct pathfinding, confirming the presence and role of axonal mRNA translation (Harris et al., 1987). One of the first precise functions identified for axonal translation is mediating the chemotropic response induced by Netrin-1 and Sema3A in Xenopus retina, where isolated axons continue to respond to these signals, but is blocked when translation is inhibited (Campbell and Holt, 2001). Application of Netrin-1 and Sema3A increases phosphorylation of eIF4e and 4EBP and also incorporation of radioactively labelled amino acids (Campbell and Holt, 2001). In addition, local protein synthesis in the axonal and dendritic compartments is also necessary for neurotrophin-mediated plasticity by Bdnf and NT-3 in the hippocampus (Kang and Schuman, 1996). Synaptic plasticity and memory consolidation was also found to depend on dendritic synthesis of CaMKIIα (Huber, 2000; Miller et al., 2002).

As would be expected, local translation is also involved in injury response of axons. Regenerating growth cones of axons of adult sensory neurons were found to contain translational initiation factors, ribosomal proteins and rRNAs. The ability to form growth cones in regenerating axons were found to be affected by treatment with protein synthesis inhibitors cycloheximide and anisomycin, even when the cell soma has been removed, demonstrating that translation does occur in axons and is involved in growth cone formation (Verma et al., 2005).

Some of the best studied axonally translated genes are importins, which are mediators of retrograde transport. Retrograde transport allows far ends of axons and dendrites to communicate with the cell soma, for example in case of an injury. Importins are mainly localised in axons, and a lesion up-regulates them by means of local translation in sciatic nerves. Disruption of importin-mediated nuclear translocation by treating the site of axotomy with synthetic peptides containing the nuclear localisation signal (NLS) inhibits regrowth of DRG axons (Hanz et al., 2007). In particular, mRNA of Importin-β1 was found to localise in axons via its 3'UTR, and axonal knockout of Importin-β1 attenuates the transcriptional response and regrowth after axotomy of DRG neurons (Perry et al., 2012).

Besides injury, retrograde transport also plays a role in neuron specification. In certain cases, when axons meet their targets, they encounter target-derived signalling molecules which induce specification of the neuron. In one such system, target-derived Bdnf induces translation of axonally localised Smad1, 5 and 8 RNAs, which are then translocated to the

cell soma where they are phosphorylated into transcriptionally active forms (Ji and Jaffrey, 2012).

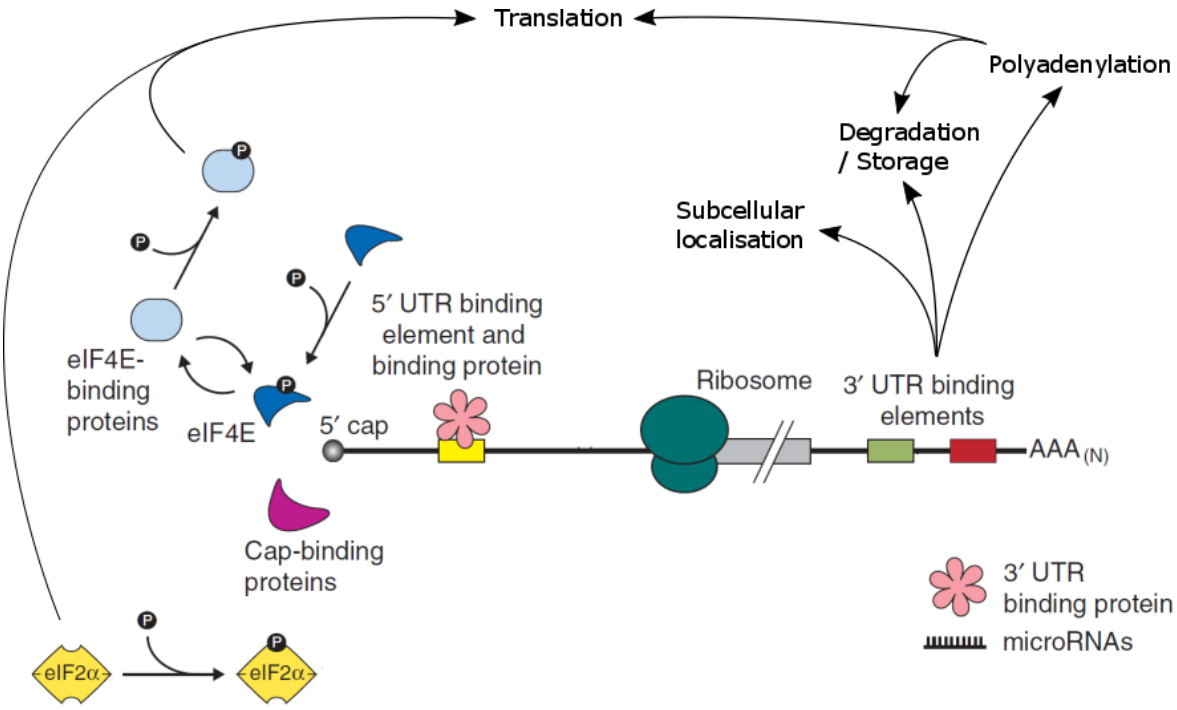


Figure 5: Overview of various post-transcriptional regulation mechanisms of gene expression. Recognition of 3'UTR motifs (e.g. zip-code, AREs, CPE) by various binding partners influences subcellular localisation, stability and polyadenylation of the mRNA. Length of the poly(A) tail in turn affects stability. Translation initiation is affected by polyadenylation status, 5'UTR elements, and the phosphorylation status of 4E-BPs and eIF2α. Adapted from (Baker and Coller, 2006).

## 1.6 Aims of study

Axons of the adult mammalian CNS have very limited ability to regenerate following an injury. For this reason, SCI often leads to drastic and pro-longed disabilities. Despite numerous studies conducted in the past decades, our understanding on what prevents regeneration in the CNS is still very limited, and a robust therapy to improve axon regeneration and functional recovery after SCI is yet to be found. Studies have recently started to show increasing evidence of the importance of post-transcriptional control in

protein expression, as well as the role of localised protein synthesis in axons towards axonal physiology. We hypothesise that post-transcriptional regulation plays an extensive role in the injury response of CNS neurons, and that by modulating post-transcriptional regulation, CNS neurons could be reprogrammed to regenerate.

Thus, the first goal of this project is to perform genome-wide profiling to uncover the extent of post-transcriptional regulation of gene expression upon SCI and its functional relevance. The second goal is to investigate major RBPs players of this regulatory process and whether CNS regeneration could be improved via manipulating these candidate RBPs, and to elucidate through which mechanisms these RBPs influence the fate of their target mRNAs.

# 2. Materials and Methods

## 2.1 Materials

### 2.1.1 Chemicals and Reagents

| Chemical / Reagent / Kit | Source |
|---|---|
| 4% Paraformaldehyde in phosphate buffer | Roth |
| Acid-Phenol:Chloroform, pH 4.5 (with IAA, 125:24:1) | Ambion |
| Actinomycin | Sigma-Aldrich |
| Agar | Roth |
| Agarose | Sigma-Aldrich |
| Agencourt Ampure XP beads | Life Technologies |
| Agilent high-sensitivity DNA kit | Agilent |
| Amicon-Ultra-15 column (100K MWCO) | Sigma-Aldrich |
| Ampicillin | AppliChem |
| AXIS Axon isolation devices, 450um | Millipore |
| B27 supplement (50X), serum free | Thermo Fisher Scientific |
| Benzonase | Millipore |
| Boric acid | Fluka |
| Caesium chloride (CsCl) | Sigma-Aldrich |
| Calcium chloride ($CaCl_2$) | Sigma-Aldrich |
| cOmplete Protease Inhibitor Cocktail Tablets | Roche |
| Cordycepin | Sigma-Aldrich |
| Cycloheximide (CHX) | Sigma-Aldrich |
| D(+)-Glucose | Sigma-Aldrich |
| Diethyl pyrocarbonate (DEPC) | Sigma-Aldrich |
| Dithiothreitol (DTT) | Sigma-Aldrich |
| DNA gel loading dye (6X) | Thermo Fisher Scientific |
| dNTP mix | Fermentas |
| Dulbecco's Phosphate buffered saline (PBS) ($Mg^{2+}$ and $Ca^{2+}$ free) | PAA |
| Dulbecco's Modified Eagles Medium (DMEM) | Life Technologies |
| EDTA | Thermo Fisher Scientific |
| Egg albumin | Gerbu |

| | |
|---|---|
| Ethanol (EtOH) | Sigma-Aldrich |
| FailSafe PCR Enzyme Mix | Epicentre |
| Fetal bovine serum | Biochrom |
| Fluoroblok cell culture insert, PET membrane, 3um pores | Corning |
| Fluoromount-G | eBioscience |
| G2 Dialysis Cassette (20K MWCO, 15ml) | Thermo Fisher Scientific |
| GeneChip Mouse Genome 430A 2.0 | Affymetrix |
| GeneChip One-Cycle Target Labeling and Control Reagents | Affymetrix |
| Glucose | Sigma-Aldrich |
| Glutamine | Life Technologies |
| Glycine | Sigma-Aldrich |
| Glycoblue | Ambion |
| Goat serum | Chemicon |
| Hank's balanced salts solution (HBSS) | Life Technologies |
| HEPES | Gibco |
| Horse serum | Biochrom |
| Isoflurane | Baxter |
| Isopropanol | Sigma-Aldrich |
| KAPA HiFi HotStart ReadyMix | KAPA Biosystems |
| Ketavet (100mg/ml) | Pfizer |
| L-Glutamine (100x L-Glutamine) | Life Technologies |
| Millicell hanging inserts, PET membrane, 3µm pores | Millipore |
| Minimum essential medium (MEM) | Thermo Fisher Scientific |
| N2 supplement (100X) | Thermo Fisher Scientific |
| Nextera XT DNA Sample preparation kit | Illumina |
| Nextera XT Index kit | Illumina |
| Nonidet P-40 | Roche |
| Oligonucleotide primers | MWG |
| PCR $H_2O$ | Braun |
| Penicillin Streptomycin (P/S) | Life Technologies |
| Phenylmethanesulfonyl fluoride solution (PMSF) | Sigma-Aldrich |
| Poly(A) Tail-Length Assay Kit | Affymetrix |
| Polyacryl carrier | Fisher Scientific |
| Polyethylene glycol (PEG) solution | Sigma-Aldrich |
| Poly-L-lysine hydrobromide | Sigma-Aldrich |
| Potassium chloride (KCl) | Applichem |
| Potassium phosphate monobasic ($KH_2PO_4$) | Gerbu |
| Pure Link Hi Pure Plasmid Filter Maxiprep | Life Technologies |

| | |
|---|---|
| Kit | |
| QIAmp Micro DNA isolation kit | Qiagen |
| Quantitect primers | Qiagen |
| Qubit dsDNA high-sensitivity (HS) kit | Life Technologies |
| Ribo-Zero Magnetic Kit | Epicentre |
| RNAqueous-Micro kit | Ambion |
| RNase-free $H_2O$ | Ambion |
| RNase-free PBS | Ambion |
| RNasin Plus RNase Inhibitor (RNAsin) | Promega |
| Rompun (2%) | Bayer |
| Round glass cover slips | Roth |
| ScriptSeq Index PCR Primers | Epicentre |
| ScriptSeq v2 RNA-Seq Library Preparation Kit | Epicentre |
| Sodium acetate | Ambion |
| Sodium azide | Merck |
| Sodium chloride (NaCl) | Sigma-Aldrich |
| Sodium deoxycholate (DOC) | Sigma-Aldrich |
| sodium dihydrogen phosphate (NaH2PO4) | Sigma |
| Sodium dodecyl sulfate (SDS) | Roth |
| sodium hydrogen phosphate ($Na_2HPO4$) | Sigma |
| Sodium pyruvate | Thermo Fisher Scientific |
| Sodium tetraborate (Borax) | Sigma-Aldrich |
| Sucrose | Sigma-Aldrich |
| SuperFrost slides | Roth, Germany |
| Superscript II reverse transcriptase | Life Technologies |
| SuperScript VILO cDNA Synthesis Kit | Life Technologies |
| SYBR® Green PCR Master Mix | Applied-Biosystems |
| Tools for mouse surgery | Fine Science Tools |
| Triton X-100 | Sigma-Aldrich |
| Trizma base | Sigma-Aldrich |
| Trypsin-EDTA (0.05%) | Life Technologies |
| TSO oligonucleotide | Exiqon |
| Tween-20 | Merck |
| Ultracentrifuge tubes | Beckman Coulter |

Table 1: List of chemicals and reagents

### 2.1.2 Solutions and Media

| Solutions | Composition |
|---|---|
| Perfusion solution | 5.71mg/ml Ketavet<br>2.8mg/ml Rompun<br>in NaCl 0.9% |
| PBS (20X) | 160g/L NaCl<br>23g/L $Na_2HPO_4$<br>28.84g/L $NaH_2PO_4$<br>4g/L KCl<br>4g/L $KH_2PO_4$<br><br>Fill up to 1L with $H_2O$ and adjust pH to 7.4 |
| TBS (10X) | 24.23g/L Trizma base<br>80.06g/L NaCl<br><br>Fill up to 1L with $H_2O$ and adjust pH to 7.6 |
| DEPC $H_2O$ | 1:1000 DEPC<br><br>Prepare in $H_2O$, leave overnight and autoclave |
| 2X Gradient buffer | 30mM Tris-HCl pH7.4<br>30mM $MgCl_2$<br>600mM NaCl<br>200µg/ml cycloheximide (CHX)<br>2mM dithiothreitol (DTT)<br><br>Prepare in DEPC $H_2O$ and sterile filter |
| Light sucrose gradient solution | 8.67 g sucrose,<br>25 ml 2X Gradient buffer<br><br>Fill up to 50 ml with DEPC $H_2O$ |
| Heavy sucrose gradient solution | 25g sucrose<br>25ml 2X Gradient buffer<br><br>Fill up to 50 ml with DEPC $H_2O$ |
| Homogenisation buffer | 0.25M sucrose<br>50mM Tris/HCl, pH7.4 |

| | |
|---|---|
| | 5mM $MgCl_2$<br>25mM KCl<br><br>Prepare in DEPC $H_2O$ and sterile filter. Add the following just before use:<br>200μg/ml CHX<br>1X Roche complete protease inhibitor<br>1mM DTT<br>1mM PMSF<br>100U/ml RNAsin |
| 0.9M sucrose solution | 30.8% sucrose<br>50mM Tris-HCl, pH7.4<br>5mM $MgCl_2$<br>25mM KCl<br><br>Prepare in DEPC $H_2O$ and sterile filter. Add the following just before use:<br>100 μg/ml CHX<br>1X Roche complete protease inhibitor<br>1mM DTT<br>1mM PMSF |
| 1.1M sucrose solution | 38.5% sucrose,<br>50mM Tris-HCl, pH7.4<br>5mM $MgCl_2$<br>25mM KCl<br><br>Prepare in DEPC $H_2O$ and sterile filter. Add the following just before use:<br>100μg/ml CHX<br>1X Roche complete protease inhibitor<br>1mM DTT<br>1mM PMSF |

| | |
|---|---|
| 2M sucrose solution | 68.4% sucrose<br>50mM Tris-HCl, pH7.4<br>5mM $MgCl_2$<br>25mM KCl<br><br>Prepare in DEPC $H_2O$ and sterile filter. Add the following just before use:<br>100µg/ml CHX<br>1X Roche complete protease inhibitor<br>1mM DTT<br>1mM PMSF |
| Benzonase buffer | 50mM TrisHCl<br>2mM $MgCl_2$<br>150mM NaCl<br><br>adjust pH to 8.5 and autoclave |
| Na-HEPES resuspension buffer | 50mM HEPES<br>0.15M NaCl<br>25mM EDTA<br><br>Prepare in $H_2O$ and sterile filter |
| CsCl topping solution | 0.55g/ml CsCl<br><br>Prepare in Na-HEPES resuspension buffer and adjust refractive index to 1.3710 at room temperature |
| 40% PEG8000/1.915M NaCl solution | 40% v/v PEG<br>1.915M NaCl<br><br>Sterile filter |
| Borate buffer | 1.24g boric acid<br>1.9g sodium tetraborate (Borax)<br><br>Adjust to 400ml with $H_2O$, adjust pH to 8.5 and sterile filter |
| PLL coating solution | 1mg/ml poly-L-lysine<br><br>Prepare in borate buffer and sterile filter |

| | |
|---|---|
| HS-MEM | 10% horse serum<br>1.2% glucose<br>2mM glutamine<br>1mM sodium pyruvate<br>0.22% $NaHCO_3$<br>1X Penicillin Streptomycin<br>1X MEM<br><br>Prepare in $H_2O$ and sterile filter |
| N2-B27-MEM | 1X N2 supplement<br>1X B27 supplement<br>0.1% w/v egg albumin<br>0.6% glucose<br>1mM glutamine<br>1mM sodium pyruvate<br>0.22% $NaHCO_3$<br>1X Penicillin Streptomycin<br>1X MEM<br><br>Prepare in $H_2O$ and sterile filter |

Table 2: List of solutions and media

### 2.1.3 Antibodies

| Antibody | Conjugate | Host species | Manufacturer | Dilution |
|---|---|---|---|---|
| Primaries antibodies | | | | |
| Cpeb1 ptg | | Rabbit | Proteintech | 1:250 |
| Cpeb1 | | Mouse | Group of Raúl Méndez | 1X |
| β-tublin | | Mouse | Millipore | 1:300 |
| Secondary antibodies | | | | |
| Anti-rabbit 488 | Alexa 488 | Goat | Life Technologies | 1:500 |
| Anti-mouse 488 | Alexa 488 | Goat | Life Technologies | 1:500 |
| Anti-mouse 633 | Alexa 633 | Goat | Life Technologies | 1:500 |

Table 3: List of antibodies

### 2.1.4 Primers

| Gene | Primer | 5'-3' sequence |
|---|---|---|
| **Apc** | qPCR-F | TGCAGGCCATTGCAGAGTTA |
| | qPCR-R | ACACAGCGTAGCCTTGTTGG |
| **c-Fos** | qPCR-F | CGACCATGATGTTCTCGGGT |
| | qPCR-R | GCGCAAAAGTCCTGTGTGTT |
| **c-Jun** | qPCR-F | TGGGCACATCACCACTACAC |
| | qPCR-R | TCTGGCTATGCAGTTCAGCC |
| **Cebpb** | qPCR-F | ATCCGGATCAAACGTGGCTG |
| | qPCR-R | GGCCCGGCTGACAGTTAC |
| **Cpeb1** | Genotyping-F | AGATGCAAATGGCTTGTGCC |
| | Genotyping-R | GGCCATCTCTTTGGAGCACT |
| **Cpeb4** | qPCR-F | TATGGGCGAAGGAGAGGTCAG |
| | qPCR-R | AGGTGACCCCAGACCACTAT |
| | PAT-F1 | ACTGTGTATGGGGAGGTTGT |
| | PAT-F2 | AGCAAGTGGGTGTCTAGTTT |
| | PAT-F3 | TCCTCTTTCTTGCTGGTGTT |
| | PAT-utrR | CCACTAGCACTTCAACAAATGA |
| **Ctnnb1** | qPCR-F | TACGAGCACATCAGGACACC |
| | qPCR-R | AAAGCAACTGCACAAACAATGG |
| | PAT-F1 | TTTATCGGGGATACGTGCGG |
| | PAT-F2 | AGCAGGTGGATCTATTTCATGTTTT |
| | PAT-F3 | AGACGTGTAACATTGTGTAGCCT |
| | PAT-utrR | CCGCATCTGTTGAAGCATTGT |
| **Egr1** | qPCR-F | CACCTGACCACAGAGTCCTTTT |
| | qPCR-R | GACTAGGCTGAAAAGGGGTTCA |
| **Fosb** | qPCR-F | CGACTTCAGGCGGAAACTGA |
| | qPCR-R | TTCGTAGGGGATCTTGCAGC |
| **Gapdh** | qPCR-F | CCAGTGAGCTTCCCGTTCA |
| | qPCR-R | GAACATCATCCCTGCATCCA |
| **Junb** | qPCR-F | CAACCTGGCGGATCCCTATC |
| | qPCR-R | GCCTGTGTCTGATCCCTGAC |
| **Kif5c** | qPCR-F | AAGAGGCCAAGGAGAATGCC |
| | qPCR-R | GATGGGCTTGGCGATCTGAG |
| **Kpnb1** | qPCR-F | AGGGCGGAGATCGAAGACTA |
| | qPCR-R | TGGTACCAGATCAAGCCTGG |
| | PAT-F1 | AGCATCAATCTGTAATTGGCATTCA |
| | PAT-F2 | AGAAGAAGTTCAAATTCCATCCACT |
| | PAT-F3 | GACTGGAGAAGTGGAGGGAC |
| | PAT-utrR | AAGGTGGTGGTATCAGTTTTGG |

| | | |
|---|---|---|
| **Map2k7** | qPCR-longutr –F | AAGCTACTTGAACACAGCTTCATC |
| | qPCR-longutr-R | CATGAGGCTACCTGAAGAAGGG |
| | qPCR-shortutr-F | AAGCTACTTGAACACAGCTTCATC |
| | qPCR-shortutr-R | CAGACTCCCACTGAAGAAGGG |
| **Nfkbia** | qPCR-F | CTCTTGTTGAAATGTGGGGCTG |
| | qPCR-R | CAGTCATCATAGGGCAGCTCAT |
| **Pten** | qPCR-F | GCATCGGGGCAAATTTTTAAAGGCA |
| | qPCR-R | GGATTGCAAGTTCCGCCACTGA |
| | PAT-F1 | ACCAAAGTTGGAGTTGTGGA |
| | PAT-F2 | AGCCTCTTGATGTGTGCATT |
| | PAT-F3 | CCCACTGGGATTTTACAGTTT |
| | PAT-utrR | TCCACAGGAAGGTATTTCTAGTC |
| **Socs3** | qPCR-F | TAGACTTCACGGCTGCCAAC |
| | qPCR-R | CGGGGAGCTAGTCCCGAA |
| **Stat3** | qPCR-F | ACCCAGGTAGTGCTGCCCCGTA |
| | qPCR-R | GGGGGACATCGGCAGGTCAAT |
| | PAT-F1 | ACTGCACTCAGATTCCAATGTA |
| | PAT-F2 | ACTGCTTAGCCTTTCAGTGC |
| | PAT-F3 | GAACAAGGTGAGGGCTTCTC |
| | PAT-utrR | CTGGAAGTTAAAGTAGTTACAGCA |
| **Stxbp1** | qPCR-F | AGGAGCTCAGCAAGTATTCGAC |
| | qPCR-R | GGATGGGGACAATGGCTCTC |

Table 4: List of primers

qPCR primers for Map2k7 (total), Neurod2, Noggin, and Zfp36l2 were purchased as QuantiTect Primers from QIAGEN.

## 2.2 Methods

### 2.2.1 Animal experiments

#### 2.2.1.1 Mice

Mice were housed under standard conditions and fed *ad libitum*. All procedures were in accordance to the DKFZ guidelines and approved by the Regierungpräsidium Karlsruhe.

C57BL/6J mice, referred to as “wild-type” hereinafter, were bred in house at the DKFZ Center for Preclinical Research facility. Cpeb1$^{flox/flox}$ mice were kindly provided by Raúl Méndez.

#### 2.2.1.2 Spinal cord injury

Female C57BL/6 mice of age 10-12 weeks were used. Females were chosen due to ease of emptying the bladders of injured animals. Mice were anesthetised by exposure to 3% isofluran in oxygen. Concentration is then reduced to 1.5% to maintain anesthesia. The back of the animal was shaved and a 1cm incision was made on the skin along the middle. The vertebral column was exposed by separating the surrounding fat and connective tissues. A laminectomy was performed at thoracic level T7/8 to reveal the spinal cord, which is then symmetrically transected with fine irridectomy scissors. The surrounding tissue was then sutured and the skin closed with surgical clamps. Sham operation were performed in the same way but without transecting the spinal cord. Bladders of injured animals were depressed and emptied once a day.

#### 2.2.1.3 Perfusion

Animals were anesthetised by injection of 200ml of perfusion solution. The thoracic cavity was then opened to reveal the heart, and the animal perfused by transcardial perfusion with 20ml of HBSS. If tissues are to be extracted for immunohistochemistry, this is followed by 10ml of 4% PFA.

#### 2.2.1.4 *Drosophila* experiments

*Drosophila* experiments were performed by Marta Koch from the lab of Bassem Hassan.

**Fly stocks and genetics**

*Drosophila* melanogaster stocks were kept on standard cornmeal media. For tissue specific overexpression of the transgenes, the GAL4/UAS system was used (Brand and Perrimon, 1993). pdf-gal4, uasgfp; pdf-gal4, uas2x egfp/cyo flies were used to drive expression of the various candidate genes, or crossed to wild-type Canton S (CS) for the outgrowth experiments, or to UAS-lacZ for the regrowth experiments. Overexpression stocks were obtained from the Bloomington Stock Centre and the pdf-gal4 line was obtained from P. Taghert. Flies were dissected 2-10 days after eclosion.

***Drosophila* outgrowth and regrowth assays**

For the outgrowth screening, a minimum of 5 fly brains (10 sLNv projections) per genotype were dissected in PBS, fixed in 4% PFA and stained with for Gfp. The degree of sLNv outgrowth was classified as "increased", "reduced" or "no observable effect" relative to that of controls.

Regrowth assay was performed on whole brain explants as described (Ayaz et al., 2008; Koch and Hassan, 2012). Briefly, flies were reared at 18°C to minimize developmental effects, and shifted to 25°C one day prior to injury. Culture plate inserts were coated with laminin and PLL. Fly brains were dissected in a sterile Petri dish containing ice cold Schneider's *Drosophila* Medium (GIBCO) and transferred to a culture plate insert containing culture medium (10 000 U/ml penicillin, 10 mg/ml streptomycin, 10% Fetal Bovine Serum and 10 µg/ml insulin in Schneider's *Drosophila* Medium). sLNv axonal injury was performed using an ultrasonic microchisel controlled by a powered device (Eppendorf), and dishes were kept in a humidified incubator at 25°C. Four days later, cultured brains were fixed and stained for Gfp. The exact location of the lesion was determined by comparison with axonal projection length at 5 hours post-injury when regrowth has not yet occurred. Injured sLNv neurons that has formed at least one new axonal sprout with a minimum length of 12µm was

measured in ImageJ. Regenerated length was defined as the regenerated axon lengths measured using the manual tracing tool. Projected distance was defined as the displacement of the axon sprouts from the lesion site, measured in a straight line. Statistical comparisons were performed with student's t-test.

### 2.2.2 Tissue and cell biology

#### 2.2.2.1 Cortical neuron culture

**Cortical neuron isolation**

Mice were put together overnight for mating and then separated. At embryonic day 16.5, the mother was sacrificed by cervical dislocation and the embryos were removed. Embryonic brains were extracted in cold HBSS with 1% P/S and cortices were dissected under a dissection microscope in a mouse hood. Cortices were washed once with HBSS with 1% P/S, then incubated in 0.5ml 0.05% trypsin at 37ºC for 5 minutes. Trypsination was stopped by adding 1 volume of HS-MEM. Cortices were washed once in HS-MEM and then triturated with flame polished glass Pasteur pipettes until a cell homogenate is formed. The cell suspension was then centrifuged at 2000G for 3 minutes at 4ºC and resuspended in HS-MEM. Cells were then counted with a counting chamber, mixed with AAV if needed, and plated accordingly.

**Plating**

For culturing neurons on glass cover slips or microscopic slides (for AXIS devices), the culture surface was immersed in concentrated nitric acid (65%) overnight, washed 5 times with deionised water, dried and sterilised by ultraviolet light irradiation in a cell culture hood for 20 minutes. PLL coating solution was added to cover the whole surface, incubated at 37ºC

overnight, and washed 2 times with deionised water before use. Transwell culture inserts were coated in the same way but without the acid treatment and UV sterilisation.

Cover slips and transwell chambers were placed into tissue culture plates with wells of fitting sizes and neurons suspended in HS-MEM were added.

For AXIS devices, the device was placed and attached to microscopic slides just before use. Cells were resuspended in 5µl and dispensed directly into the channel on the cell soma side. The soma side wells were then filled with medium, followed 5 minutes later by axon side wells, to allow time for medium to pass through the microgrooves to the axon side and prevent bubbles from blocking the groove openings. Cells were then plated as follows:

| | **Number of cells** | **Volume of medium** |
|---|---|---|
| 18mm round cover slip (12 well) | $3x10^5$ | 1ml |
| 12mm round cover slip (24 well) | $1x10^5$ | 0.5ml |
| Transwell cell culture insert (12 well) | $3x10^5$ | 0.5ml upper side,<br>1.5ml lower side |
| Fluoroblok cell culture insert (24 well) | $1x10^5$ | 0.3ml upper side,<br>0.7ml lower side |
| AXIS | $1x10^5$ | 200µl soma side<br>100µl axon side |

Table 5: Number of neurons plated and volume of medium

Cultures were kept in a humidified cell culture incubator at 37ºC. One day after plating, the HS-MEM was replaced with N2B27-MEM.

#### 2.2.2.3 Cell culture

HEK293T cells were maintained in DMEM supplemented with 10% FBS, 1% P/S and 1% L-glutamine. When confluent, the culture flasks were washed one with PBS. The cells were dissociated with 0.25% Trypsin–EDTA at 37ºC. Trypsination was stopped by addition of 1 volume of culture medium. Cells were washed off the culture surface and pelleted by

centrifugation at 4ºC at 1500rpm for 3 minutes. Cells were resuspended in new culture medium, splitted and plated accordingly.

#### 2.2.2.4 Adeno-associaded virus (AAV) Production

AAV production was performed in collaboration with the research group of Dirk Grimm, who provided the plasmids and protocols and did the initial rounds of virus production.

**Transfection**

30 15cm cell culture dishes were seeded with $4.5x10^6$ HEK293T cells. 2 days later cells were co-transfected with three plasmids: 1) pSSV9-CAG-CreGfp, which contains a Cre Gfp fusion under a CAG promoter, flanked by viral ITR sequences for packaging; 2) AdH, which contains the helper factors from adenovirus essential for activating the AAV gene expression programme; and 3) Wdc2, which contains *rep* and *cap2* that encode AAV replication factors and serotype type 2 capsid proteins respectively.

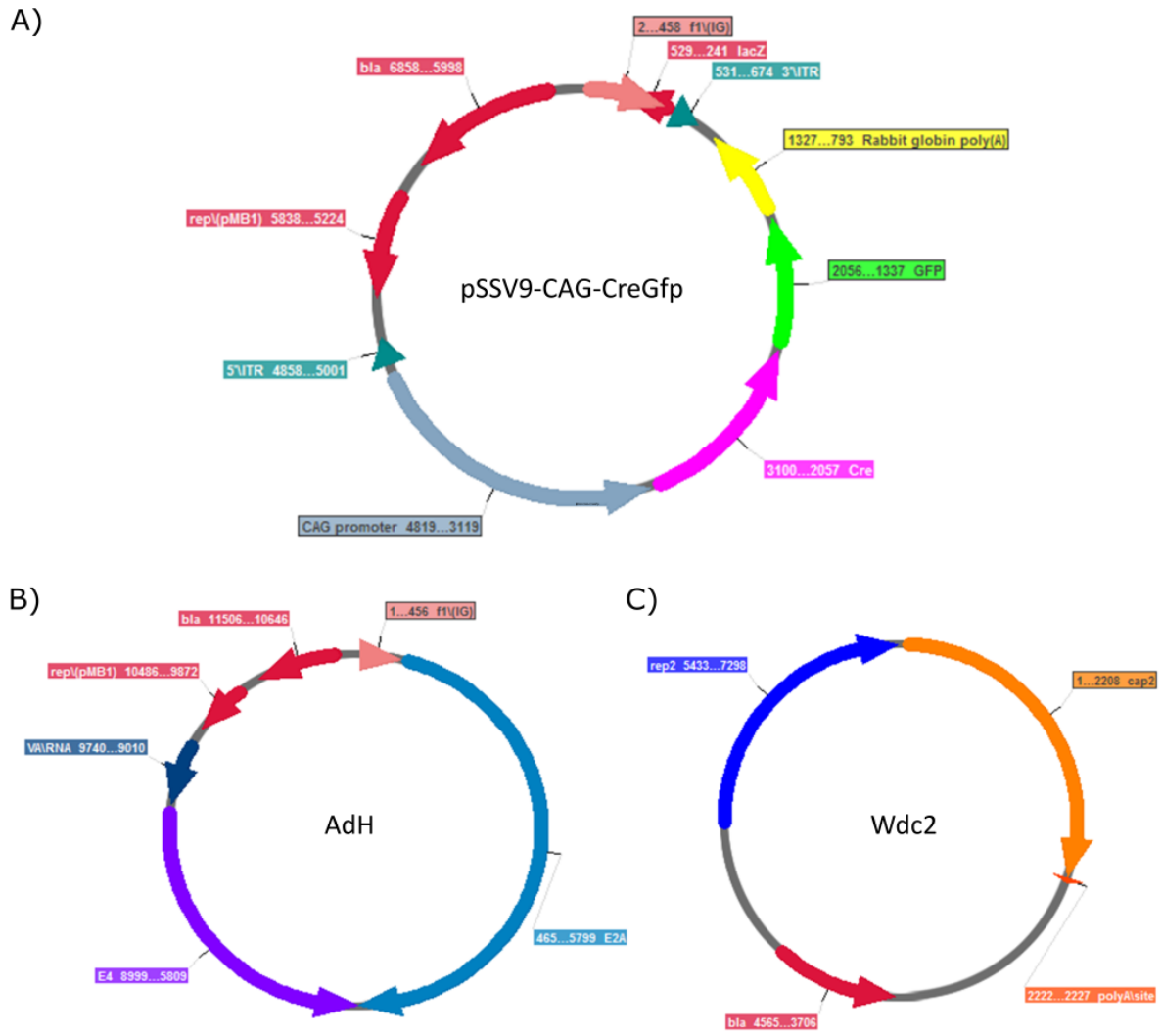


Figure 6: Plasmids used in AAV production. A) pSSV9-CAG-CreGfp, expressing a Cre Gfp fusion protein under the CAG promoter. 2) AdH, expressing the adenovirus helper factors. 3) Wdc2, expressing replication factors and serotype type 2 capsid proteins.

A DNA solution was prepared from 440ug of each plasmid, mixed with 23.7ml of 300mM NaCl and filled up to 47.4ml with $H_2O$. Then 1.7ml PEI (2ug/ul) was mixed with 23.7ml of 300mM NaCl and filled up to 47.4ml with $H_2O$. The PEI solution was then added dropwise into the DNA solution. The mixture was vortexed and left to stand at room temperature for 10 minutes. Then 3.2ml of the mixture was added dropwise onto each plate while swirling the medium constantly.

**Cell lysis and AAV precipitation**

3 days after transfection, cells were harvested by scraping and all the culture medium was also collected in order to also save detached cells. The cell suspension was pelleted by centrifugation at 400G for 15 minutes, washed once with PBS, and resuspended in 15ml benzonase buffer. Cells were then lysed by freeze-thawing. The tube was immersed in liquid nitrogen for 5 minutes, then transferred to a 37ºC water bath until the cell suspension is completely thawed. The process is repeated 4 times. In order to digest host cell DNA and RNA, the tube was sonicated for 80 seconds, and benzonase was added to a concentration of 50U/ml and incubated for 1 hour at 37ºC with vortexing at 10 minutes intervals. Debris was then pelleted by centrifugation at 4000G for 15 minutes and the supernatant was collected. Subsequently proteins were precipitated by addition of calcium chloride to a final concentration of 25mM, incubation on ice for 1 hour and centrifugation at 10,000G at 4ºC for 15 minutes. The supernatant was collected and AAV was precipitated by addition of ¼ volume of 40% PEG8000/1.915M NaCl and incubation at 4ºC for 3 hours.

**Caesium chloride (CsCl) purification**

The tube was centrifuged at 2500G at 4ºC for 30 minutes and the supernatant was discarded. The pellet was resuspended in 10ml Na-HEPES resuspension buffer and incubated overnight at 4ºC. The tube was then centrifuged at 2500G at 4ºC for 30 minutes, the supernatant was collected and the volume brought up to 24ml with Na-HEPES resuspension buffer and 13.2g of CsCl was added. The refractive index (RI) was then measured using a refractometer. RI of the virus sample was adjusted to 1.3710 by adding Na-HEPES resuspension buffer when it is too high and CsCl when it is too low. Meanwhile the RI of topping solution is adjusted in the same manner. The virus sample was then transferred to an ultracentrifuge tube and the tube was filled to the top with CsCl topping solution. The tubes were balanced and centrifuged with a SW70Ti rotor at 45,000rpm at 21ºC for 22 hours. Subsequently the bottom of the tube was punctured with a needle and the contents were separated into 0.5ml fractions starting from the bottom by draining into 15ml tubes, while taking care to maintain the sequence of

the fractions. The RI of the fractions were measured and those with RI within 1.3711 and 1.3766 were pooled.

**Dialysis and concentration**

The virus solution was dialysed to exchange caesium chloride with PBS using a G2 Dialysis Cassette (20K MWCO, 15ml). The cassette was first equilibrated by immersing in PBS for 2 minutes. The volume of the virus sample was brought up to 9ml with PBS and added into the cassette. The cassette was first immersed in cold PBS and kept at 4ºC without stirring and the PBS replaced after 30 minutes for better removal of caesium chloride. Stirring was started after the first PBS replacement. PBS was replaced again after 1 hour, 2 hours, 2 hours, overnight, and 2 hours.

An Amicon-Ultra-15 column (100K MWCO) was then used to concentrate the virus. The filter on the column was first equilibrated by washing 2 times with 15ml PBS and centrifugation at 1000G for 2 minutes. Virus sample was applied to the column and centrifuged at 400G until a volume of 1-1.5ml was reached. The AAV sample was collected, aliquoted and stored at -80ºC.

**Titration**

Virus samples were lysed by alkaline lysis. 10µl of virus aliquot was mixed with 10µl TE buffer and 20µl 2M NaOH and incubated at 56ºC for 30 minutes. Then the lysis was stopped by addition of 38µl 1M HCl and diluted with 922µl $H_2O$. qPCR together with serially diluted standards was performed and the titer of the sample was deduced by plotting a standard curve.

#### 2.2.2.5 Drug treatment

Actinomycin was added to the culture medium to a final concentration of 10µM. For transwell chambers, the medium from both compartments were pooled, actinomycin was added, and the medium was redistributed to both compartments. For AXIS cultures, the medium was removed from the axon side. Then medium containing 200µM of cordycepin or cycloheximide was dispensed back into the axon side channel and wells.

#### 2.2.2.6 Regeneration assays

For cultures on cover slips, a glass Pasteur pipette was drawn across the culture surface to cut processes. For transwell chambers, the underside of the Fluoroblok cell culture inserts were scraped with a sterile cotton swap to remove the processes growing there. For AXIS cultures, vacuum was applied directly to the axon side channel to suck away the axons.

For cultures on cover slips and AXIS devices, the cultures were imaged live with a phase contrast filter. For transwell chamber cultures, the live cell dye Calcein AM was added to the medium 30 minutes before imaging and processes are visualised using a Gfp filter. Imaging was performed using a Zeiss Cell Observer from the DKFZ Light Microscope Core Facility.

Images were analysed and regenerating processes were traced with ImageJ in a blinded manner. In order to ease the effort for tracing and reduce subjective biases, a custom written ImageJ macro kindly provided by Damir Krunic from the DKFZ Light Microscope Facility was used for supervised automated tracing. Firstly, the rollerball function was applied to equalise background signal. Gaussian blur was then applied to smooth out any part of the processes with weak signal, which would otherwise be considered as a break. Then a threshold was manually set to subtract the background signal while minimising the breaks created in the processes. The skeletonise and analyse particles functions were used to trace all the processes, with a lower limit of 60 pixels to discount debris. Comparison of data from manually and macro traced images revealed the two to be highly similar to each other.

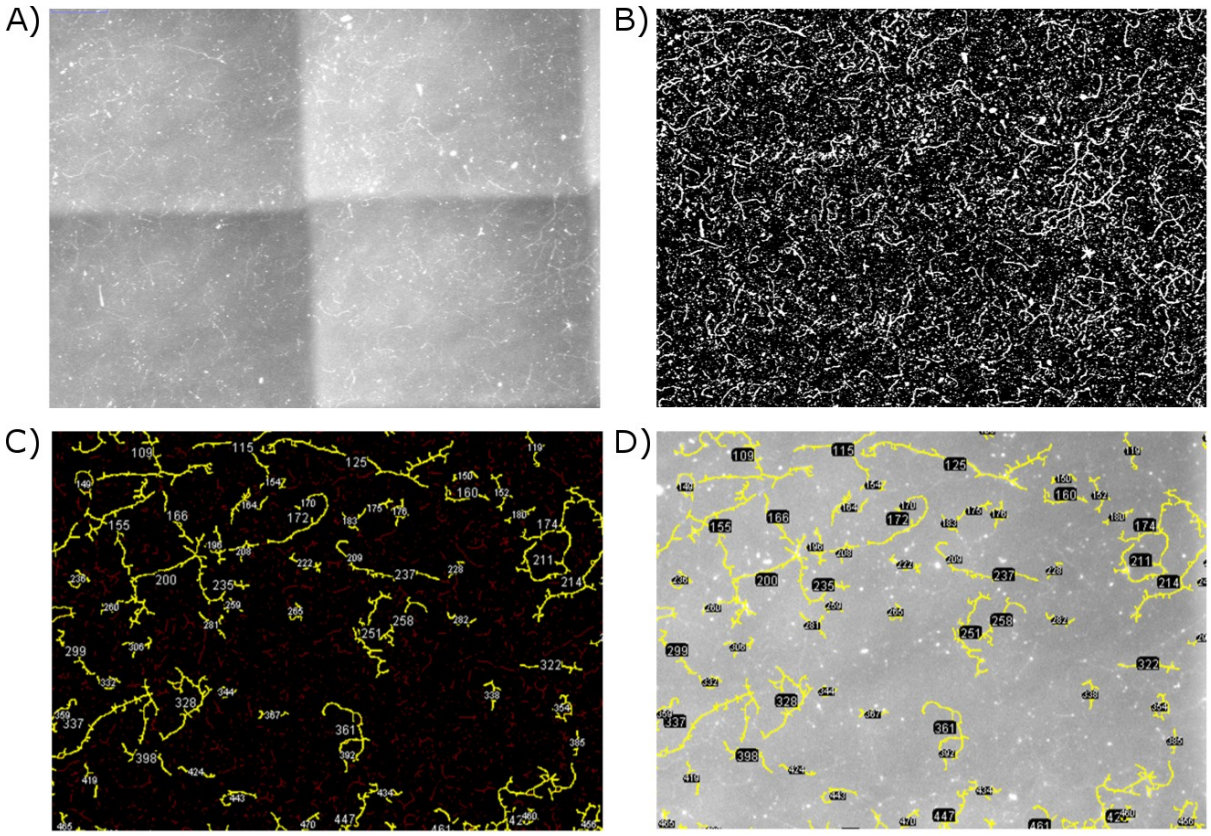


Figure 7: Supervised automated tracing of neuronal processes. A) Input from stitched tile scan images. B) Background signal across tiles is equalised and subtracted. C) Processes are skeletonised and traced. D) Tracings superimposed on the original image.

#### 2.2.2.7 Immunohistochemistry

Extracted tissues were fixed with 4% PFA at 4ºC overnight. After washing 2 times with PBS, tissues were sectioned using a vibrotome to appropriate thicknesses and kept in PBS with 0.02% sodium azide at 4ºC until use. Sections were washed 3 times 15 minutes each in TBS, then blocked with TBS supplemented with 0.25% Triton X-100 and 3% serum (TBS++) for 1 hour. Primary antibody was diluted in TBS++ and incubated with the sections overnight at 4ºC with shaking. Afterwards the sections were washed 3 times 15 minutes each with TBS, and incubated with secondary antibody diluted in TBS++ at room temperature for 2 hours with shaking. The sections were then washed again with TBS 3 times 15 minutes each, and finally mounted on glass slides with Fluoromount-G and left to dry in the dark.

### 2.2.3 Molecular biology

#### 2.2.3.1 DNA Extraction

DNA was isolated using the QIAmp DNA Micro kit from QIAGEN according to the manufacturer's protocol. 180µl of Buffer ATL was added to neurons grown on cover slips and lysis was assisted with a cell scrapper. The lysate was transferred to a 1.5ml tube. 20µl Proteinase K was added and the tube was incubated at 56ºC for 45 minutes. 200µl Buffer AL containing 1µl of polyacryl carrier was then added to each sample, followed by 200µl of 100% ethanol. The tube was then incubated for 5 minutes at room temperature, and the lysate was transferred to a QIAamp MinElute colutm and centrifuged at 6000G at room temperature for 1 minute. The flow-through was discarded, and the column was washed with 500µl Buffer AW1 and then with 500µl Buffer AW2. The column was centrifuged a further 3 mintues to dry the membrane completely. To elute the DNA, 30µl of nuclease-free water was added to the membrane, the column was incubated at room temperature for 1 minute, then centrifuged at full speed for 1 minute.

#### 2.2.3.2 Polysome fractionation

**Sucrose gradient preparation**

Heavy and light sucrose gradient solutions were prepared and added to the corresponding chambers of the gradient maker with magnetic stirrers. The gradient maker is placed on a stir plate on an elevated platform and the output was connected to a glass capillary placed at the bottom of an ultracentrifuge tube. The valves were then opened to allow the sucrose solutions to mix and flow into the tube via gravity, starting with light sucrose. The sucrose solution that comes out becomes denser over time, and displaces the lighter sucrose upwards, thus generating a gradient in the tube. The gradients were prepared at least 1 hour before fractionation and kept at 4ºC until use.

**Tissue preparation**

Animals were anesthetised and perfused with 20ml of HBSS supplemented with 0.2mg/ml cycloheximide which immobilizes ribosomes on associated transcripts. Tissues were extracted to homogenisation buffer (40µl for brains and 10µl for spinal cords) on ice and diced into small pieces to allow better penetration of cycloheximide and incubated for at least 15 minutes. Tissue pieces were then homogenised with a Dounce tissue grinder with specific number of strokes (5 times with a tight pestle for brains, 5 times with a loose pestle followed by 5 times with a tight pestle for spinal cords) to disrupt cells while keeping the nuclei intact. 20% volume of the lysate is fresh frozen for later extraction of total RNA. Nuclei and tissue fragments were pelleted and removed by centrifugation at 500G at 4ºC for 10 minutes. Remaining membrane fragments in the supernatant were lysed by addition of NP-40 and sodium deoxycholate detergents to a final concentration of 1% each.

**Myelin floatation**

Fatty components mainly coming from myelin in the samples have to removed or the signal in the polysome profile might be masked. The lysate is first mixed with 1.22 volumes of 2M sucrose solution and transferred to a polyethylene ultracentrifuge tube, and filled up to approximately 10ml volume with 1.1M sucrose solution. Then 0.9M sucrose solution is carefully overlaid on top to the rim of the tube. Subsequently the tubes were centrifuged with SW40Ti rotor and buckets at 24,000rpm at 4ºC for 3 hours. During this step fatty lipids float up and ribosomes are deposited as a pellet at the bottom.

**Sucrose gradient fractionation**

The supernatant was carefully removed completely without disturbing the pellet, and the pellet was resuspended in 400µl homogenisation buffer supplemented with 1% NP-40 and

1% sodium deoxycholate. The samples were then carefully overlaid on top of sucrose gradients, and centrifuged at 40,000rpm at 4ºC for 1.5 hours. The gradients were then fractionated using an Isco density gradient fractionator. The UV detector was switched on at least 15 minutes before fractionation to allow the UV lamp to warm up and set to the appropriate sensitivity (0.2 for brains, 0.05 for spinal cords). The tube piercer was assembled and connected to 60% sucrose solution via a rotating pump. The setup was tested by pumping for a few minutes to ensure there were no leaks in the connections. Water was pumped into the UV detector with a syringe and baseline was set to an appropriate level.

The ultracentrifuge tubes containing the samples was carefully attached to the UV detector and pierced from the bottom with the tube piercer. 60% sucrose solution was then pumped from below to slowly displace the samples upwards into the UV detector and into the drop dispenser. The absorbance at 260nm was recorded to generate the absorption profile for the sample. The samples were collected in 0.5ml fractions and frozen at -80ºC until use.

#### 2.2.3.3 RNA Extraction

**Neurons**

Due to the small amount of material available from neuron cultures, the RNAqueous-Micro kit is used following the manufacturer's instructions. Cover slips were washed briefly with PBS, then 300µl of Lysis Solution was added. The cover slips were then scraped using a cell scrapper and the lysate transferred to a 1.5ml tube. If RNA is to be extracted from either processes or cell soma from transwell chambers, then the side not needed was scraped with a DNAse- and RNAse-free cotton swap (when extracting processes, the upper surface was scraped, when taking cell soma, the lower surface was scraped). The membrane was then cut out with a scalpel, rinsed briefly in PBS, then put into a 1.5ml tube containing 300µl Lysis Solution and vortexed. Subsequently 150µl of 100% ethanol was added and the tube was vortexed. The lysate was then loaded into a Micro Filter Cartridge Assembly and centrifuged using a table-top centrifuge at full speed for 10 seconds, and the flow-through was discarded. The cartridge was washed once with 180µl of Wash Solution 1, then 2 times with 180µl of

Wash Solution 2/3, with full speed centrifugation for 10 seconds in between. The cartridge was centrifuged at full speed for a further 1 minutes to remove residue fluid. To elute RNA, 15µl of 75ºC RNAse-free water was added to the centre of the filter, incubated for 1 minute in room temperature, and then centrifuged at full speed for 30 seconds. This step is repeated once to increase RNA yield.

DNA was then removed by DNAse treatment. 3µl of 10X DNAse I buffer and 1µl of DNAse I was added to each sample and then incubated at 37ºC for 20 minutes. Afterwards 3.4µl of DNAse Inactivation Reagent was added and incubated at room temperature for 2 minutes. The tube was centrifuged at full speed for 1.5 minutes, and the supernatant taken and stored at -80ºC.

**Polysome fractions**

To each individual fraction or pooled fractions, 10% SDS was added to a final concentration of 1% to unfold proteins and dissociate ribosomes. One volume of acidic phenol chloroform was added and the samples incubated at 65ºC for 10 minutes. After centrifugation at 17,000G at room temperature for 20 minutes, the aqueous phase was transferred to a new tube. In samples with high sucrose concentrations the aqueous phase may be at the bottom due to phase inversion. Then 1 volume of isopropanol, 1/9 volume of sodium acetate (pH 5.2) and 1µl of GlycoBlue was added to each sample and the RNA was precipitated by incubation at -80ºC for at least 1 hour. The samples were then centrifuged at 17,000G for 30 minutes at 4ºC and the supernatant was discarded. The pellet was washed once with 80% ethanol, then air dried and dissolved in nuclease-free water.

#### 2.2.3.4 Reverse transcription

Reverse transcription was performed using the SuperScript VILO cDNA Synthesis Kit, with the following reaction mix and thermo cycle:

| | |
|---|---|
| RNA | 100-1000ng |
| 10X SuperScript Enzyme Mix | 2µl |
| 5X VILO Reaction Mix | 4µl |
| Nuclease-free water | To 20µl |

| | |
|---|---|
| 25ºC | 10 minutes |
| 42ºC | 60 minutes |
| 85ºC | 5 minutes |

#### 2.2.3.5 Quantitative Real-time PCR (qPCR)

qPCR is performed using a 7500 Fast Real-Time PCR System Cycler (Applied Biosystems) with the following reaction mix:

| | |
|---|---|
| $H_2O$ | 9.7µl |
| Forward primer (1:20 diluted) (stock 100µM) | 1.8µl |
| Reverse primer (1:20 diluted) (stock 100µM) | 1.8µl |
| 2x SYBR Green PCR Master Mix | 12.5µl |
| cDNA template | 1µl |

If Qiagen Quantitect primers were used, they were not further diluted. All reactions were run as technical triplicates.

**2.2.3.6 Poly(A) tail (PAT) assay**

PAT assay was performed using the Poly(A) Tail-Length Assay Kit from Affymetrix according to the manufacturer's protocol. Firstly, a number of guanosine and inosine residues were added to the 3' end of the poly(A) tails, to facilitate priming, with the following reaction mix:

| | |
|---|---|
| DNase-treated RNA | 1μg |
| 5X Tail Buffer Mix | 4μl |
| 10X Tail Enzyme Mix | 2μl |
| Nuclease-free water | To 20μl |

The reaction mix was incubated at 37ºC for 60 minutes, and the reaction was stopped by adding 2μl of 10X Tail Stop Solution. Next the G/I-tailed RNAs were reverse transcribed into cDNA with the following reaction mix:

| | |
|---|---|
| G/I tailed RNA | 5μl |
| 5X RT Buffer Mix | 4μl |
| 10X RT Enzyme Mix | 2μl |
| Nuclease-free water | 9μl |

The reaction mix was incubated at 44ºC for 60 minutes, 92ºC for 10 minutes, and then hold at 4ºC. cDNA samples were diluted 1 fold with nuclease-free water. Two different PCRs were then performed. A "Tail PCR" with primers flanking the poly(A) tail of a specific gene to measure the length of the tail, and a "UTR PCR" with primers priming within the 3'UTR as a semi-quantitative measure of sample amount. Gene-specific primers were designed to have a Tm of 60ºC. At least 3 different forward primers were designed and tested, and the best one was picked based on amplification efficiency and specificity. The reaction mix and thermo cycle of the PCRs are as follows:

| | Tail PCR | UTR PCR |
|---|---|---|
| Diluted cDNA | 2µl | 2µl |
| 5X PCR Buffer Mix | 5µl | 5µl |
| 10µM Gene-Specific Forward Primer | 1µl | 1µl |
| 10µM Universal Reverse Primer | 1µl | - |
| 10µM Gene-Specific Reverse Primer | - | 1µl |
| 1.25U/µl HotStart-IT Taq DNA Polymerase | 1µl | 1µl |
| Nuclease-free water | To 25µl | To 25µl |

| | | |
|---|---|---|
| 94ºC | 2 minutes | |
| 94ºC | 10 seconds | 30 cycles |
| 60ºC | 30 seconds | |
| 72ºC | 5 minutes | |
| 4ºC | hold | |

PCR products were mixed with loading buffer and run on a 2.5% agarose gel to determine the range of poly(A) tail lengths.

#### 2.2.3.7 Microarray

Total and polysome-bound RNA fractions from polysome fraction of spinal cords were profiled with microarrays (GeneChip Mouse Genome 430A 2.0, Affymetrix) by Stefan Klußman. Input amounts of 5µg and 3µg were used for total and polysome-bound RNA fractions respectively. Details of the following steps consisting of cDNA synthesis, *in vitro* transcription, cRNA purification and fragmentation, microarray hybridisation, washing and staining, could be found in the thesis of Stefan Klußman. The microarray chips were scanned using a HP GeneArray scanner (Affymetrix).

#### 2.2.3.8 Library preparation for whole genome RNA-seq from neuronal processes

**Library preparation by ScriptSeq protocol**

Sample RNAs were first depleted of rRNAs using the Ribo-Zero Magnetic Kit (Epicenter) and purified using AMPure XP beads. The quality of the RNA was then checked using a Bioanalyzer RNA Pico Chip. RNAseq libraries were then prepared using the ScriptSeq v2 RNA-Seq Library Preparation Kit (Epicentre) according to the manufacturer's protocol. Briefly, the rRNA-depleted samples were fragmented and subjected to cDNA synthesis. The resulting cDNA was tagged at the 3' end using a Terminal-Tagging Oligo (TTO). The cDNA was then purified again with AMPure XP beads, and subjected to 15 cycles of PCR amplification with ScriptSeq Index Primers. Finally the amplified cDNA was purified once more with AMPure XP beads, quantified with Qubit and ran on a High Sensitivity Bioanalyzer DNA Chip to access sample amount and quality.

**Library preparation by Smart-seq2 protocol**

RNAseq libraries were prepared using the Smart-seq2 protocol as published in (Picelli et al., 2014). Briefly, 1ng of DNAse-treated RNA from neuronal processes were used as input material. Reverse transcription was performed using SuperScript II reverse transcriptase, an oligo(dT) primer and a locked nucleic acid (LNA)-containing template-switching oligonucleotide. The resulting cDNA was then amplified by 14 cycles of PCR with KAPA HiFi DNA polymerase. Amplified cDNA was then purified by 1x volume of AMPure XP beads, quantified with Qubit and ran on a High Sensitivity Bioanalyzer DNA Chip to access sample amount and quality. 500pg of purified cDNA was then taken for tagmentation and 11 cycles of amplification using the Nextera XT DNA sample preparation kit (Illumina), after which the cDNA is converted into libraries with unique barcodes. After a further cleanup using AMPure XP beads at a ratio of 0.6:1, the cDNA libraries were measured with Qubit and Bioanalyzer to access again the quality and concentration.

**Next generation RNA-sequencing**

A total of 10 libraries were generated, 3 each from developing and regenerating wild type processes, and 2 each from developing and regenerating Cpeb1 knockout processes. 20ng from each library were used to create a multiplex, which is measured again with Qubit and Bioanalyzer to calculate the final molarity.

Sequencing was performed at the DKFZ Genomics and Proteomics core facility. Amplified cDNA libraries were subjected to 100bp paired-end sequencing with Illumina HiSeq 2000. Samples were allocated into 2 lanes so that each sample will exceed the minimal requirement of 30 million reads.

### 2.2.4 Bioinformatics analysis

#### 2.2.4.1 Microarray

Analysis of microarray data was performed by Alvaro Mateos. Array data corresponding to each fraction were normalized separately using the vsn method implemented in the R/bioconductor package vsn (Huber et al., 2002). lts.quantile=0.5 was used to allow robust normalization when many genes are differentially expressed. Differential expression was calculated using limma (Smyth, 2004) from R/bioconductor at the level of probesets. The threshold for significance was set at Benjamini-Hochberg false discovery rate (FDR) < 0.05. Probesets were then translated to Ensembl gene ids (Ensembl v72; www.ensembl.org). Probesets mapping to multiple Ensembl gene ids were excluded from subsequent analysis.

GO enrichment analysis was performed by comparing abundance of annotated GO terms among the up- to the down-regulated genes using the GOstats package (Falcon and Gentleman, 2007) and the annotation package org.Mm.eg.db v2.14.0 from R/bioconductor. The background was defined as the combination of up- and down-regulated groups, while excluding any intersections (when multiple probesets mapping to the same gene show both

up- and down-regulation). Under-representation of up-regulated genes is displayed as enrichment of down-regulated genes.

To perform the enrichment study in the mouse and fly genomes, GO annotations from the R/Bioconductor annotation packages org.Mm.eg.db v2.14.0 and org.Dm.eg.db v2.14.0 were used. Only annotations derived from experimental evidence were used, in order to prevent circularity when annotations derived from homology are used. To prevent artificially inflating the number of motifs when genes have more than one transcript with a common 3'UTR, enrichment analysis was performed at the level of genes.

Cytoscape v3.0.2 (Shannon et al., 2003) was used to visualize the results from the enrichment analysis. Only significant terms (Benjamini-Hochberg FDR < $1^{-4}$) were shown on the GO network, with each node referring to a GO category. The colour represents the direction of enrichment, with the colour intensity and size of the node representing significance of enrichment.

To associate fold changes from transcripts to motifs in their 3'UTR, probesets were translated to Ensembl transcript id (Ensembl v72), and only probesets that map to a single unique transcript were used. 3'UTR sequences were obtained from Ensembl v72 and searched for sequences of the investigated RNA motifs. Distributions of fold change were compared using the Kolmogorov-Smirnov test (http://cran.r-project.org/). To represent the fold change profiles for transcripts from specific GO categories, we used GO annotation at the level of transcript from the R/Bioconductor tool biomaRt.

#### 2.2.4.2 RNA-seq

Computational analysis of RNAseq data was performed in collaboration with Sheng Zhao. Quality of raw reads was checked by FASTQC (http://www.bioinformatics.babraham.ac.uk/projects/fastqc/). Adapter sequences in raw reads were trimmed with Btrim64 (http://graphics.med.yale.edu/trim ) (Kong, 2011). Trimmed reads were then mapped to mouse genome GRCm38 (ENSEMBL v78) using STAR_2.4.0g (Dobin et al., 2013) and quantified with HTSeq 0.6.1p2 (Anders et al., 2014). RNAseq data

quality metrics, such as total number of reads, transcriptome mapped reads and mapping rate were calculated by picard-tools-1.123 (https://broadinstitute.github.io/picard/).

Gene expression matrices were generated as previously described in (Shalek et al., 2013). Briefly, expression level of each gene was quantified by transcript per million (TPM) and fragments per kilobase of transcript per million fragments mapped (FPKM) using RSEM 1.2.18 (Li and Dewey, 2011).

Principal component analysis (PCA) was performed using custom developed R scripts based on FactoMineR library (http://factominer.free.fr/) using counts. GO and KEGG pathway enrichment analysis was performed using the the tool Metascape (http://metascape.org/) with default parameters. Genes with calculated $\log_2$FC > 0.75 or < -0.75 and an adjusted p-value < 0.05 were used as input and the whole genome was used as background. Bonferroni correction of the hypergeometric p-value was used to calculate statistical significance of the enrichment. Upstream Regulator Analysis from Ingenuity (QIAGEN) was used to look for upstream regulators of gene expression, which makes the prediction based on the input gene list and their corresponding fold change.Genes with calculated $\log_2$FC > 0.75 or < -0.75 and an adjusted p-value < 0.05 were used as input, and ran with default parameters.

#### 2.2.4.3 Dynamic analyses of Alternative PolyAdenylation from RNA-Seq (DaPars)

Analysis of alternative polyadenylation (APA) events in the RNAseq data using DaPars (Xia et al., 2014) was performed by Mechthild Lütge.

Briefly, an extended gene model was applied, which extends the 3'UTRs of annotated genes by 10kb until a neighbouring gene is reached. The RNAseq data was then annotated using this model. Each 3'UTR was then scanned in a 5' to 3' direction, and a drop in reads coverage, defined as having < 5% of the coverage of the previous exon, is considered as a distal polyA site. A regression model is then used to identify the location of a proximal polyA site. Relative poly(A) site usage is indicated by Percentage of Distal poly(A) site Usage Index (PDUI), which is calculated by:

$$\mathrm{PDUI} = \frac{W_L}{W_L + W_S}$$

Where $W_L$ and $W_S$ are the estimated expression levels of transcripts with usage of distal and proximal poly(A) site respectively. Statistical test for significance for differential polyA site usage between conditions is performed using Fisher's exact test and adjusted using Benjamini-Hochberg false-discovery rate (FDR). APA is considered to occur in a gene between two conditions (X and Y) when a) FDR ≤ 0.05; b) $|PDUI_X - PDUI_Y| \geq 0.2$ ; and c) $|\log_2\left(\frac{PDUI_X}{PDUI_Y}\right)| \geq 1$

### 2.2.5 Statistical analyses

Statistical tests used varied according to the type of data and are specified in the respective figures. All analyses were performed in Prism 5.0 (Graphpad) or in R (http://cran.r-project.org/).

# 3. Results

## 3.1 Uncoupling of transcription and translation in injury response of the CNS

### 3.1.1 Widespread uncoupling between transcriptional and translational responses to SCI

To simultaneously profile the transcriptional and translational response to neuronal injury in the mammalian CNS, translational state array analysis (TSAA) was performed in our group by Stefan Klußmann (Fig. 8A). A time point of 9 hours after SCI was chosen, which is during the early phase after injury where axons are attempting to regenerate (Cajal et al., 1991; Kerschensteiner et al., 2005). The time point is also desirable as the infiltration of immune cells is still limited (Gadani et al., 2015; Hausmann, 2003), and that there is enough time for transcriptional and translational changes to take place (Schwanhäusser et al., 2011). TSAA was performed by isolating total and polysome-bound RNAs from the same injured or naïve spinal cords. Polysome-bound RNAs were isolated by sucrose gradient fraction (Lou et al., 2014) and collecting fractions that contain more than one ribosome. The different pools of sample RNAs were then subjected to microarray analysis. Changes in the total RNAs and polysome-bound RNAs represent changes in mRNA abundance and ribosome-loading respectively. Bioinformatics data analysis was performed by Alvaro Mateos.

As expected, a large number of genes were found to be differentially expressed upon SCI (Fig. 8B). In the total RNA fraction, there are slightly more genes that are up-regulated than down. In the polysome-bound RNA fraction, there are a lot less differentially regulated genes, with the majority of them being down-regulated. This agrees with the notion that upon stress, there is a general shut down of translation to maximise cell survival (Park et al., 2008; Yamasaki and Anderson, 2008). For many genes, there is a discrepancy between the direction of change in mRNA abundance and ribosome loading (Fig. 8C and D), and the correlation between the two is low ($R = 0.036$). This suggests strong and widespread uncoupling between transcriptome and translatome response of SCI.

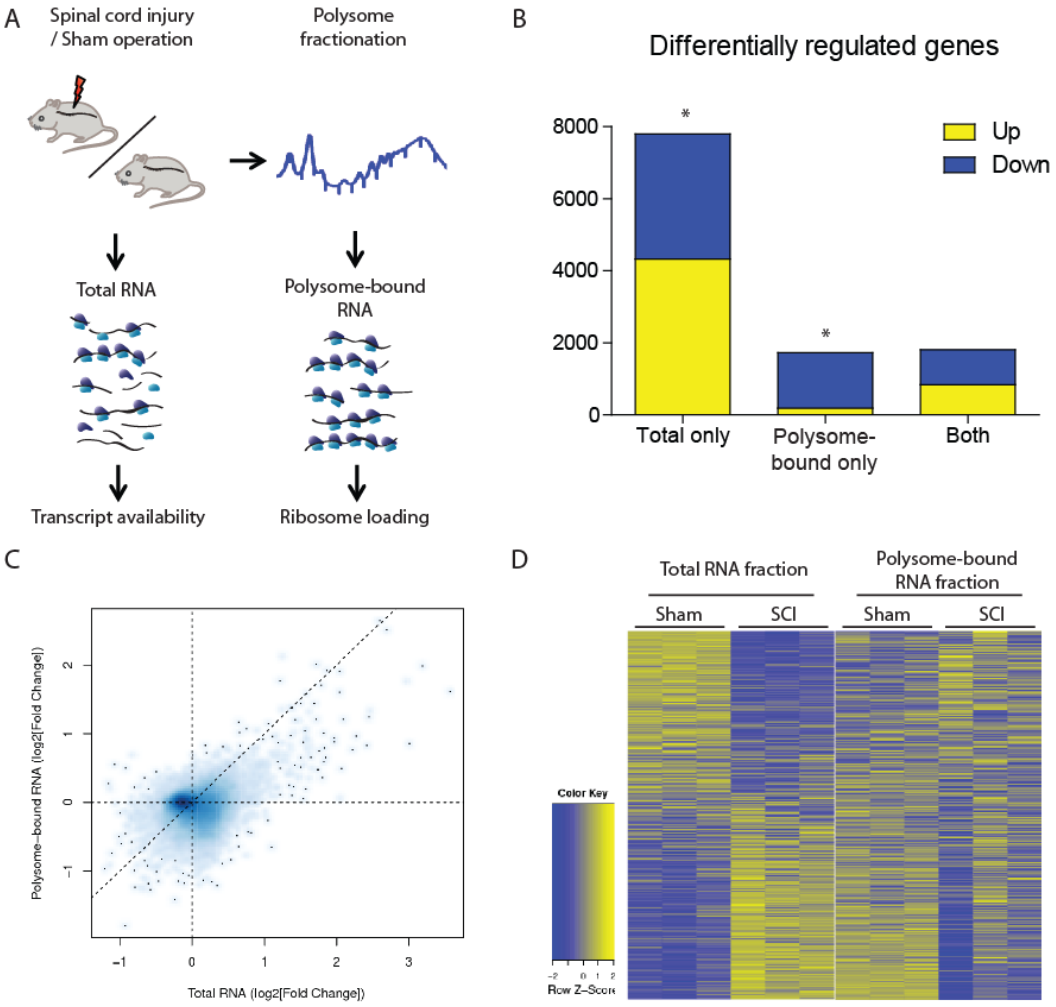


Figure 8: Spinal cord injury induces uncoupled changes in mRNA abundance and ribosome loading. A) Experimental scheme of TSAA of mouse naïve and injured spinal cord. n=3 mice per group. B) Number of differentially expressed genes upon injury in mouse spinal cord from different RNA fractions with false discovery rate (FDR) < 0.05. Chi-square of distribution of up- and down-regulated genes in total and polysome-bound RNA fractions: $p < 0.0001$. C) Fold changes in total and polysome-bound RNA upon spinal cord injury. D) Heat map representation of gene expression with z-score in total and polysome-bound RNA from naïve and injured mice spinal cords. Each column represents one biological replicate and each row represents the same gene across lanes. (Data by Stefan Klußman and Alvaro Mateos)

### 3.1.2 Functional clustering of uncoupled genes

To investigate the functional relevance of this uncoupling effect, Gene Ontology (GO) analysis (Ashburner et al., 2011) was performed for biological processes (BP) GO categories

and visualized using Cytoscape (Shannon et al., 2003). The different pattern of GO enrichment of up- and down-regulated genes in the total and polysome-bound RNA fractions suggests that uncoupling is functionally relevant (Fig. 9). mRNA abundance for genes related to RNA processing and splicing, ribosome biogenesis, translation and protein localisation were increased upon SCI; and genes related to CNS development, neurogenesis, neuron differentiation and cytokine responses were decreased (Fig. 9A). On the other hand, ribosome loading for genes related to inflammatory and cytokine response, cell death regulation and transcription was increased (Fig. 9B). Interestingly, no enrichment of down-regulated genes in ribosome bound RNAs was observed, suggesting the decrease in translation is a general effect and not specific to any particular function. Of particular note, CNS development genes have reduced mRNA abundance upon SCI but their ribosome loading remained similar. This suggests a preferential translation of these genes, possibly underlying the temporary regeneration at this phase after SCI. The down-regulation of mRNA abundance could explain the later termination of regeneration, as these mRNAs are not replenished when they reach the end of their lifespan.

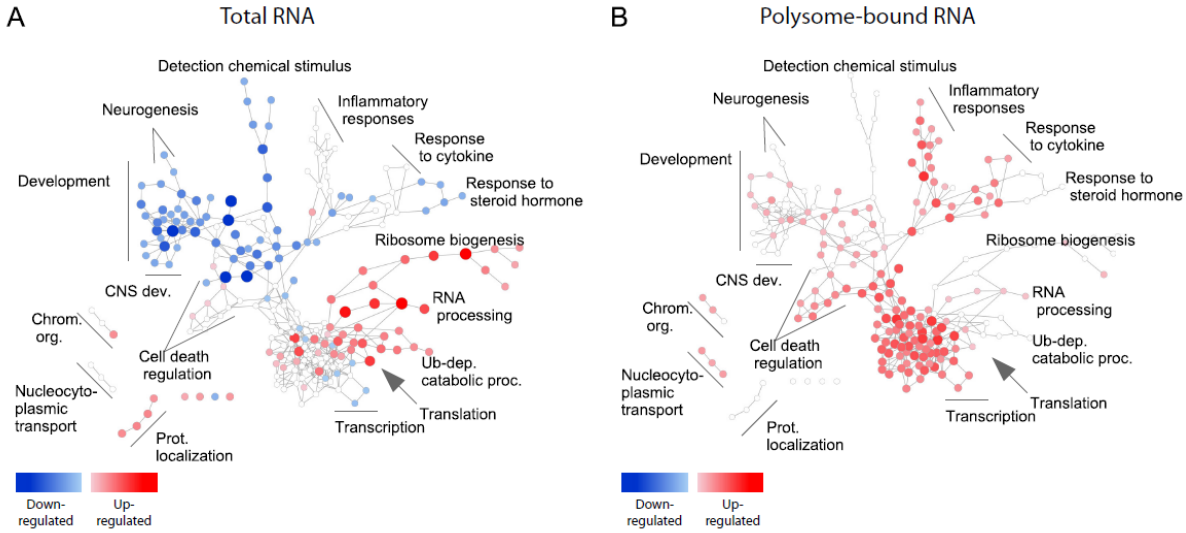


Figure 9: Functional clustering of the injury response in the A) total and B) polysome-bound RNA fractions. Each node represents one GO category. Enrichments of up- and down-regulated- genes are indicated as red and blue nodes respectively. Colour intensity and size of the node represent significance by FDR. (Data by Stefan Klußman and Alvaro Mateos)

### 3.1.3 Uncoupled genes regulate axonal growth in Drosophila

To investigate if transcripts exhibiting this uncoupled behaviour do indeed affect axonal growth, a screening of axonal growth following exogenous expression of candidate genes was performed in Drosophila by Marta Koch in the group of Bassem Hassan in VIB, Belgium. A list of 38 candidate genes that exhibited uncoupling after SCI, and for which a fly homologue exists and a UAS line was available, was chosen. These genes were expressed in the small ventral lateral neurons (sLNvs), a population of CNS neurons in the fly brain, using the UAS-Gal4 system (Brand and Perrimon, 1993). Most of these genes have reduced mRNA abundance but similar ribosome loading upon spinal cord injury (Table 6). It was discovered that 19 (50%) tested candidates influenced the developmental growth of the sLNv axonal projection, from which 12 increased the outgrowth and 7 had a negative effect (Fig. 10 and Table 6). The high proportion of uncoupled genes influencing axonal outgrowth supports the notion that uncoupling is functionally related to axonal regeneration.

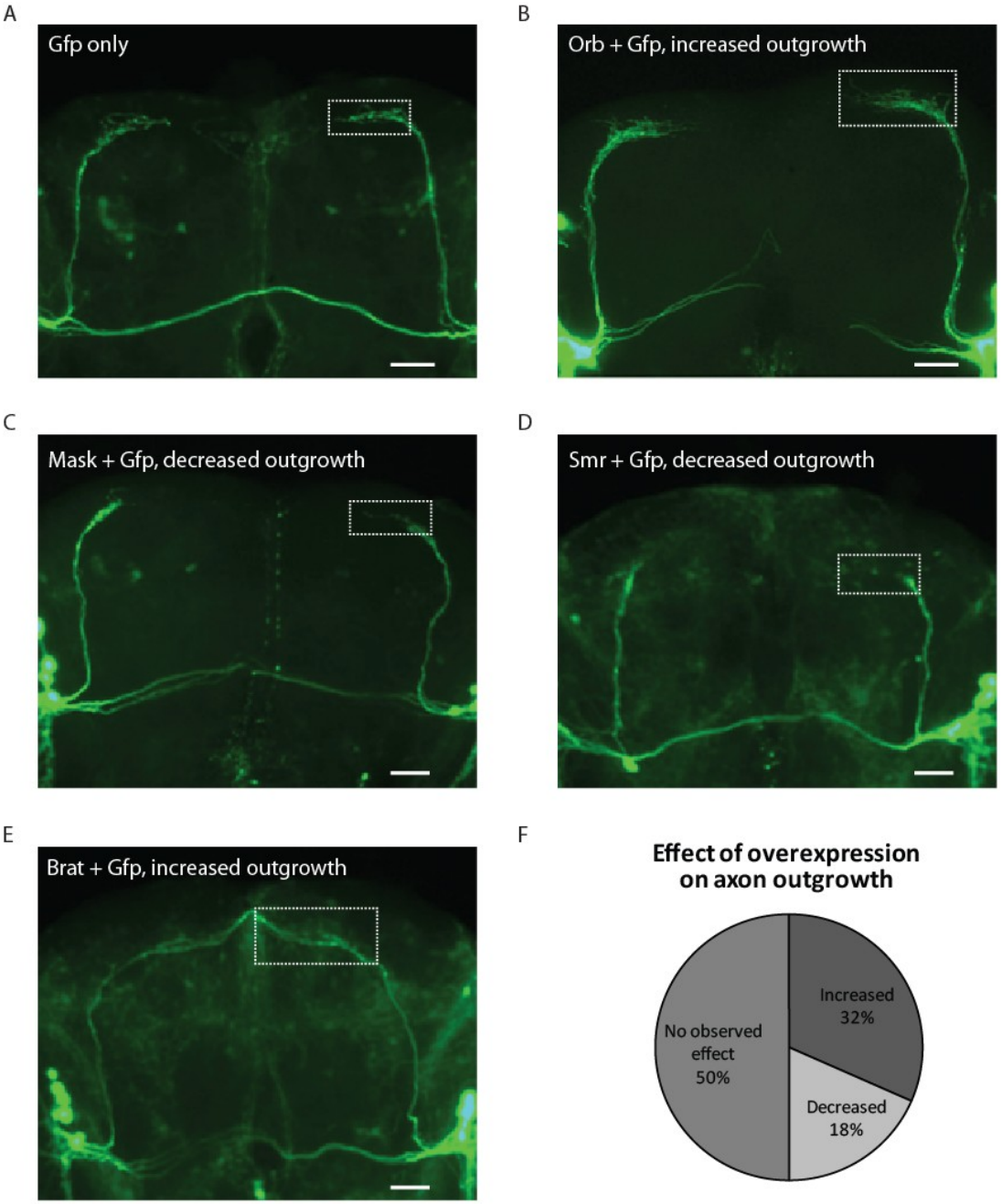


Figure 10: Overexpression of uncoupled genes modifies axonal outgrowth in Drosophila sLNv neurons. A-E) Representative pictures of Drosophila brain slice cultures with sLNv neurons overexpressing the indicated genes, and the grade given for the degree of axonal outgrowth. F) Number of genes inducing increased, decreased or no change in axonal outgrowth. A minimum of 5 brains were quantified per genotype. Scale bars: 50µm. (Data by Marta Koch)

| | | SCI/Naïve fold change | | Phenotype in Drosophila overexpression |
|---|---|---|---|---|
| **Mouse gene symbol** | **Fly gene symbol** | **total RNA fraction** | **polysome-bound RNA fraction** | **Axonal outgrowth** |
| Ankhd1 | mask | -0.304 | 0.342 | decreased |
| Anp32a | Mapmodulin | -0.075 | 0.494 | decreased |
| Bbx | bbx | -0.363 | 0.149 | decreased |
| Lphn1 | Cirl | -0.023 | 0.273 | decreased |
| Ncor1 | Smr | -0.264 | 0.347 | decreased |
| St13 | CG2947 | -0.055 | -0.109 | decreased |
| Tenm3 | Ten-m | -0.026 | 0.218 | decreased |
| Cdc25a | stg | -0.092 | 0.190 | increased |
| Cpeb1 | Orb | 0.257 | -0.334 | increased |
| Eif3c | eIF3-S8 | 0.149 | 0.271 | increased |
| Prkacb | Pka-C1 | -0.308 | 0.165 | increased |
| Rad50 | rad50 | 0.079 | 0.111 | increased |
| Rbfox2 | CG32062 | -0.209 | 0.148 | increased |
| Rhou | Cdc42 | 0.533 | 0.513 | increased |
| Sfswap | su(wa) | -0.331 | -0.094 | increased |
| Trim family | Brat | NA | NA | increased |
| Txnrd1 | Trxr-1 | 0.020 | 0.428 | increased |
| Wnk1 | CG7177 | -0.254 | 0.431 | increased |
| Ywhaz | 14-3-3ζ | 0.274 | -0.270 | increased |
| Atrx | XNP | -0.343 | 0.192 | no observable effect |
| Aurka | Aur | -0.064 | 0.109 | no observable effect |
| Bptf | e(Bx) | -0.062 | 0.381 | no observable effect |
| Brd2 | fs(1)h | -0.038 | 0.555 | no observable effect |
| Chd4 | Mi-2 | -0.279 | 0.362 | no observable effect |
| Ctcf | CTCF | -0.085 | 0.126 | no observable effect |
| Eif2c2 | Ago1 | NA | NA | no observable effect |
| Gnrhr | GRHR | -0.173 | 0.029 | no observable effect |
| Kif5b | Khc | -0.120 | 0.050 | no observable effect |
| Lpin2 | CG8709 | -0.174 | 0.284 | no observable effect |
| Magi2 | Magi | -0.560 | 0.316 | no observable effect |
| Mll3 | CG5591 | -0.848 | -0.016 | no observable effect |
| Naa15 | Nat1 | 0.314 | 0.099 | no observable effect |
| Nedd4 | Nedd4 | -0.246 | -0.072 | no observable effect |
| Nr4a2 | Hr38 | 0.079 | 0.032 | no observable effect |
| Rest | crol | -0.309 | 0.126 | no observable effect |
| Trip12 | CG17735 | 0.075 | 0.228 | no observable effect |

| | | | | |
|---|---|---|---|---|
| Vps35 | CG5625 | 0.044 | 0.009 | no observable effect |
| Wdfy3 | bchs | -1.076 | 0.547 | no observable effect |

Table 6: List of genes screened for effects on Drosophila sLNv axonal outgrowth and fold changes in TSAA. (Data by Marta Koch and Stefan Klußman)

## 3.2 Identification of RNA motifs that regulates uncoupling behaviour

### 3.2.1 Association of 3'UTR motifs with smaller reductions in mRNA abundance upon SCI

In order to uncover the mechanisms of post-transcriptional regulation leading to uncoupling behaviour of transcripts, the association of common features in the 3'UTR of the mRNA to its expression in the RNA fractions from TSAA was investigated. Many regulatory motifs reside within the 3'UTR and govern the dynamics of the mRNA, such as degradation, transport and translation (Moore, 2005; Szostak and Gebauer, 2013). In addition, many neuronal mRNAs crucial to axon physiology such as Gap43, β-actin, Map2 and Bdnf are regulated via their 3'UTRs (Blichenberg et al., 1999; Donnelly et al., 2011; Lau et al., 2010). The analysis has to be performed on the transcript level, since transcript variants of the same gene can have different 3'UTRs. To this end, data from probesets that map to only one transcript was used.

The motifs studied here are the cytoplasmic polyadenylation element (CPE), Pumilio binding element (PBE), Musashi binding element (MBE), and the hexanucleotide (Hex) which is involved in polyadenylation. The change in mRNA abundance after SCI was more positive for mRNAs that contain the studied motifs versus those that do not (Fig. 11A). Specifically, mRNAs that do not possess the motif in question suffer a greater decrease in the total RNA fraction than those that do possess it. In contrast, no significant difference is observed in changes in the polysome-bound fraction upon SCI (Fig. 11B). To ensure that this is not an artefact, the analysis was repeated using the same motifs but on the 5'UTR (Fig. 12A) or random sequences between 5 and 9 base pairs long (Fig. 12B), and no association with changes in mRNA abundance was observed. These results suggest that these motifs within the 3'UTR confer increased transcript stability upon injury.

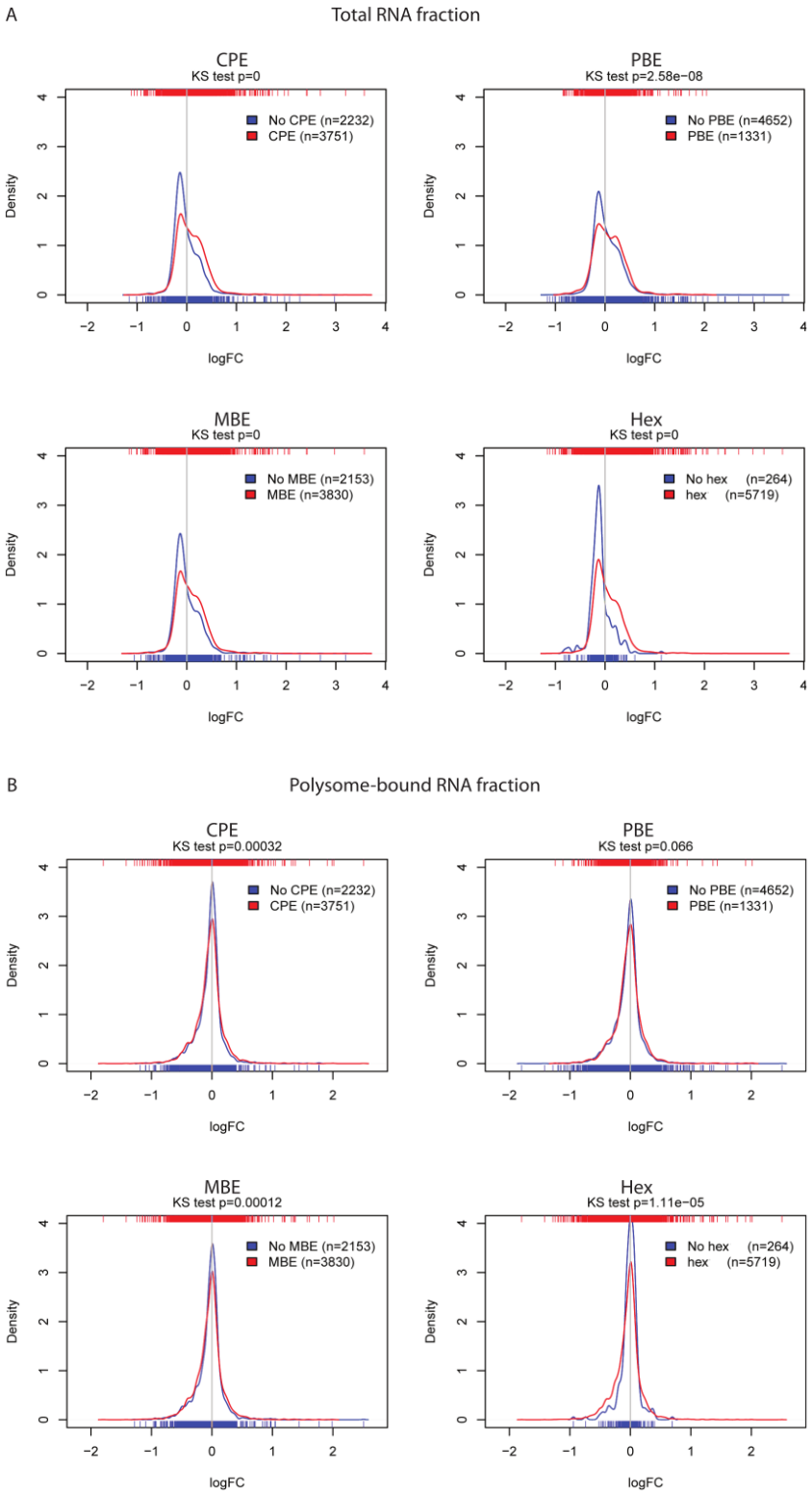


Figure 11: Transcripts possessing specific motifs in their 3'UTR have higher mRNA abundance upon spinal cord injury. Density plot of fold changes in the A) total and B) polysome-bound RNA fraction of transcripts possessing the indicated motifs versus those that do not. Comparison of similarity between curves: Kolmogorov-Smirnov test. (Data by Stefan Klußman and Alvaro Mateos)

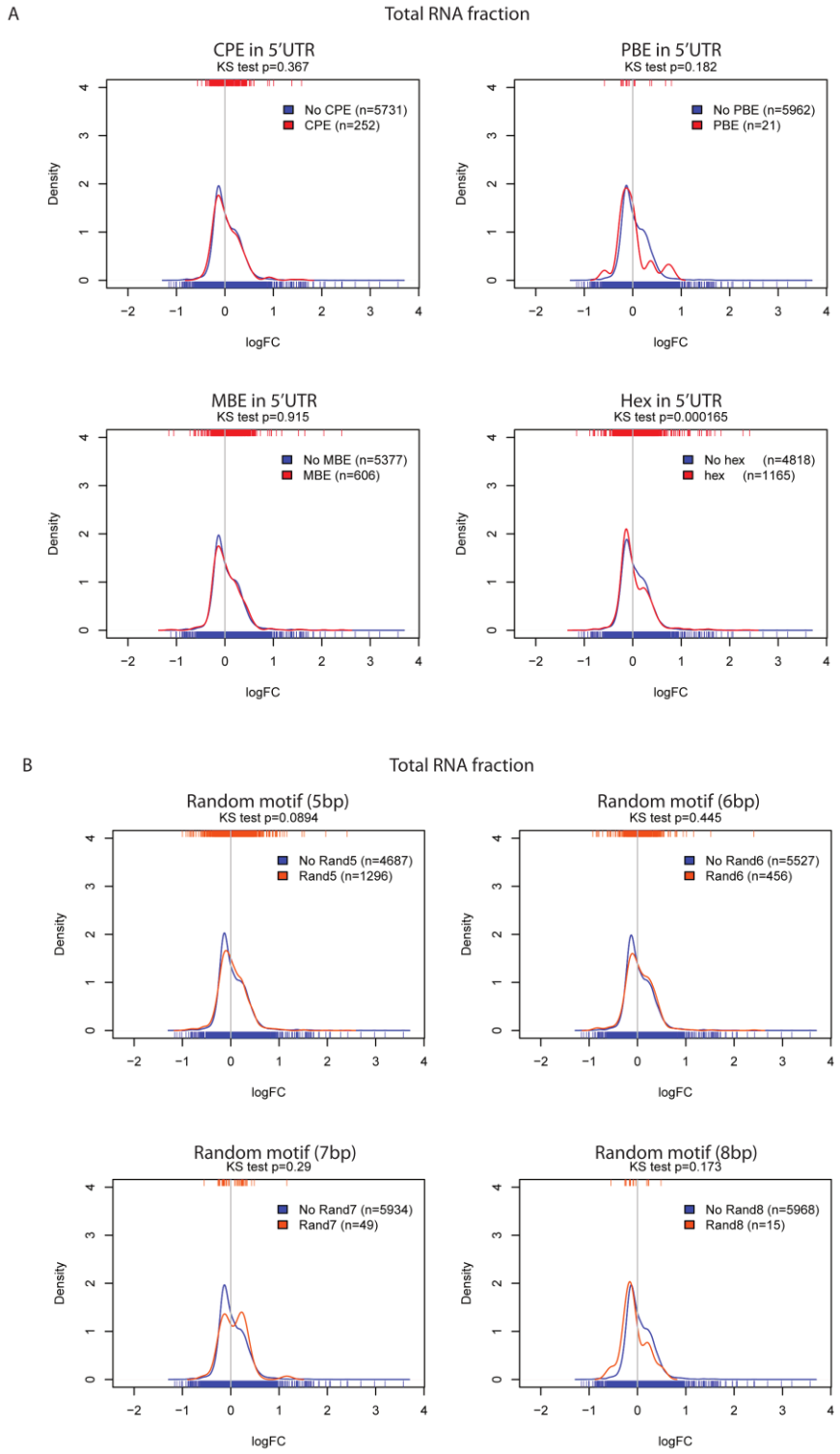


Figure 12: Lack of association of motifs in the 5'UTR and random motifs towards changes in mRNA abundance. A) Density plot of fold changes in the total RNA fraction of transcripts possessing the indicated motifs in the 5'UTR versus those that do not. B) Density plot of fold changes in the total RNA fraction of transcripts possessing the indicated random motifs in the 3'UTR versus those that do not. Comparison of similarity between curves: Kolmogorov-Smirnov test. (Data by Stefan Klußman and Alvaro Mateos)

### 3.2.2 Association of CPE with smaller reductions in mRNA abundance upon SCI in regeneration and mRNA processing genes

Special attention was paid to CPE, as it has been shown to play a role in neuron physiology, including synaptic plasticity and dendritic transport (Hake and Richter, 1994; Lin et al., 2009; Wu et al., 1998), and its exogenous expression increases axonal outgrowth in Drosophila sLNv (Fig. 10B). To investigate this in depth, the association of CPE with differential expression in the total RNA fraction was repeated in specific GO categories. The association of CPE with a smaller decrease in mRNA abundance upon SCI was found to be conserved for transcripts of genes related to CNS development, axon development and cell morphogenesis (Fig. 13A). This effect is likewise not observed in ribosome loading (Fig. 13B). In addition, for RNA processing categories, transcripts containing CPE show a general increase upon injury, compared to the stable level of those that do not. This agrees with a recent study that RNA repair and splicing pathways regulate axon regeneration (Song et al., 2015).

To address this, the motif analysis was also performed for AU-rich elements (AREs), which regulate RNA degradation or stability. In a similar manner to CPE, transcripts containing AREs are less down-regulated in the total RNA fraction following injury (Fig. 14A). Also CPE and AREs were found to co-occur in the mouse transcriptome, suggesting the two motifs function in conjunction with each other (Fig. 14C). Transcripts possessing both elements likewise show higher changes in mRNA abundance than those that do not (Fig 14D). Taken together, this data suggests that CPE confers stability in mRNA abundance against the global decrease induced by SCI, possibly by increasing RNA stability in conjunction with AREs.

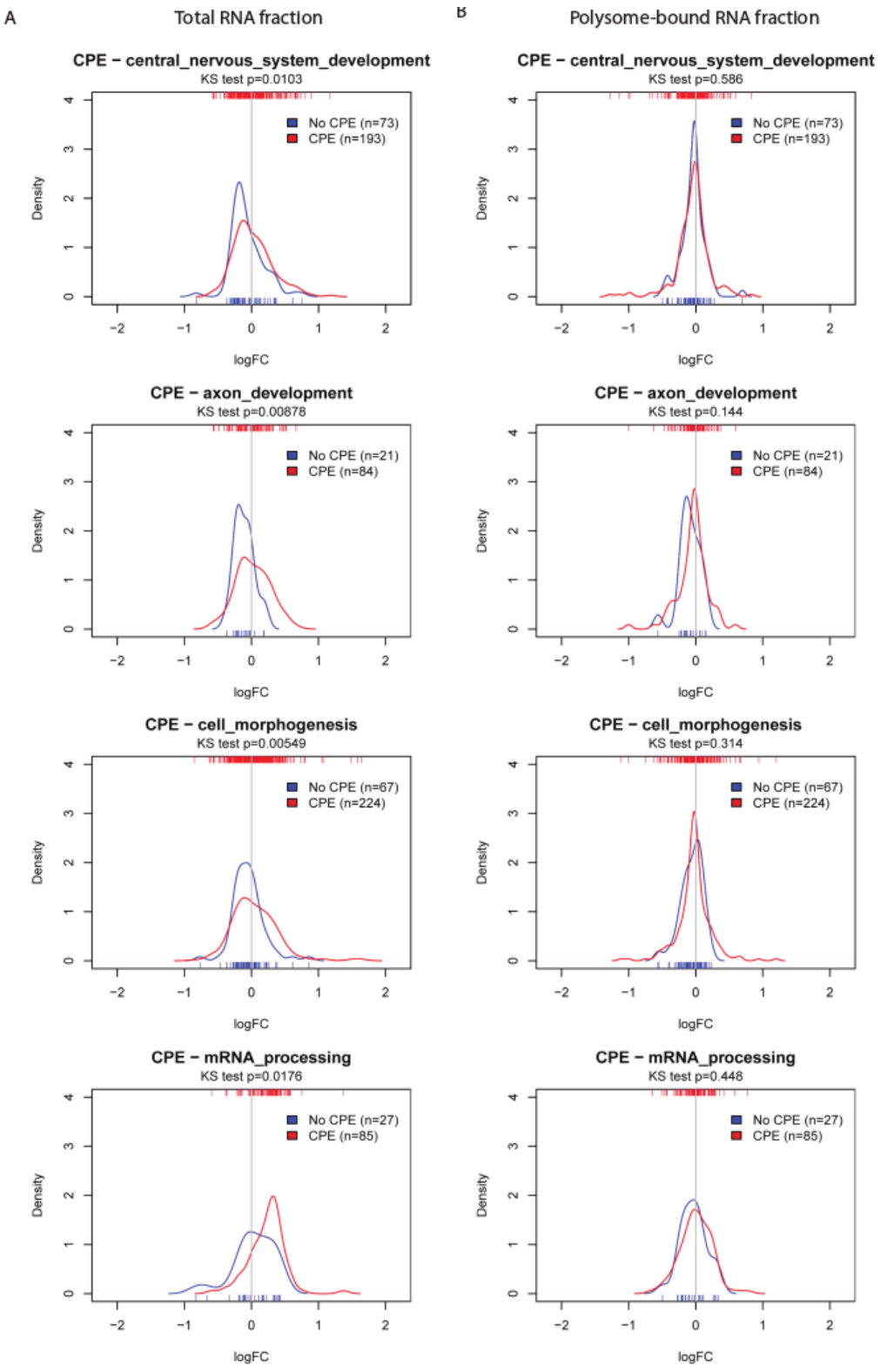


Figure 13: Transcripts possessing CPE in the 3'UTR have higher mRNA abundance in GO categories of CNS development, axon development, cell morphogenesis and mRNA processing. Density plot of fold changes in the A) total and B) polysome-bound RNA fraction of transcripts with and without CPE in their 3'UTR. Comparison of similarity between curves: Kolmogorov-Smirnov test. (Data by Stefan Klußman and Alvaro Mateos)

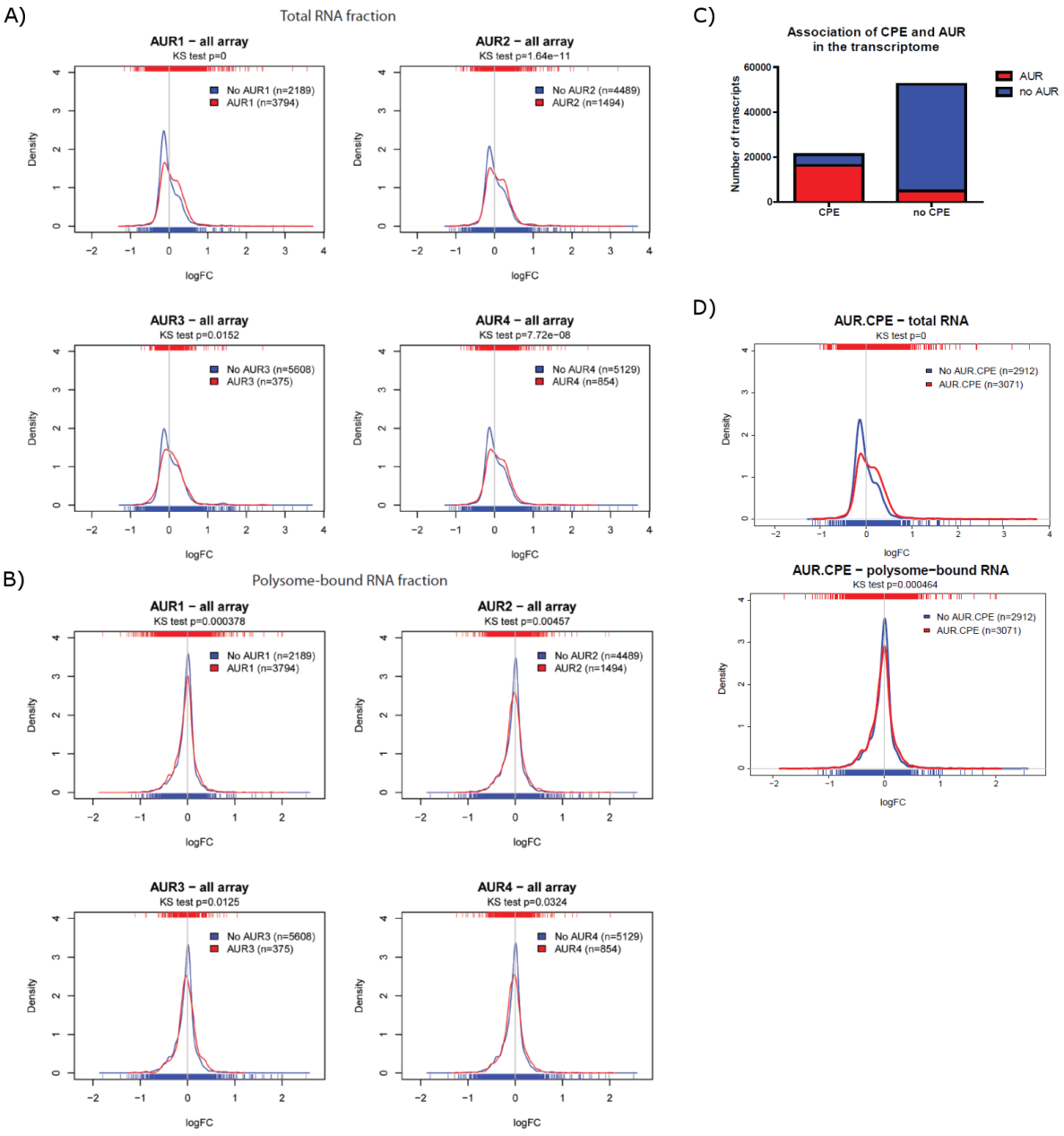


Figure 14: AREs are associated with CPE and a lesser decrease in fold change in the total RNA fraction after spinal cord injury. A) Density plot of fold changes in the total RNA fraction of transcripts possessing the indicated ARE versus those that do not. B) Density plot of fold changes in the polysome-bound RNA fraction of transcripts possessing the indicated ARE versus those that do not. C) Number of transcripts harbouring CPE and AUR in the whole transcriptome. Chi-square test of distribution: $p < 0.0001$. D) Density plots of fold changes in the total and polysome-bound RNA fractions of transcripts possessing both AUR and CPE versus those that do not. Comparison of similarity between curves: Kolmogorov-Smirnov test. (Data by Stefan Klußman and Alvaro Mateos)

### 3.2.3 Conserved enrichment of CPE in nervous system development genes between mouse and Drosophila genomes

In order to investigate the general role of CPE, GO enrichment analysis was performed on protein coding genes of the mouse and fly genomes. Only GO annotations based on experimental evidence were used, in order to exclude annotations derived from evolutionary homology which will create circularity when comparing two species. Of the categories enriched for CPE containing genes, many relate to nervous system development, including neuron projection morphogenesis, axonogenesis and axon guidance (Fig. 15A). In Drosophila, CPE-enriched categories are more prevalent, and the association with nervous system development genes is stronger (Fig. 15B). Interestingly, CPE-enriched categories encompass almost all of those enriched in the mouse genome, suggesting a high level of conservation of CPE function between the two species.

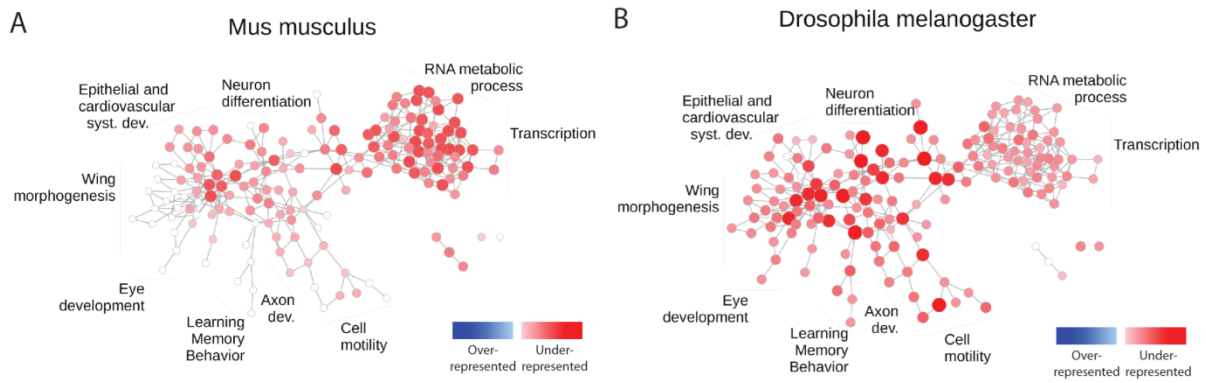


Figure 15: Functional clustering of CPE containing genes in the mouse and Drosophila genomes. Each node represents one GO category. Over- and under-representation is represented as red and blue respectively. Colour intensity and size of the node represent significance. (Data by Alvaro Mateos)

## 3.3 Cpeb1 is a conserved enhancer of neuronal regeneration

### 3.3.1 Lack of satisfactory Cpeb1 antibodies limits potential experiments

Since CPE is associated with axon regeneration and regulation of RNA dynamics, the next logical step would be to study Cpeb1 expression in neurons and localisation to growth cones, and to identify target mRNAs of Cpeb1. Immunohistochemical staining of transected spinal cords shows enriched signal in the tips of severed axons from wild-type mice (Fig. 16A). However, subsequent validations on brains from Cpeb1 full knockout mice, also using other antibodies, showed that the staining is non-specific (Fig. 16B and C). Despite a number of antibodies against Cpeb1 being available commercially or otherwise, none of them are satisfactory, showing no or highly unspecific immunoreactivity. This likewise renders RNA immunoprecipitation experiments unreliable (data not shown). This is intriguing as these antibodies were raised using peptides from different regions of Cpeb1. This could be due to the conformation of Cpeb1 being delicate or unstable, or having a high similarity with other proteins. Studies conducted so far on Cpeb1 in neurons mostly made use of RNA in situ hybridization or Cpeb1-Gfp fusion proteins (Wilczynska, 2005; Lin, 2009).

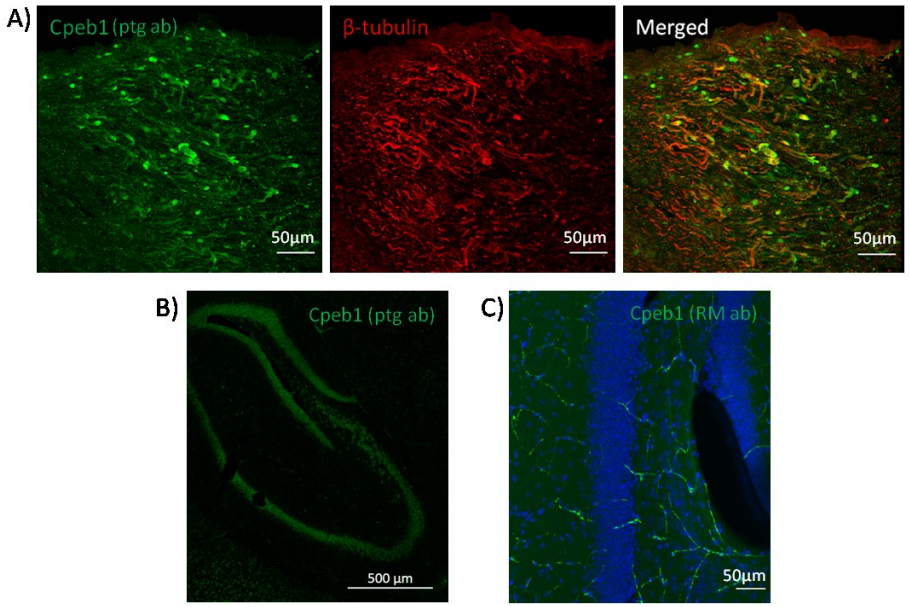


Figure 16: Stainings with Cpeb1 antibodies. A) Proximal end of wild-type transected spinal cord 9 hours after injury. B and C) Dendate gyrus stainings from Cpeb1 full knockout mice. ptg ab: antibody from ProtinTech; RM ab: antibody provided by the group of Raúl Méndez.

### 3.3.2 Generation of Cpeb1 knockout mouse neuronal cultures

In order to investigate the effects of Cpeb1 in mammalian CNS regeneration, a system inducing deletion of Cpeb1 in primary cultures of mouse embryonic cortical neurons was established. Transgenic mice with exon4 of Cpeb1 floxed were obtained from the group of Raúl Méndez. Cre-mediated recombination will remove the floxed exon, introducing a frameshift. Domains affected by the frameshift include the RNA recognition motifs (RRMs) and activating phosphorylation site, which would cripple the essential functions of the protein. Cre was introduced via AAV of serotype 2 expressing a Cre-Gfp fusion protein under a CAG promoter, which was produced in collaboration with Elena Senis from the group of Dirk Grimm in the University of Heidelberg.

Neuronal cultures were prepared from cortices of E16.5 mouse embryos and plated on poly-L-lysine treated surfaces (Kaech and Banker, 2006), and experiments were performed between 6 to 8 days in culture, when the neurons have matured. Due to potentially high stability of Cpeb1 protein when involved in RNP complexes, infection was performed as early as possible. To achieve this, initially AAVs were injected *in utero* to the ventricles of E14.5 embryos and Gfp-expressing cells from the cortex were isolated at E16.5. However Gfp positive cells were found to be very dispersed in the cortex (Fig. 17A). An attempt was made to isolate these cells with FACS sorting. However the Gfp positive population constituted only about 0.5% of the total population and were too few for any experiments (data not shown). Subsequently, infections were performed *in vitro* during neuron plating. A range of moiety of infection (MOI) was tested for infection efficiency. The lowest MOI that produces a near complete infection was determined to be $1x10^5$. PCR with primers flanking exon4 indicated high efficiency of deletion (Fig. 17B).

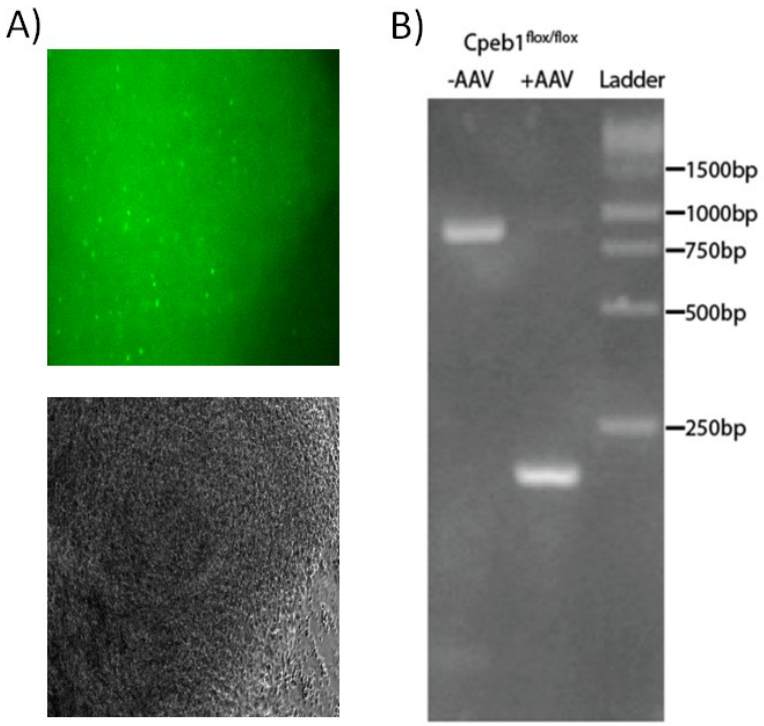


Figure 17: Efficiency of different strategies to produce Cpeb1 knockout neurons. A) Gfp signal from infected cells within E16.5 cortices with AAV-CAG-Cre-Gfp injected into ventricles at E14.5. B) Efficient deletion of Cpeb1 as detected by PCR from DIV6 cultured cortical neurons, with or without addition of AAV during plating. Expected sizes: floxed: 884bp; deleted: 186bp

### 3.3.3 Knockout of Cpeb1 inhibits regeneration in processes of mouse cortical neurons

Regrowth assay was initially performed on primary cultures of embryonic cortical neurons grown on glass cover slips. A glass capillary was drawn across cover slips at 6 days *in vitro* (DIV) to induce injury. The scratched area was imaged 24 hours later, and neuronal processes that have regrown into the tract were traced and measured (Fig. 18A-C). The number and length of the regenerated processes were not found to be significantly different between Cpeb1 knockout and wild-type neurons (Fig. 18D and E). However this model was found to be too variable, as it is hard to precisely determine the position of the cut and where regeneration starts. Also the presence of debris, from cells destroyed from the scratching, influences image quality and tracing.

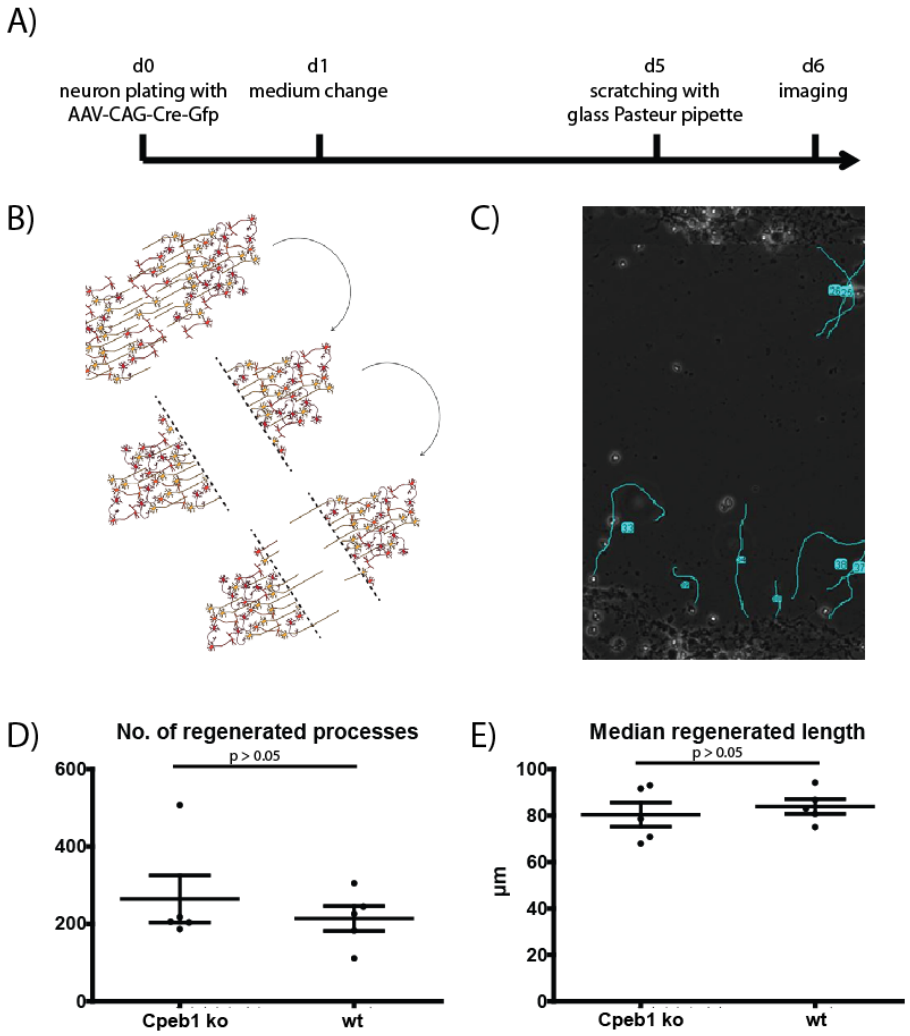


Figure 18: Regrowth assay using cover slips. A) Timeline of experimental setup. B) Schematic representation of inducing neuronal injury via scratching. C) Representative image of the scratched area and regenerated processes that were being traced. D and E) Number and median lengths of regenerated processes were not significantly changed. Each dot represents one cover slip. n = 5 per group. wt: wild-type + AAV; ko: Cpeb1$^{flox/flox}$ + AAV. Statistical analyses: Mann-Whitney. Error bars: mean +/- S.E.M.

Another approach based on transwell chambers was thus used, where neuronal processes can grow to the underside of the chamber via pores on the membrane (Fig. 19). Injury was induced at 7 DIV by gently scraping the underside with a cotton swab and imaging was performed 24 hours after injury. Calcein AM, a live cell dye, was applied 1 hour before to facilitate imaging (Fig. 19A). The processes were traced with an ImageJ macro provided by Damir Krunic from the DKFZ Light Microscope Core Facility. Deletion of Cpeb1 was found

to reduce the number of regenerated processes in knockout neurons (Fig. 20B). In addition, the lengths of regenerated processes were also reduced (Fig. 20C).

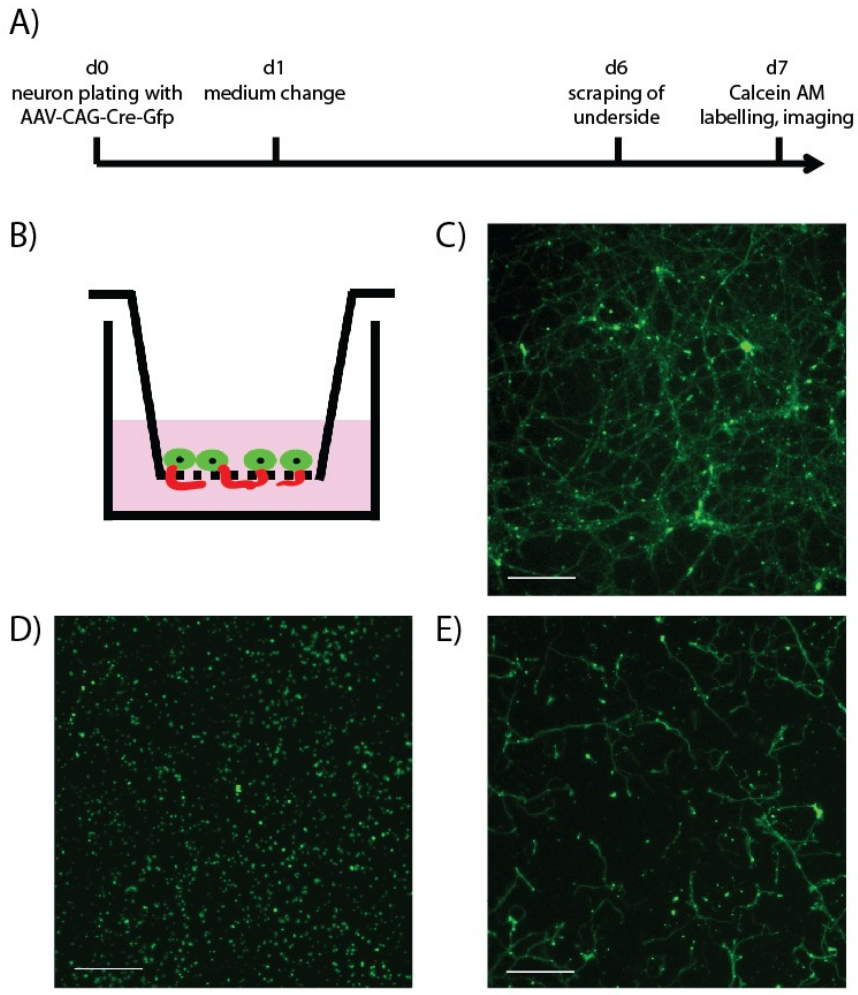


Figure 19: Establishing regrowth assay with transwell chambers. A) Timeline of experimental setup. B) Schematic representation of culturing neurons in a transwell culture insert. C-E) Representative images of the underside of the transwell chamber with processes labelled by Calcein AM C) before, D) right after and E) 24 hours after scraping. Dots are signal from the upper side passing through pores on the membrane. Scale bars: 100µm

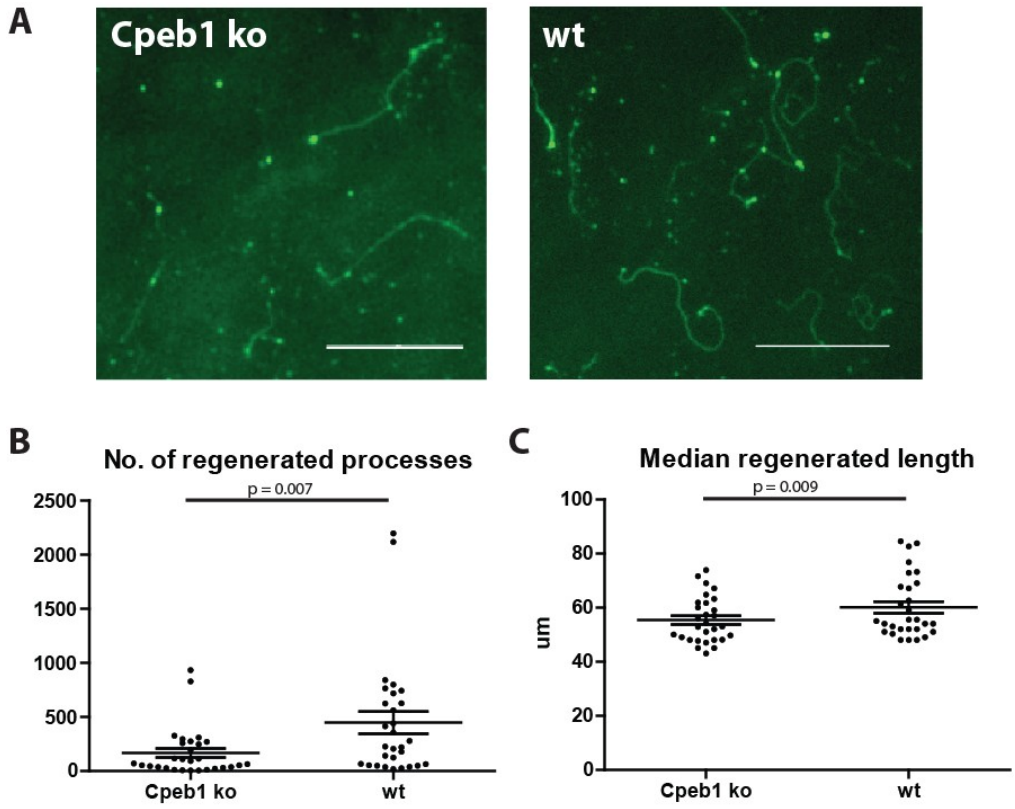


Figure 20: Knockout of Cpeb1 impairs regeneration in mouse cortical neurons. A) Representative images taken from the lower side 24 hours after injury. F,G) Number and median length of regenerated processes are decreased upon Cpeb1 knockout. Each data point represents one culture chamber. n=29 per group. Cpeb1 ko: Cpeb1$^{flox/flox}$ + AAV; wt: wild-type + AAV. Scale bars: 100µm. Statistical analyses: Mann-Whitney. Error bars: mean +/- S.E.M.

### 3.3.4 Expression of Cpeb1 in Drosophila sLNv neurons increases axonal regeneration

A regrowth assay was also performed in Drosophila sLNv neurons by Marta Koch from the group of Bassem Hassan. Brain slice cultures were prepared from flies with exogenous expression of Orb in sLNvs, whose axons were lesioned mechanically injured and the regenerative response was quantified after four days (Ayaz et al., 2008) (Fig. 21A). Overexpression of Orb was found to increase both the number and length of sprouts following axonal injury (Fig. 21B-D).

Together, data from the genome enrichment of Cpeb1 and regrowth assays in mouse and fly suggests that Cpeb1 enhances neuronal regeneration, and that this function is conserved across species.

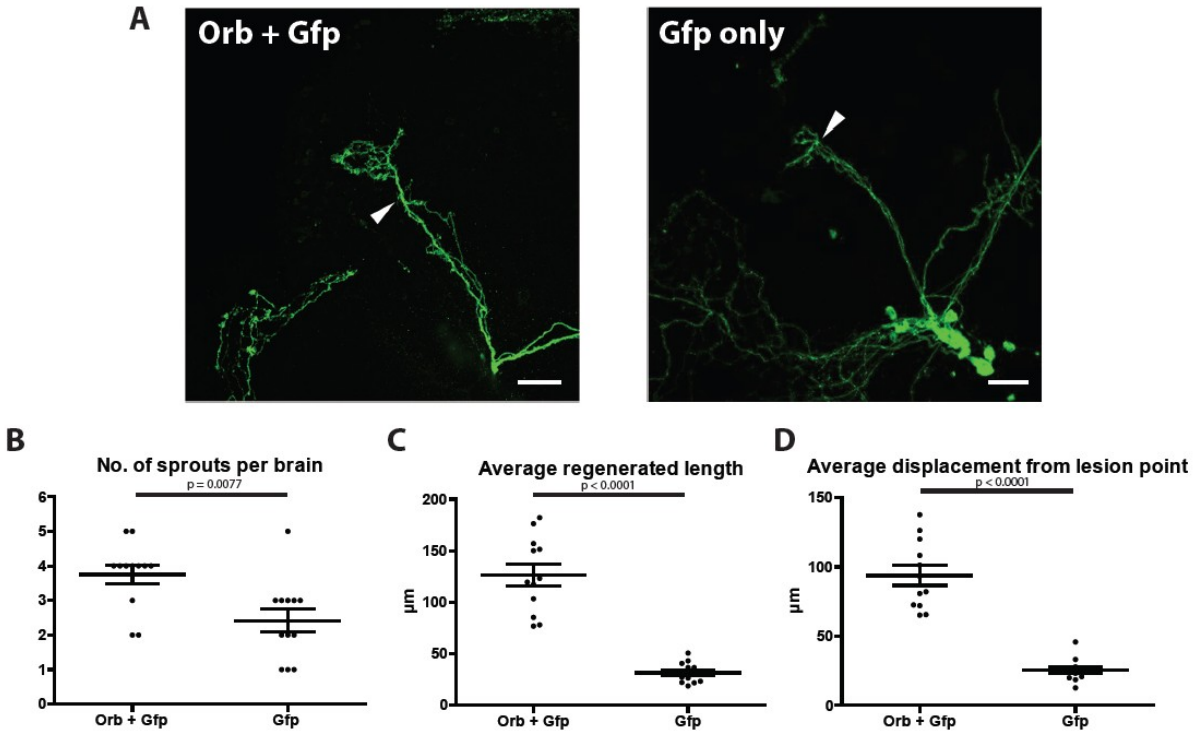


Figure 21: Exogenous expression of Orb (Cpeb1 homolog) enhances axonal regrowth in Drosophila sLNv neurons. A) Representative images of sLNv neurons 4 days after axotomy. Arrowheads indicate lesion points. B-D) Number, length and displacement from lesion point of regenerated axon sprouts are increased upon Orb expression. Each data point represents one brain slice from one fly. n=13 (flies) for Orb+Gfp and 12 for Gfp only. Scale bars: 30µm. Statistical analyses: Mann-Whitney. Error bars: mean +/- S.E.M. (Data by Marta Koch)

## 3.4 Cpeb1 mediates the transcriptome response of neuronal injury

### 3.4.1 RNA sequencing of injured and naïve processes from Cpeb1 knockout neurons

Previous data has shown that changes in mRNA abundance are associated with regeneration after SCI, and that Cpeb1 likely plays an essential role therein. As a result we investigated

changes in global mRNA abundance after injury specifically in neuronal processes, as well as the effect of Cpeb1 depletion, with next-generation RNA sequencing. RNA from neuronal processes was isolated from naïve and injured processes from wild-type and Cpeb1 knockout neurons (Fig. 22A). Libraries were prepared with the help of Klara Zwadlo, sequencing was performed in the Genomics and Proteomics Core Facility of the DKFZ, and mapping and bioinformatics analysis were performed with the help of Sheng Zhao.

Since Cpeb1 is a known regulator of polyadenylation, random priming was used to generate the cDNA library. Thus the ScriptSeq library preparation protocol was used and libraries were processed for 100bp paired-end sequencing. However the total mapping rates were very low (<35%) (Fig. 22C). The problem probably comes from the low amount of RNA collected when the cell somas have to be excluded.

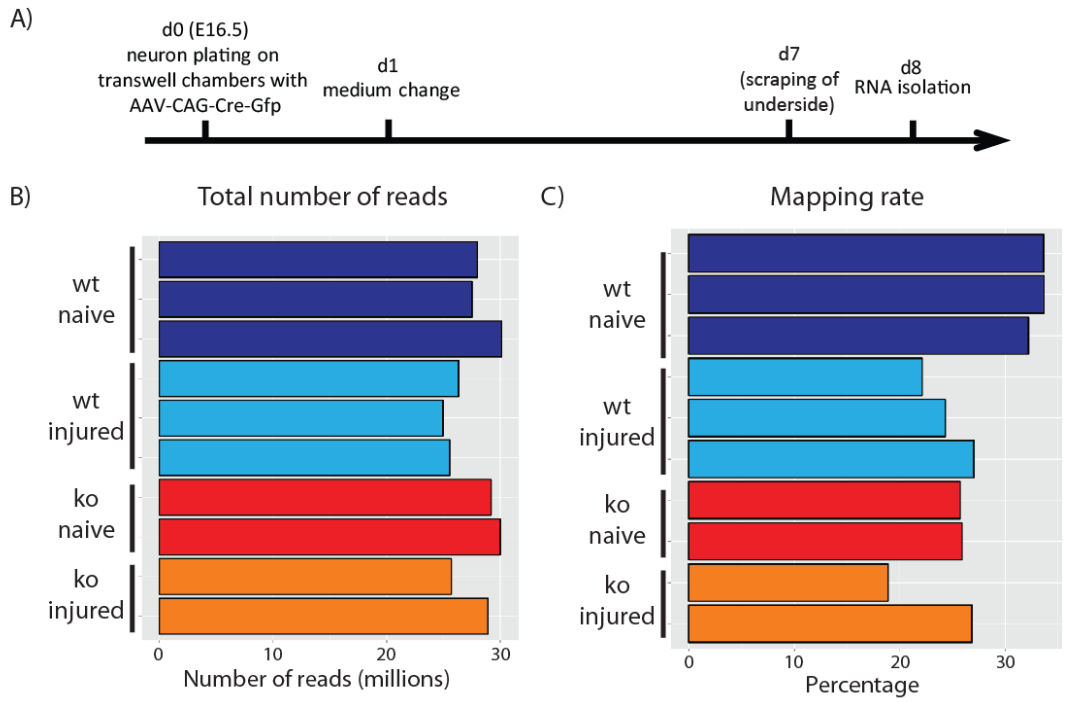


Figure 22: RNAseq of neuronal processes with ScriptSeq protocol. A) Timeline for generating samples for RNA-seq. B and C) Total number of reads are satisfactory but mapping rate is very low. n=3 for wild-type and n=2 for Cpeb1 knockout samples.

Library preparation was repeated with the Smart-seq2 protocol (Picelli et al., 2014), which requires far less input. Although this protocol makes use of primers with a stretch of 30bp poly(T)s to select for poly(A)-containing RNAs, it has been shown that few mRNAs have a

poly(A) tail shorter than 30bp (Chang et al., 2014; Subtelny et al., 2014). Thus the bias against mRNAs with short poly(A) tails would be minimal. Samples were submitted for 100bp paired-end sequencing as before.

Quality control metrics shows great improvement over the ScriptSeq protocol, with high total mapping rates and with mRNAs constituting more than 70% of mapped reads in all samples (Fig. 23A-C). Principle component analysis (PCA) shows biological replicates cluster together (Fig. 23D). There is no reads coverage on exon 4 of Cpeb1 in the knockout samples, showing efficient deletion (Fig. 23E).

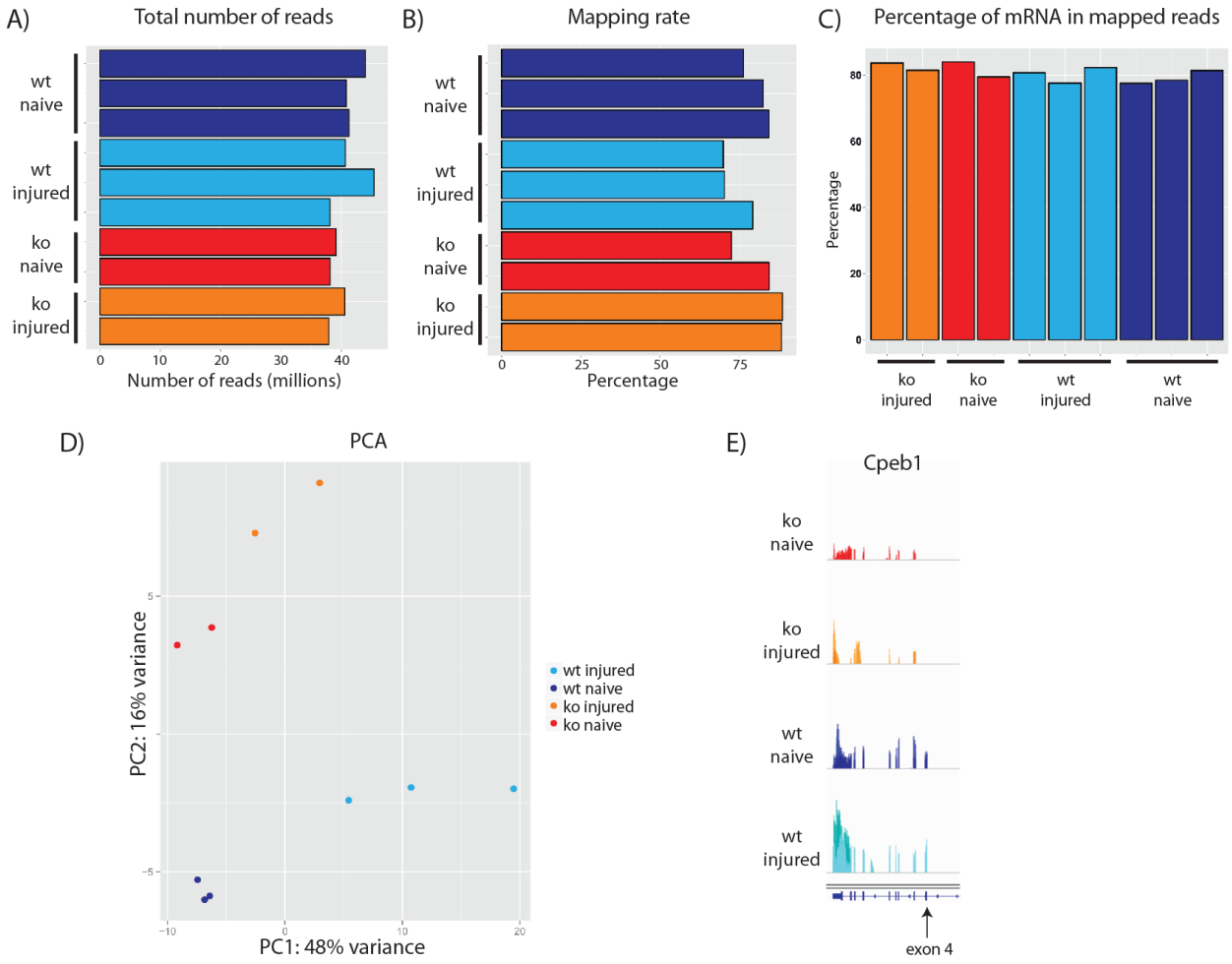


Figure 23: Quality control of RNAseq of neuronal processes with SmartSeq2 protocol. A-C) Total number of reads, mapping rate and percentage of mRNAs in mapped reads are satisfactory and similar across samples. D) PCA shows samples cluster together by replicates. E) Genome tracks of Cpeb1 showing exon 4 is efficiently deleted in knockout samples. n=3 for wild-type and n=2 for Cpeb1 knockout samples. wt: wild-type + AAV-CAG-Cre-Gfp; ko: Cpeb1$^{flox/flox}$ + AAV-CAG-Cre-Gfp.

### 3.4.2 Cpeb1 mediates the transcriptome injury response in neuronal processes

Two different approaches in comparing the samples were used to elucidate the role of Cpeb1 in injury response. In the first approach, injured and naïve samples were compared separately for wild-type and Cpeb1 knockout processes (Fig. 24A). It was found that the injury response is smaller in Cpeb1 knockout than in wild-type processes, with much less differentially regulated genes (Fig. 24B and C), suggesting that the transcriptome response is hindered upon Cpeb1 knockout. In addition, most differentially regulated genes in Cpeb1 knockout processes are down-regulated (Fig. 24D). On functional clustering, up-regulated genes in wild-type processes are enriched in TNFα signalling and the p53 pathway (Fig. 24E). Interestingly, down-regulated genes are enriched in dendrite development, neuron projection morphogenesis and CNS development. This mimics the decrease of CNS development genes in the total RNA fraction after SCI (Fig. 9A), and suggests that this *in vitro* model serves as good surrogate of SCI for studying neuronal intrinsic programs activated upon injury.

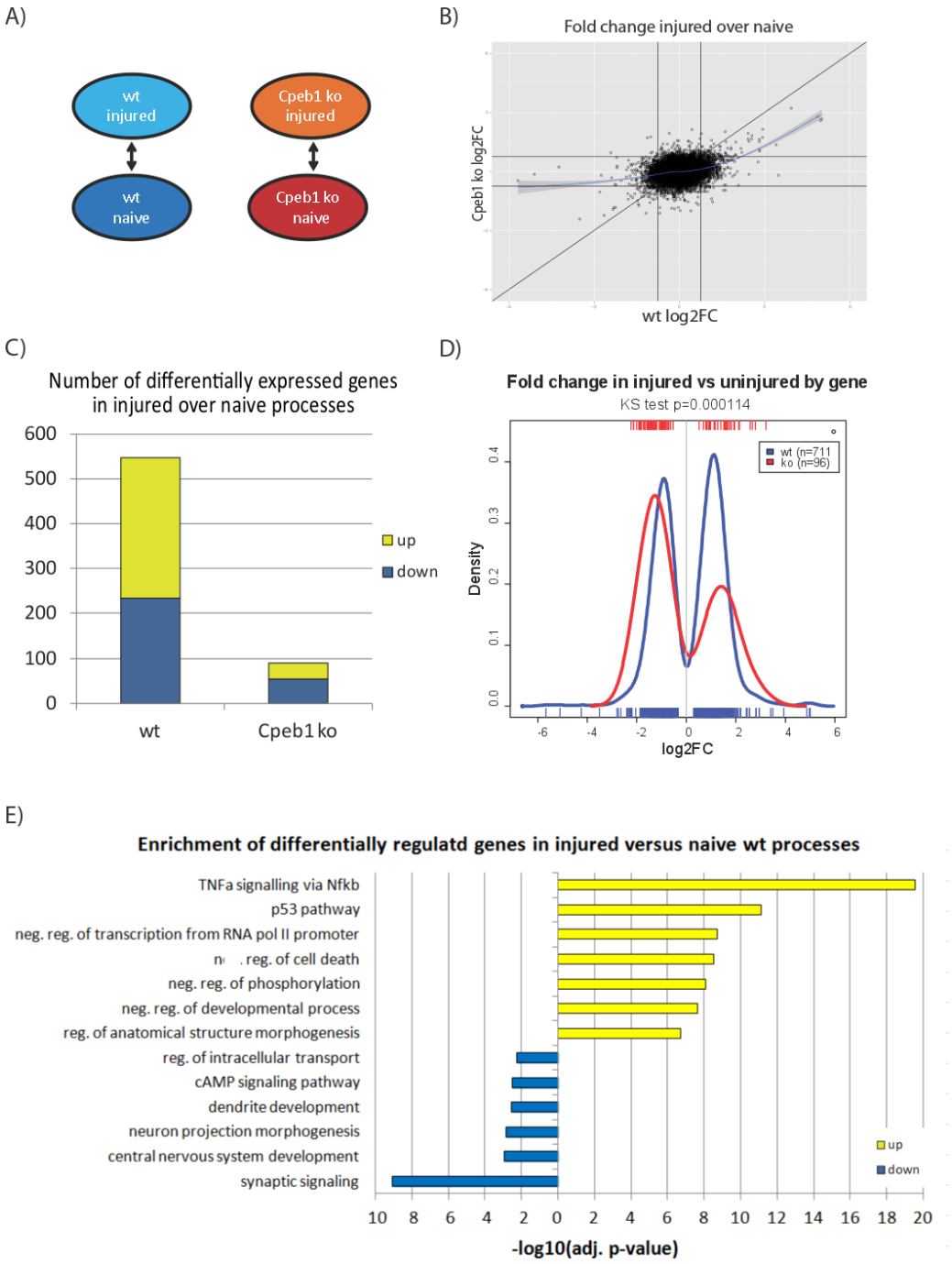


Figure 24: Injury-induced changes in mRNA abundance is reduced in Cpeb1 knockout processes. A) Schematics for the current sample comparison: injured versus naïve in wild-type and Cpeb1 knockout processes. B) Dot plot of fold change of genes upon injury in Cpeb1 knockout and wild-type processes. Loess fitness curve shows fold changes in wild type are higher than in Cpeb1 knockout processes. C) Number of genes differentially regulated upon injury ($p_{adj}$<0.05 and with log2FC either >0.75 or <-0.75). D) Density curve of fold change of genes differentially regulated upon injury ($p_{adj}$<0.05). E) Selected enriched GO categories of genes differentially regulated upon injury in wild-type processes ($p_{adj}$<0.05 and with log2FC either >0.75 or <-0.75). Statistics: Differential expression: Wald test; comparison of similarity between curves: Kolmogorov-Smirnov test; GO enrichment: Bonferroni adjusted p-value.

To ascertain the role of Cpeb1 in the observed transcriptome response after neuronal injury transcripts were separated into CPE-containing and -non-containing ones, and their profiles of expression after injury in wild-type processes were investigated. Surprisingly, mRNAs containing CPE are less differentially regulated than those that do not contain CPE (Fig. 25A). Looking more deeply into differentially regulated transcripts, there is no significant difference in distribution of fold changes between the two groups (Fig. 25B). Although when transcripts are further sub-divided according to the number of CPEs they possess, there is a mild trend that transcripts with more CPEs tend to be less down-regulated (Fig. 25C). A likely scenario that could explain this phenomenon is that at 24 hours after the injury, indirect effects and late response have already become prominent, and direct effects of Cpeb1-CPE binding are already diluted out and therefore constitute a small part of the observed changes in RNA levels.

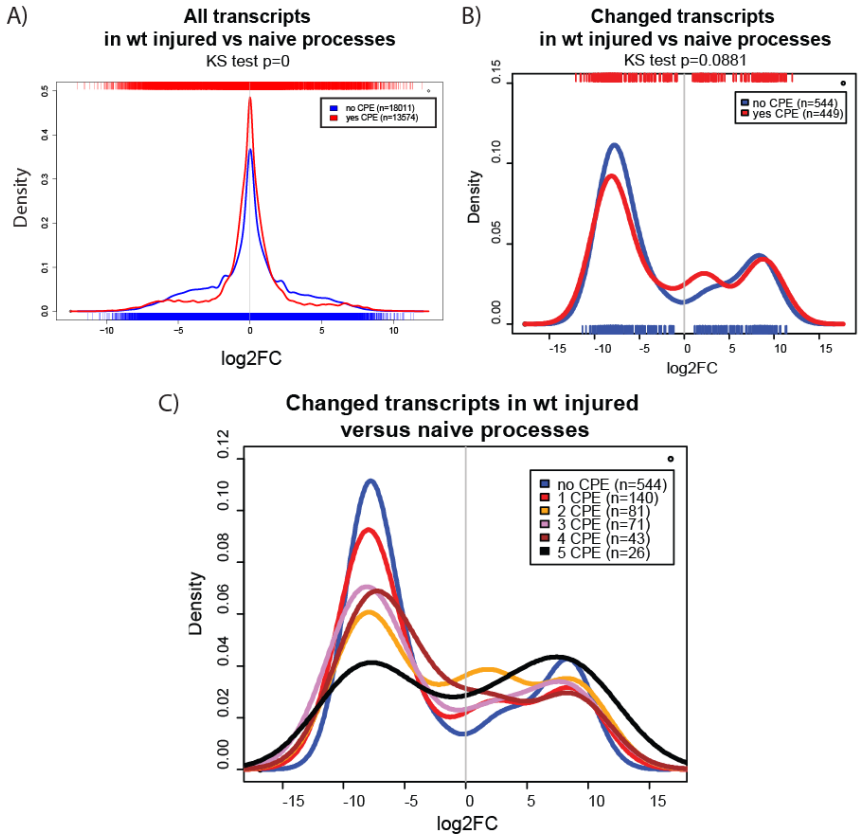


Figure 25: Association of CPE with changes in mRNA abundance upon injury. A-B) Density curve of fold change of CPE containing and non-containing transcripts upon injury for A) all detected transcripts and B) differentially regulated transcripts ($p_{adj}$<0.05). C) Density curve of fold change upon injury for differentially regulated transcripts ($p_{adj}$<0.05) segregated according to the number of CPEs possessed. Statistics: Differential expression: Wald test; comparison of similarity between curves: Kolmogorov-Smirnov test.

The second approach compares differences upon Cpeb1 knockout within injured or naïve processes (Fig. 26A). There is a much greater response upon Cpeb1 knockout in injured processes than in naïve ones, with many more genes being differentially regulated (Fig. 26B-D). Thus, Cpeb1 appears to play a much greater role in regeneration. Genes related to nuclear import and TNFα signalling are down-regulated upon Cpeb1 knockout (Fig. 26E).

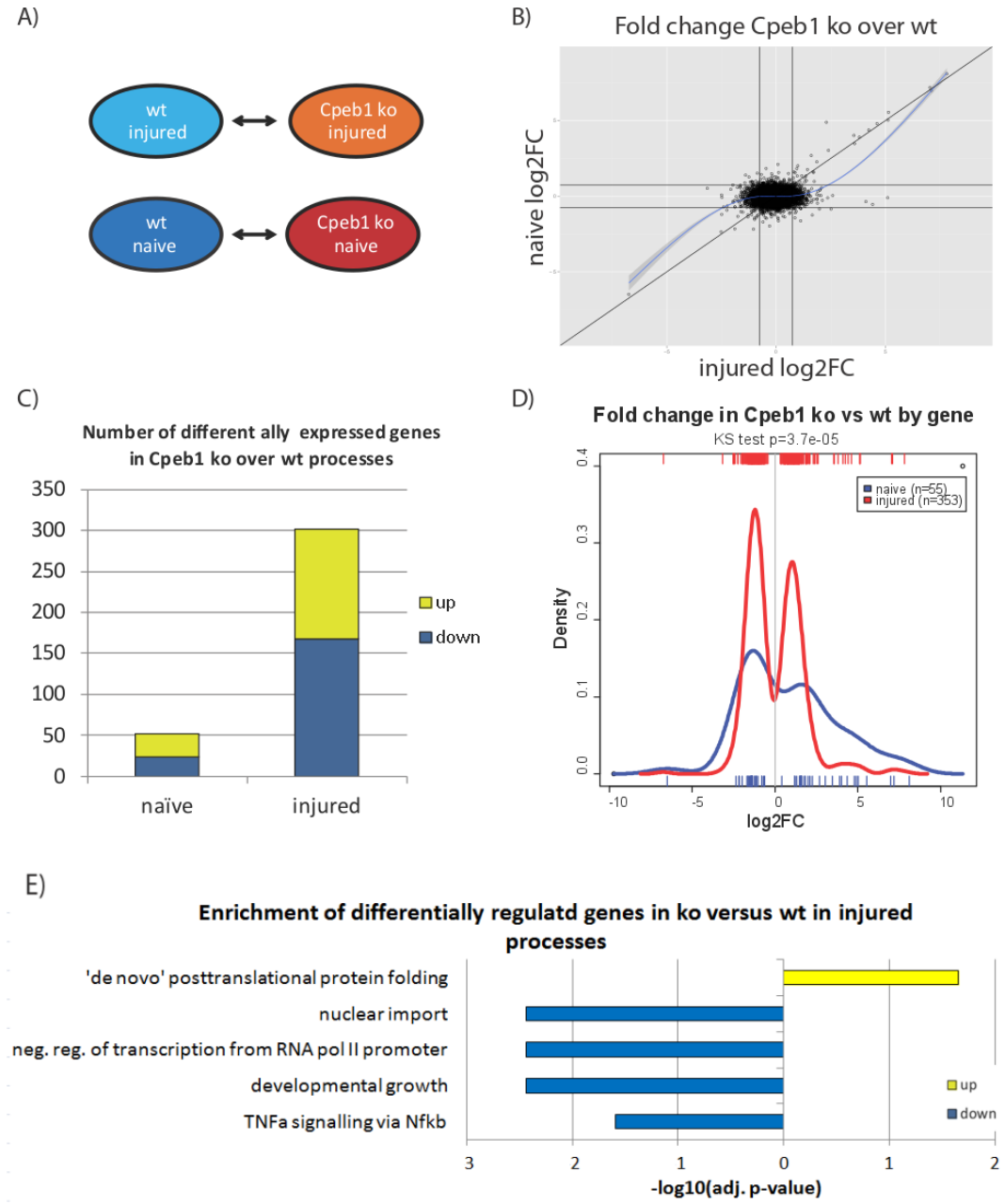


Figure 26: Cpeb1 knockout induces greater changes in mRNA abundance in injured processes. A) Schematics for the current sample comparison: Cpeb1 knockout versus wild-type in naïve and injured processes. B) Dot plot of fold change of genes upon Cpeb1 knockout in naïve against injured processes. Loess fitness curve shows fold changes is higher in injured than in naïve processes. C) Number of genes differentially regulated upon Cpeb1 knockout ($p_{adj}$<0.05 test and with log2FC either >0.75 or <-0.75). D) Density curve of fold change of genes differentially regulated upon Cpeb1 knockout ($p_{adj}$<0.05). E) Selected enriched GO categories of genes differentially regulated upon Cpeb1 knockout in injured processes ($p_{adj}$<0.05 and with log2FC either >0.75 or <-0.75). Statistics: Differential expression: Wald test; comparison of similarity between curves: Kolmogorov-Smirnov test; GO enrichment: Bonferroni adjusted p-value.

Transcripts were divided into CPE-containing and -non-containing ones and their distribution of fold changes upon Cpeb1 knockout was investigated, to ascertain the role of Cpeb1 towards CPE containing transcripts in the response to injury. Similar to before, CPE containing transcripts are less changed upon Cpeb1 knockout (Fig. 27A). Within differentially expressed transcripts, the presence of CPE did not bias towards up- or down-regulation upon Cpeb1 knockout (Fig. 27B), and there is no clear trend of association between fold change and the number of CPEs (Fig. 27C). This could again be explained by the time point being too late, with indirect effects of Cpeb1 regulation taking over the majority of the observed changes in RNA levels.

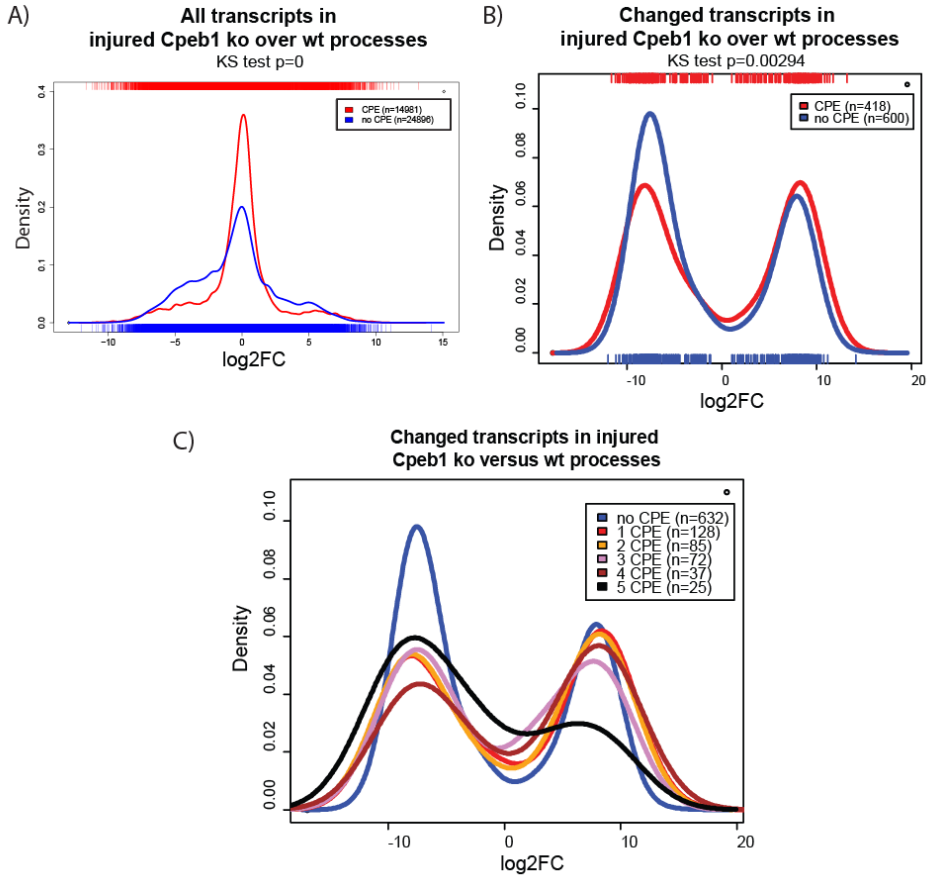


Figure 27: Association of CPE with changes in mRNA abundance upon Cpeb1 knockout. A-B) Density curve of fold change of CPE containing and non-containing transcripts upon Cpeb1 knockout for A) all detected transcripts and B) differentially regulated transcripts ($p_{adj}$<0.05). C) Density curve of fold change upon Cpeb1 knockout for differentially regulated transcripts ($p_{adj}$<0.05) segregated according to the number of CPEs possessed. Statistics: Differential expression: Wald test; comparison of similarity between curves: Kolmogorov-Smirnov test.

## 3.5 Mechanisms of post-transcriptional regulation mediated by Cpeb1

### 3.5.1 Effect of Cpeb1 knockout on mRNA expression of CPE containing regeneration associated genes (RAGs) and RBPs

Taking a deeper look into the RNAseq data, the first question was how do known RAGs behave? In particular, we focused on those that contain CPE, in order to infer direct targets of Cpeb1 (Fig. 28). Stat3 (Bareyre et al., 2011), Cebpβ (Yan et al., 2009), and Kpnb1 (Perry et al., 2012) are pro-regenerative genes that contain CPE. Among them, Cpeb1 knockout hindered injury-induced increase of axonal Cebpβ mRNA, suggesting that Cebpβ could be a direct target of Cpeb1. Pten and Socs3 are negative regulators of axon regeneration (Liu et al., 2010; Sun et al., 2011), both also CPE-containing. The injury-induced decrease of Pten mRNA is dampened upon Cpeb1 knockout, agreeing with a previous report showing that Pten is a direct target of Cpeb1 (Alexandrov et al., 2012).

We also looked into Cpeb4, a family member of Cpeb1 which binds to the same motif (Charlesworth et al., 2013). It has been reported that Cpeb1 activates the translation of Cpeb4, thereafter it replaces Cpeb1 and creates a positive translation loop for CPE-containing mRNAs (Igea and Méndez, 2010). Interestingly, Cpeb1 knockout prevents an injury-induced decrease in Cpeb4 mRNA, suggesting that Cpeb1 mediates the degradation of Cpeb4 mRNA.

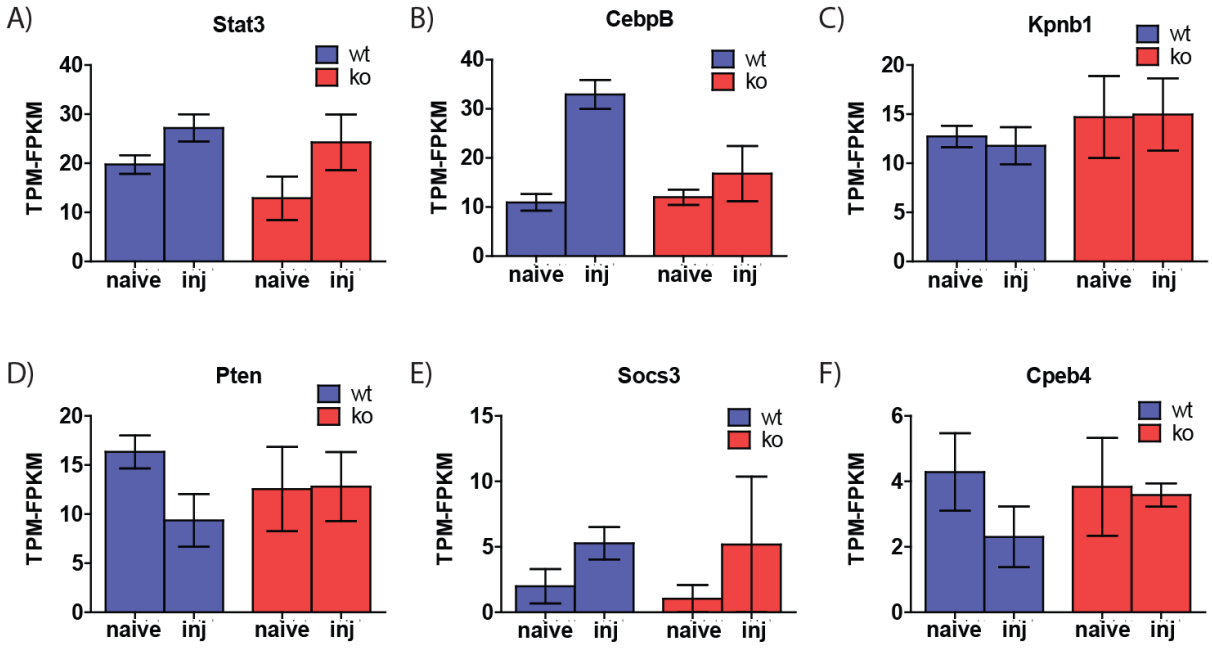


Figure 28: Gene expression values for putative Cpeb1 effector genes from RNAseq. ko: Cpeb1 ko. n=3 for wild-type and n=2 for ko. Error bars: mean +/- S.E.M.

### 3.5.2 Role of Cpeb1 on RNA stability of putative target mRNAs

As previous data suggests that Cpeb1 regulates the stability of its target mRNAs (Fig. 11, 12, 28), we directly investigated the stability of its putative targets. Firstly, the mRNA levels of putative targets on whole neurons upon Cpeb1 knockout was measured by qPCR, as a screening to narrow down the list of candidates. The rationale being that their global levels would change if they are targets of Cpeb1-mediated degradation. Genes studied were selected from known targets of Cpeb1 from the literature, or from CPE-containing genes that were significantly changed upon injury from the TSAA or RNAseq experiments. For all the genes that were studied, most have their expression reduced slightly upon Cpeb1 deletion, with Stat3 and Kif5c showing the greatest decrease (Fig. 29B).

To ascertain whether the differences observed are due to degradation, RNA degradation assay was performed by treating neurons with actinomycin D, which blocks transcription, and tracking the mRNA levels over time. In addition to Stat3 and Kif5c, the assay was also performed on Cebpβ, as it is among the most highly up-regulated genes in the total RNA

fraction from the TSAA. Surprisingly, deletion of Cpeb1 appears to confer a slightly greater stability on the tested genes (Fig. 29C-F).

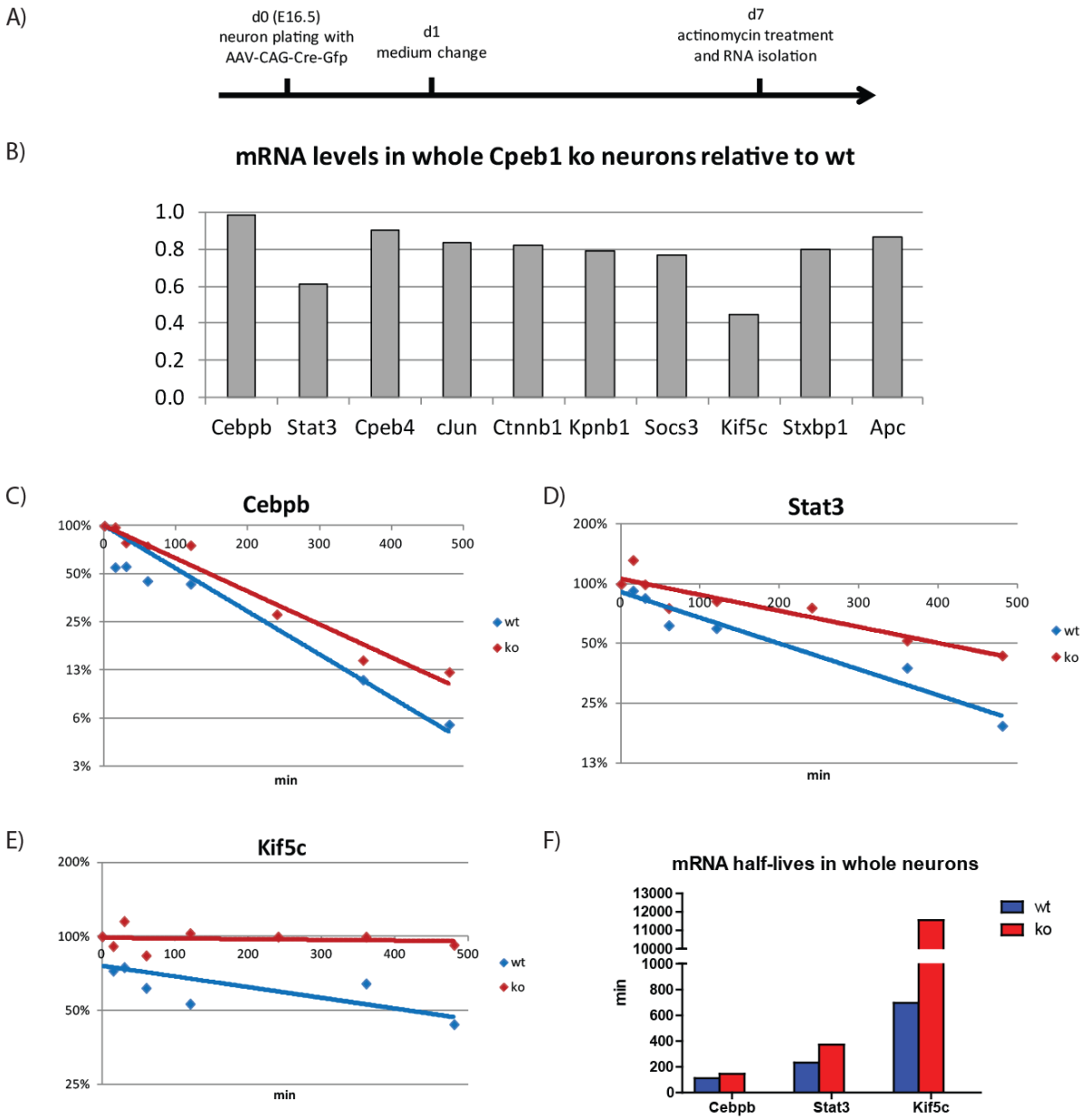


Figure 29: Levels and stability of putative Cpeb1 target mRNAs upon Cpeb1 knockout in whole neurons. A) Timeline of experiment setup. B) Relative abundance of candidate mRNAs upon Cpeb1 knockout. C-E) Degradation curve of candidate RNAs after actinomycin treatment. F) Calculated mRNA half-lives. ko: Cpeb1 knockout. RNA levels are measured by qPCR and normalised to Gapdh.

It was suspected that Cpeb1 mediated RNA stability may differ between processes and somas, due to different environmental cues; and by analysing RNA from the whole neuron, the effect is averaged out. As a result, the degradation assay was repeated on RNAs from processes and somas, isolated separately by culturing neurons on transwell chambers. Data from the RNAseq shows that Cpeb1 knockout hindered the injury-induced up-regulation of many genes in neuronal processes (Fig. 24 and 26). Consequently, attention was turned to these genes, in particular c-Jun, Junb, c-Fos, Egr1 and Nfkbia, which show the aforementioned behaviour (Fig. 30A-F). qPCR shows that the mRNAs of these genes in both processes and somas, with the exception of Nfkbia, are reduced upon Cpeb1 knockout (Fig. 30G). Interestingly, deletion of Cpeb1 confers little change in mRNA stability in processes and somas (Fig. 31). Only a slight reduction in stability was seen for c-Jun in somas and Junb in processes. In most cases, a minor increase in stability was observed after knockout. This is perhaps not surprising, as RNAseq data shows there are little changes in mRNA abundance upon Cpeb1 knockout in naïve processes (Fig. 26).

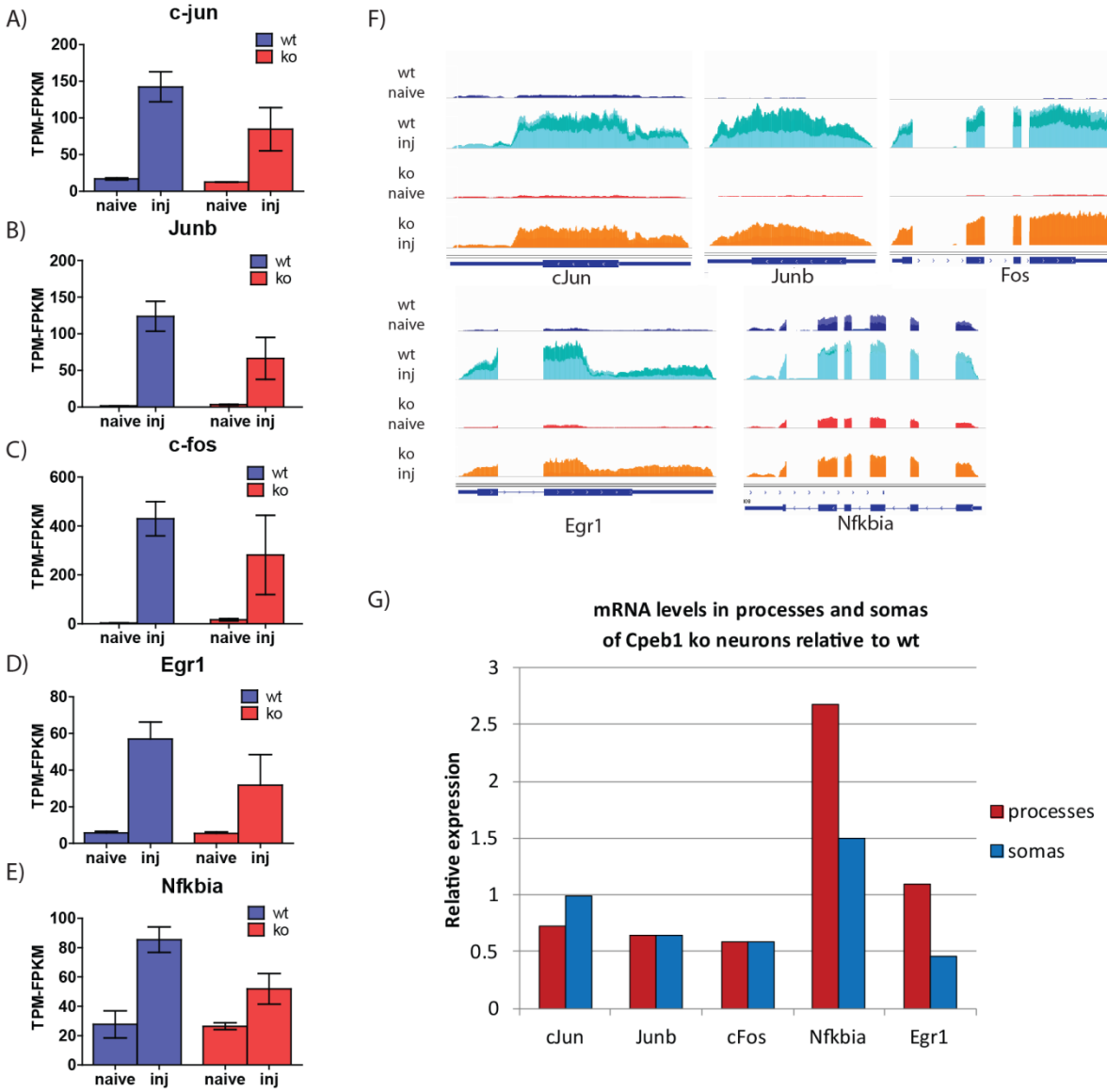


Figure 30: Expression of for putative Cpeb1 target transcription related genes. n=3 for wild-type and n=2 for ko. Error bars: mean +/- S.E.M. A-E) Gene expression values from processes from RNAseq. F) Genome tracks showing expression. G) Relative abundance of candidate RNAs upon Cpeb1 knockout in processes and somas by qPCR. ko: Cpeb1 ko.

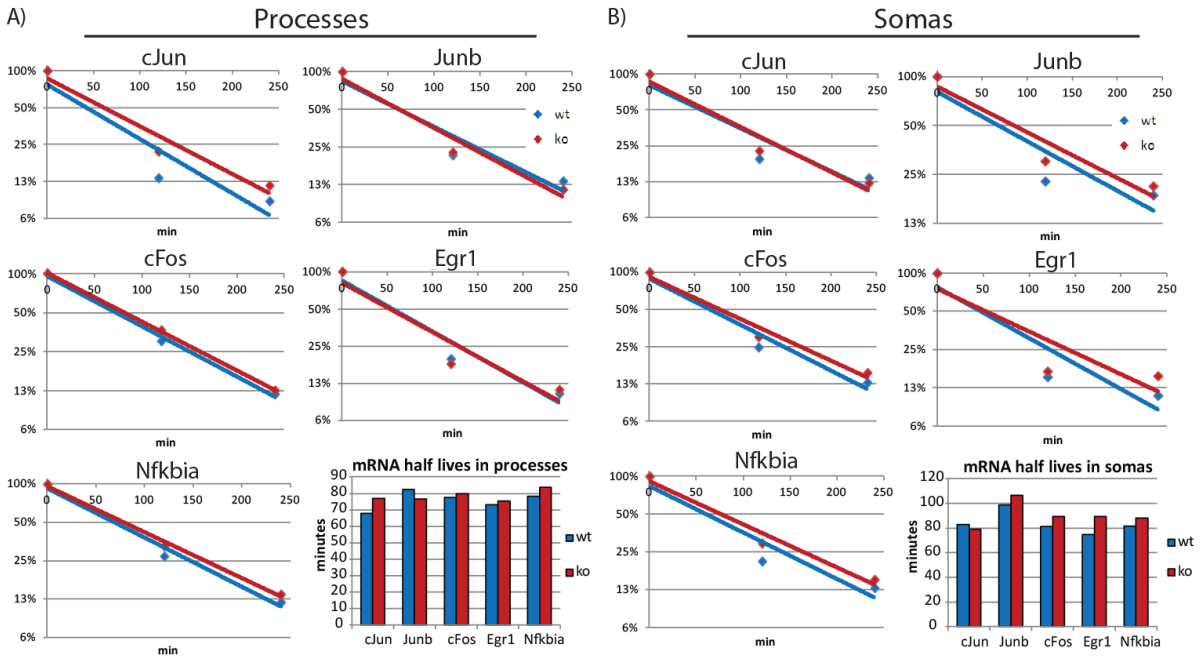


Figure 31: Stability of putative Cpeb1 target transcription related mRNAs upon Cpeb1 knockout in processes and somas. A) Degradation curve of candidate mRNAs after actinomycin treatment and calculated mRNA half-lives. ko: Cpeb1 knockout. RNA levels are measured by qPCR and normalised to Gapdh.

Accordingly, the experiment was repeated also on injured processes. The panel of targets tested was extended to include genes regulating axon regeneration: Klf6 (Moore et al., 2009; Veldman et al., 2010) and Zfp36l2 (Cargnin et al., 2014); axon guidance: Noggin (Dionne et al., 2002) and Neurod2 (Ince-Dunn et al., 2006); and synaptic development: Ptbp1 (Zheng et al., 2012). Zfp36l2 and Ptbp1 are also RBPs and post-transcriptional regulators themselves. These candidates all show a hindered injury-induced up-regulation upon Cpeb1 knockout in the RNAseq.

Upon Cpeb1 knockout, Fosb, Klf6 and Zfp36l2 expression was decreased in injured processes (Fig. 32). However, RNA degradation assay showed that for the most, Cpeb1 knockout has little effect stability of the candidate mRNAs (Fig. 33). Although there are differences in the calculated half-lives for c-Fos, Fosb, Noggin and Ptbp1, the observation is not reliable, as the data points for the degradation curves do not fit well to a straight line.

Hence, direct targets for Cpeb1-mediated RNA stability requires more extensive screening to be identified. One other possibility that explains the increased abundance of mRNAs in

injured processes is that CPE mediates the localisation of its host mRNA to the processes upon injury. This would require further experiments to elucidate, for example replacing actinomycin D treatment with microtubule destabilising chemicals that would inhibit RNA transport. Interestingly though, there is a general trend among the tested genes that mRNA half lives are increased upon injury, independent of the presence of Cpeb1 (Fig. 33). Therefore, it is evident that other factors are also responsible for the up-regulation of these genes upon injury, and perhaps these are the direct targets of Cpeb1.

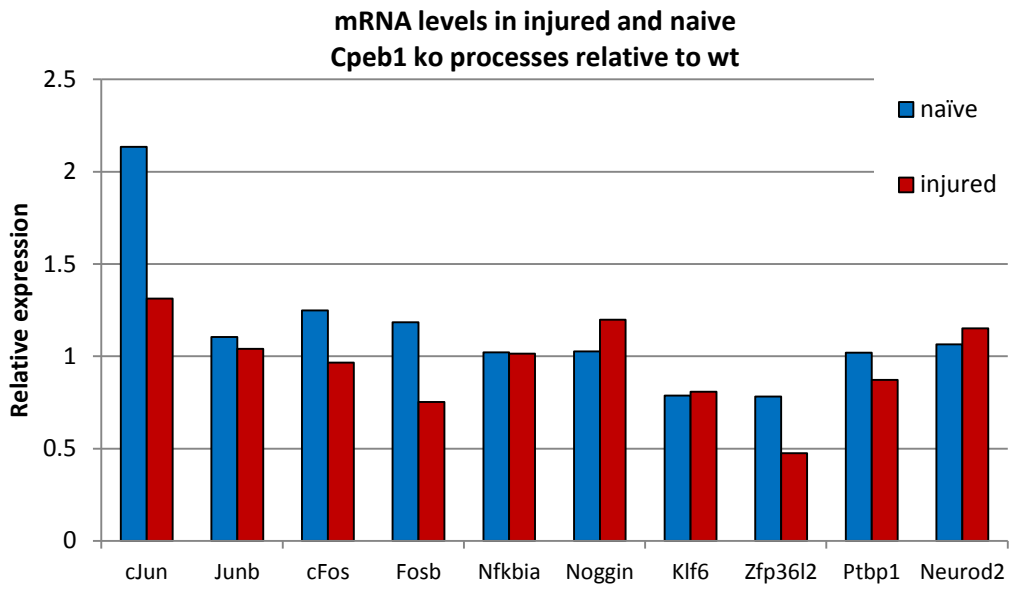


Figure 32: Relative abundance of Cpeb1 putative target mRNAs upon Cpeb1 knockout in injured and naïve processes. RNA levels are measured by qPCR and normalised to Gapdh.

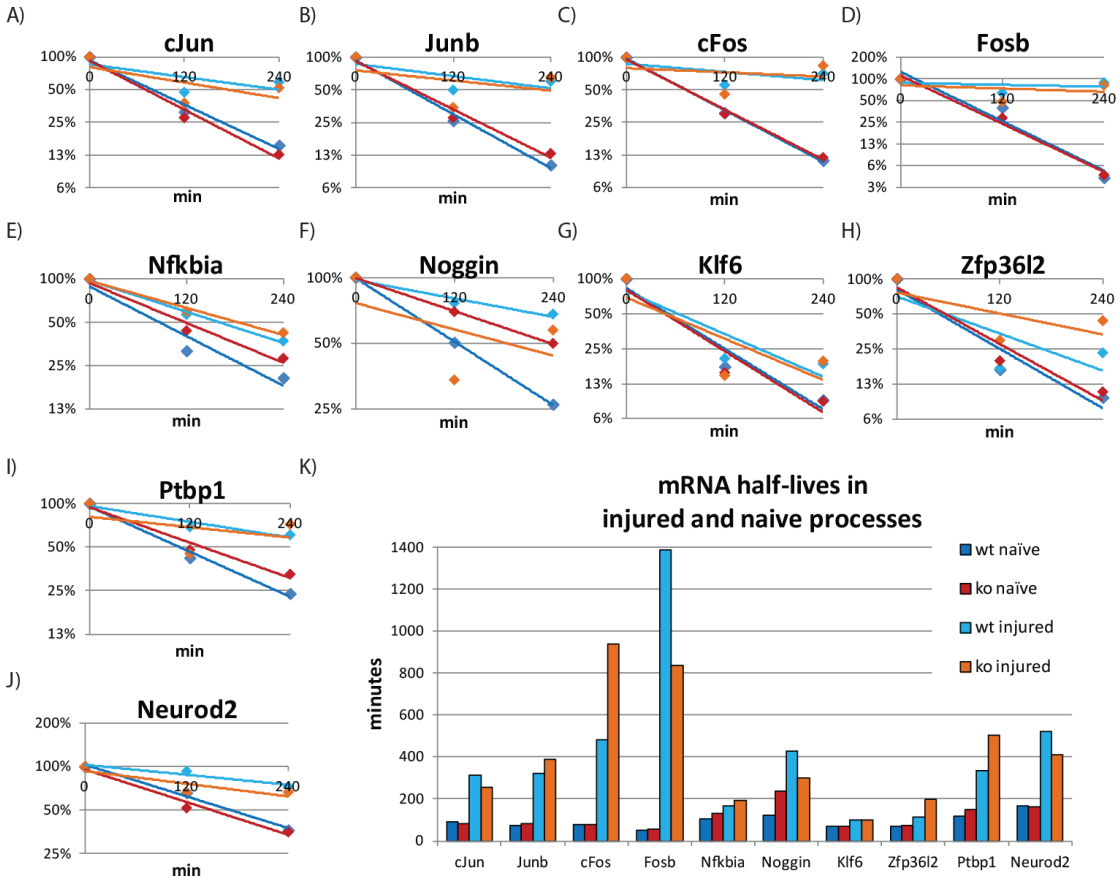


Figure 33: Stability of putative Cpeb1 target mRNAs upon Cpeb1 knockout in injured and naïve processes. A-J) Degradation curve of candidate mRNAs after actinomycin treatment. K) Calculated mRNA half-lives. ko: Cpeb1 knockout. RNA levels are measured by qPCR and normalised to Gapdh.

### 3.5.3 Cpeb1 in alternative polyadenylation

It has been reported that Cpeb1 could mediate alternative polyadenylation (APA) of target mRNAs (Bava et al., 2013). This process creates transcript variants with different 3'UTRs, affecting the presence of cis-acting elements such as RBP and miRNA binding sites and thus its post-transcriptional fate. Recently an algorithm called Dynamic analyses of Alternative PolyAdenylation from RNA-Seq (DaPars) has been developed that allows genome-wide screening of APA events using RNAseq data (Xia et al., 2014). With the help of Mechthild Lütge, DaPars was performed to screen for differential APA events using the RNAseq data.

It was found that injury and Cpeb1 both influence the usage of 3'UTR isoforms (Fig. 34). In the comparison within wild-type samples (Fig. 34C), injury induces a shift towards longer 3'UTRs and a down-regulation in these genes. This agrees with the general notion that longer 3'UTRs contain more miRNA binding sites and thus are more readily degraded (Mayr and Bartel, 2009).

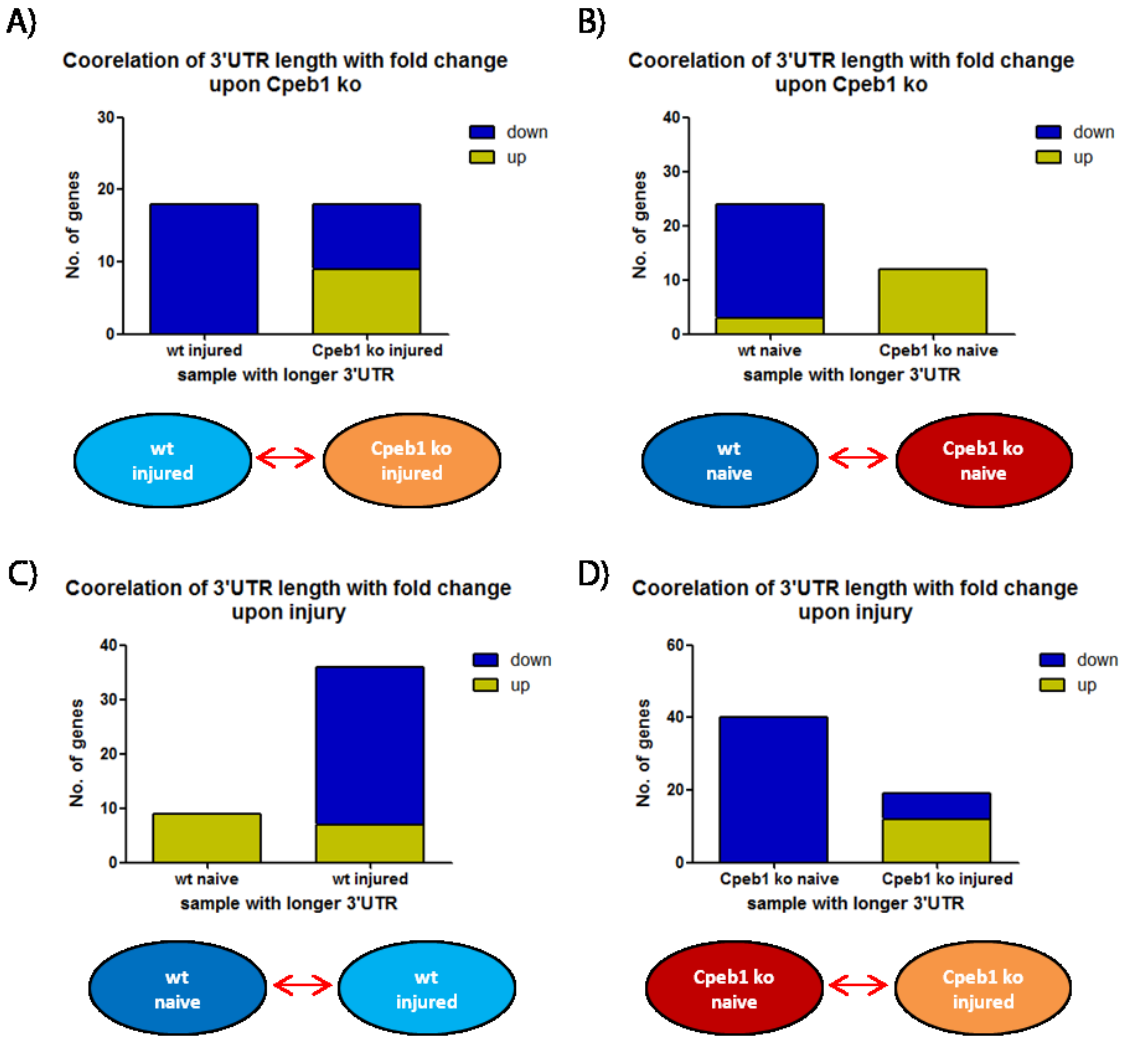


Figure 34: Differential expression of genes with alternative polyadenylation identified by DaPars. Genes listed are identified by DaPars with $p<0.05$; and with log2FC either $>0.75$ or $<-0.75$ and, $p<0.05$ by Wald's test. Chi-square test of distribution: A): $p=0.001$; B-D) $p<0.0001$.

Among the genes identified to have differential APA upon Cpeb1 knockout, one is Map2k7, an upstream kinase of JNK signalling which in turn activates c-Jun. Map2k7 activates JNK signalling, leading to microtubule bundling and elongation of neurites (Yamasaki et al.,

2011). Map2k7 isoforms possess either a long or a short 3'UTR. The longer 3'UTR causes increased localization of the mRNA to neurites, phosphorylation and activation of the Map2k7 protein, and elongation of neurites (Feltrin et al., 2012). Importantly, the long 3'UTR contains 3 CPE motifs whereas the short 3'UTR contains none, and Cpeb1 knockout causes a shift to the short 3'UTR in injured processes (Fig. 35A). Therefore, Map2k7 presents an attractive candidate for investigation, with the hypothesis that Cpeb1 increases the usage of the longer 3'UTR of Map2k7 and thus its activation, which in turn increases the activation of the JNK pathway, leading to regeneration.

The ratio of long to short 3'UTR of Map2k7 upon Cpeb1 knockout was thus further investigated, by performing qPCR with primers amplifying specifically only one of the isoforms. It was found that Cpeb1 knockout causes a shift to the short 3'UTR in whole neurons, albeit the difference is not significant (Fig. 35B). In processes the difference is minimal, however more replicates are needed to ascertain this.

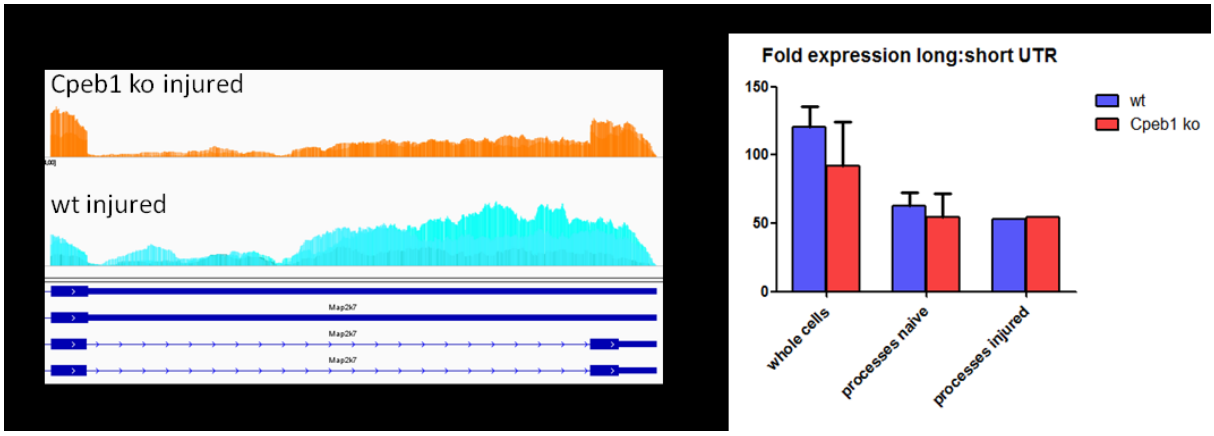


Figure 35: Effect of Cpeb1 knockout on Map2k7 alternative polyadenylation. A) Genome tracks showing expression of Map2k7 3'UTR of wild-type and Cpeb1 knockout injured processes. B) Ratio of long to short 3'UTR of Map2k7 determined by isoform-specific qPCR.

### 3.5.4 Polyadenylation status of putative Cpeb1 target mRNAs after neuronal injury

Localised translation in axons is essential towards regeneration (Kalinski et al., 2015; Merianda et al., 2015; Verma et al., 2005). This means spatial control over translation is in place, with it being repressed initially and only activated when the mRNAs are in their target

location. Precise control over mRNA translation occurs via cytoplasmic polyadenylation, a process best studied in Xenopus oocytes but also shown in neuronal growth cones (Brittis et al., 2002; Lin et al., 2009). Since Cpeb1 is a key regulator of cytoplasmic polyadenylation, putative targets of Cpeb1 related to regeneration were studied for their polyadenylation status by poly(A) tail (PAT) assays (Fig. 36A). In addition to amplifying the poly(A) tail, an extra "UTR" PCR was performed as a control for RNA quality. In the beginning, 3 different forward primers were designed for each gene, which were then tested and the best picked for subsequent assays. The number of PCR cycles was also tested for a balance between signal intensity and accuracy, as the polymerase could slip when amplifying long stretches of the same base, and 30 cycles was found to be optimal.

The PAT assay was first performed on naïve and injured spinal cord tissue for known binding targets of Cpeb1: Pten, Cpeb4, and Stat3. However, no difference between naïve and injured spinal cords could be observed (Fig. 36B). It was suspected that in spinal cord tissue, RNA from other cell types as well as from neuronal cell somas might mask the signal coming from the axonal compartment. As a result, the assay was repeated with the length of spinal cord taken reduced from 2.5cm to 1cm around the lesion area. However, there was still no observable change in poly(A) tail length upon injury (Fig. 36C). Perhaps despite reducing the amount of tissue taken, the influence from other cell types and neuronal cell soma is still too large.

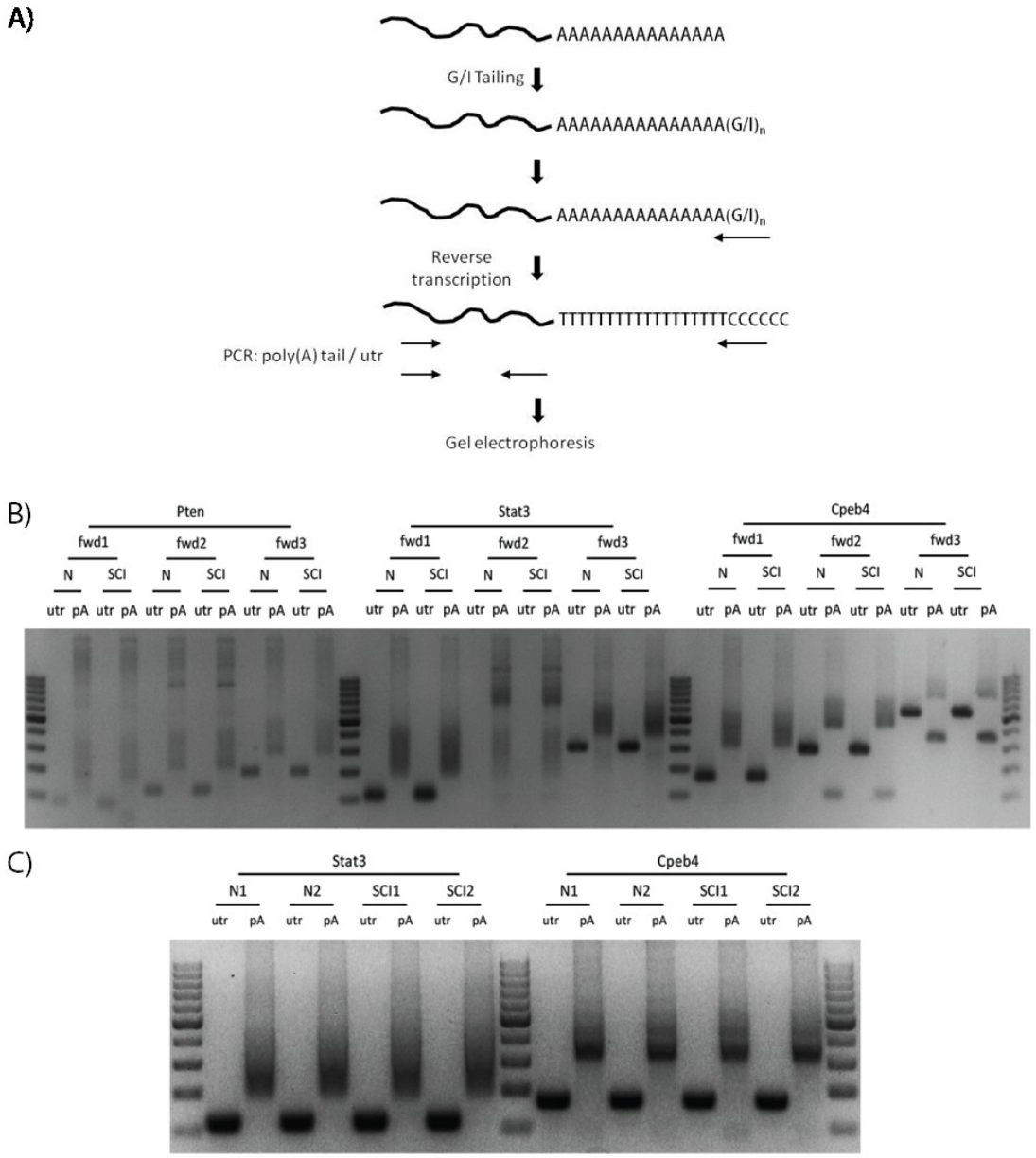


Figure 36: Effect of SCI on polyadenylation. A) Schematics for PAT assay. B) PAT assay with 2.5cm of spinal cord tissue around the operated area. C) PAT assay with 1cm of spinal cord tissue around the operated area. N1 and N2: replicates of naive spinal cord; SCI1 and SCI2: replicates of injured spinal cord; fwd1-3: different forward primers priming on the 3'UTR of the same gene; utr: amplified 3'UTR; pA: amplified poly(A) tail.

Consequently, the assay was performed on RNAs isolated from processes or cell somas from embryonic cortical neurons by culturing them on transwell chambers (Fig. 37). Injury induced an increase in poly(A) tail length for Kpnb1, agreeing with the fact that localized translation of Kpnb1 in axons is a part of injury induced response (Perry et al., 2012). On the

other hand, a shortening of poly(A) tail for Cpeb4 was observed. Knockout of Cpeb1 increases the poly(A) tail length for Cpeb4 and β-catenin in injured processes, suggesting that Cpeb1 shortens the poly(A) tails of these two mRNAs upon injury.

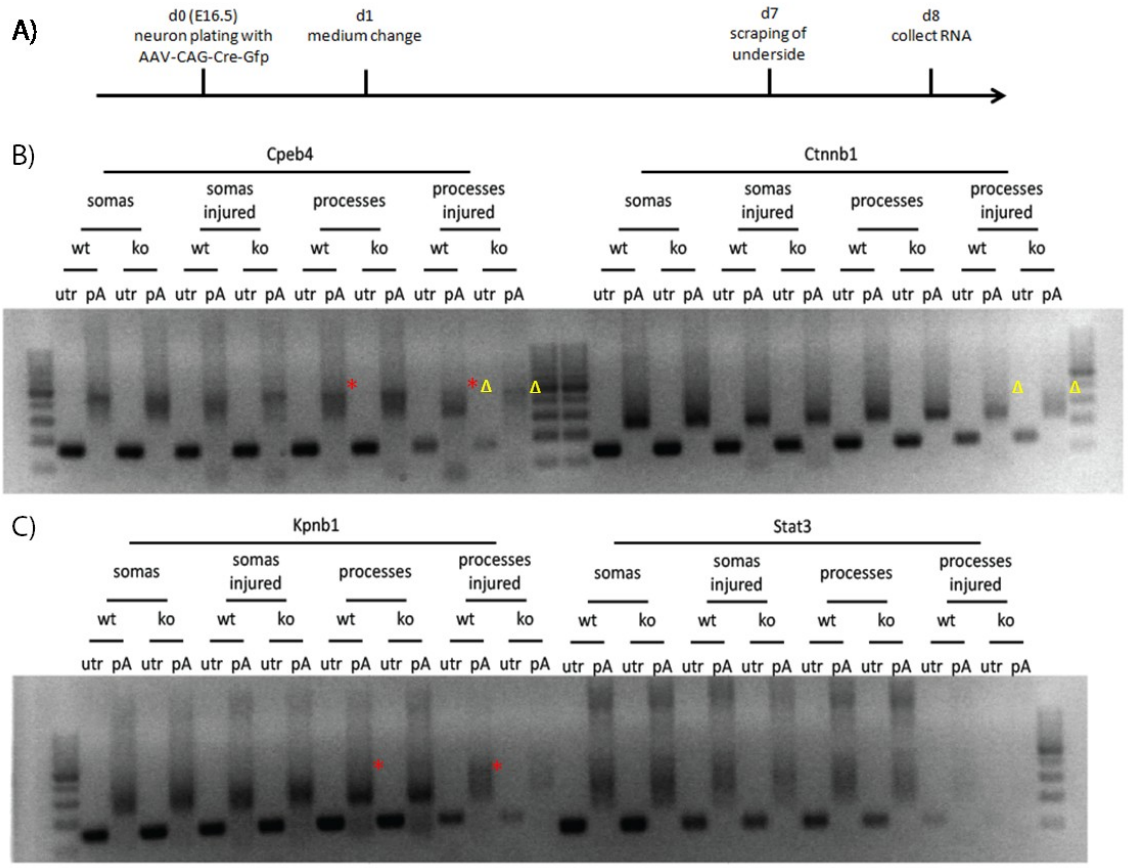


Figure 37: Effect of injury and Cpeb1 knockout on polyadenylation. A) Timeline for experimental setup. B and C) PAT assay on cell somas and somas of wild-type and Cpeb1 knockout neurons. Red asterisk: difference between injured and naïve; yellow triangle: difference between Cpeb1 knockout and wild-type. utr: amplified 3'UTR; pA: amplified poly(A) tail.

### 3.5.5 Role of polyadenylation on axonal regeneration

To investigate if regeneration mediated by localised translation occurs via polyadenylation, the effect on axonal regrowth by inhibiting polyadenylation with cordycepin was studied. To allow axon specific treatment, cortical neurons were cultured in axis isolation devices (AXISs) (Park et al., 2006). Microfluidic pressure forces axons to develop through narrow channels that block cell somas (Fig. 38B). Axotomy was performed by applying vacuum to

the axonal compartment to suck away the medium together with the axons. The compartment was then refilled with medium containing the corresponding inhibitor, and regrowth was quantified 14 hours later. However no significant differences in terms of either number or length of regenerated axons was observed (Fig. 38C and D). Inhibition of translation with cycloheximide causes a small but insignificant decrease in these parameters. Culturing neurons within tight environment of the chamber caused bad viability and high variability, possibility the reason causing the lack of reliable observations.

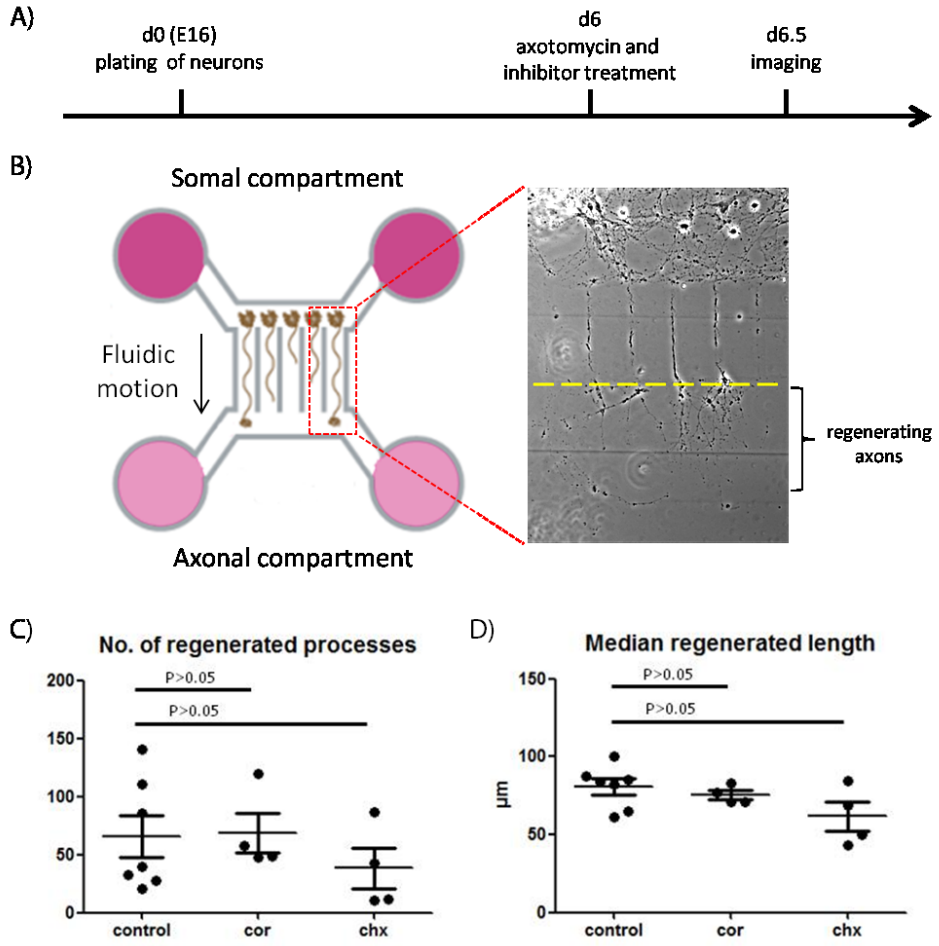


Figure 38: Effect of axonal inhibition of polyadenylation and translation on regrowth. A) Timeline for experimental setup. B) Schematics and representative picture showing the working of an AXIS device. B and C) Number and median length of regenerated axons. cor: cordycepin treated; chx: cycloheximide treated. n=7 for control, n=4 for cordycepin and cycloheximide. Error bars: Mean +/- S.E.M. Statistical test: Mann-Whitney.

### 3.5.6 Mediators of Cpeb1 regulated injury response

Since most injury-induced changes in mRNA abundance in neuronal processes were found to be unrelated to CPE (Fig. 25 and 27), it was postulated that much of the response comes from indirect targets of Cpeb1. To investigate through which molecules this is mediated, which will give an idea on what could be the direct targets of Cpeb1, Upstream Regulator Analysis from Ingenuity was performed. This predicts the upstream regulators based on the provided expression data. Two lists were analysed: genes exclusively regulated in wild-type and not Cpeb1 knockout processes upon injury (Table 7) and genes regulated in Cpeb1 knockout versus wild-type in injured processes (Table 8). The analysis does not predict Cpeb1 as an upstream regulator, but manual inspection of the database revealed there are very few annotated targets of Cpeb1, making prediction of Cpeb1 unlikely.

Within the first list, a number of transcription regulators were predicted to be both activated and repressed upstream regulators, reflecting the increased gene expression changes in wild-type compared to Cpeb1 knockout processes (Table 7). Among them, Crem and Myc have increased expression upon injury in the RNAseq data. These two genes also possess CPEs in at least in some of their isoforms, thus suggesting they may be direct targets of Cpeb1-mediated RNA stability. In particular, Crem, which is a part of the cAMP-mediated signal transduction and binds the cAMP responsive element (CRE) in promoters of many genes, is predicted to be repressed in the injured processes upon Cpeb1 knockout (Table 8). Crem possesses a large number of transcript isoforms which translates into both activators and repressors of transcription (Behr, 2000; Foulkes et al., 1992), thus it could also be a target for Cpeb1-mediated alternative splicing or polyadenylation. Targets of Crem found to be up-regulated include Btg2 and Cebpb, both enhancers of axonal growth (Miyata et al., 2008; Yan et al., 2009) (Fig. 39). For the other transcription factors predicted to be activated upstream regulators, there is no significant change in mRNA levels in the RNAseq. However, this does not rule out that they are not regulated by Cpeb1 via polyadenylation and translation.

Interestingly, a number of growth factors and the pro-regeneration cytokine IL6 are predicted to be activated upstream regulators (Table 7). This likely reflects only the fact that a repertoire of growth-related genes was up-regulated, as neurons are not known to produce growth factors or cytokines themselves. This is confirmed by checking the genome tracks of

these growth factors. In addition, the mRNA levels of these predicted growth factors are not significantly different upon injury.

| Upstream Regulator | log2FC in dataset | Molecule Type | Predicted Activation State | Activation z-score | p-value of overlap |
|---|---|---|---|---|---|
| IL6 | | cytokine | Activated | 2.779 | 4.36E-04 |
| MAP2K1/2 | | group | Activated | 2.177 | 6.64E-03 |
| Jnk | | group | Activated | 2.187 | 7.13E-02 |
| Vegf | | group | Activated | 3.613 | 5.80E-03 |
| Akt | | group | Activated | 2.011 | 1.54E-01 |
| ERK | | group | Activated | 2.088 | 3.73E-04 |
| NGF | | growth factor | Activated | 2.009 | 1.53E-08 |
| BMP4 | | growth factor | Activated | 2.026 | 2.64E-02 |
| FGF1 | | growth factor | Activated | 2.095 | 4.70E-05 |
| FGF10 | | growth factor | Activated | 2.2 | 1.25E-02 |
| FGF2 | | growth factor | Activated | 3.13 | 3.08E-09 |
| TGFB1 | | growth factor | Activated | 2.696 | 1.27E-13 |
| EGF | | growth factor | Activated | 3.19 | 2.38E-07 |
| IKBKG | | kinase | Activated | 2.373 | 1.03E-01 |
| CREM | 1.779 | transcription regulator | Activated | 2.181 | 3.81E-07 |
| GLI1 | | transcription regulator | Activated | 2.123 | 1.80E-05 |
| CREB1 | | transcription regulator | Activated | 5.328 | 5.47E-21 |
| YBX1 | | transcription regulator | Activated | 2 | 1.35E-02 |
| SMAD4 | | transcription regulator | Activated | 2.182 | 1.06E-02 |
| MYCN | | transcription regulator | Activated | 2.639 | 7.70E-09 |
| TP53 | | transcription regulator | Activated | 2.642 | 1.88E-22 |
| MYC | 1.092 | transcription regulator | Activated | 2.418 | 5.12E-15 |
| EIF4E | | translation regulator | Activated | 2.21 | 1.01E-03 |
| DICER1 | | enzyme | Inhibited | -2.375 | 8.71E-05 |
| MIR124 | | group | Inhibited | -2 | 7.53E-03 |
| BDNF | | growth factor | Inhibited | -3.043 | 2.07E-17 |

| | | | | |
|---|---|---|---|---|
| miR-155-5p (miRNAs w/seed UAAUGCU) | mature microrna | Inhibited | -2.425 | 7.04E-04 |
| miR-34a-5p (and other miRNAs w/seed GGCAGUG) | mature microrna | Inhibited | -2.605 | 4.01E-04 |
| miR-124-3p (and other miRNAs w/seed AAGGCAC) | mature microrna | Inhibited | -4.2 | 3.24E-05 |
| mir-155 | microrna | Inhibited | -2.177 | 6.22E-02 |
| let-7 | microrna | Inhibited | -3.504 | 6.34E-05 |
| mir-122 | microrna | Inhibited | -2.538 | 1.05E-04 |
| mir-22 | microrna | Inhibited | -2.2 | 6.17E-04 |
| SOX1 | transcription regulator | Inhibited | -2.236 | 4.31E-02 |
| SOX3 | transcription regulator | Inhibited | -2.236 | 1.68E-02 |

Table 7: Predicted upstream regulators in genes exclusively regulated in wild-type and not in Cpeb1 knockout processes upon injury.

| Upstream Regulator | log2FC in dataset | Molecule Type | Predicted Activation State | Activation z-score | p-value of overlap |
|---|---|---|---|---|---|
| STAT4 | | transcription regulator | Inhibited | -2,216 | 1,57E-01 |
| CREM | | transcription regulator | Inhibited | -2,219 | 1,29E-02 |
| CREB1 | | transcription regulator | Inhibited | -3,192 | 6,88E-05 |
| MYCN | | transcription regulator | Inhibited | -2,425 | 9,90E-02 |
| IL1B | | cytokine | Inhibited | -2,309 | 3,08E-01 |
| HOXA10 | | transcription regulator | Activated | 2,000 | 2,04E-01 |
| miR-125b-5p (and other miRNAs w/seed CCCUGAG) | | mature microrna | Activated | 2,193 | 6,36E-03 |

Table 8: Predicted upstream regulators in injured processes upon Cpeb1 knockout.

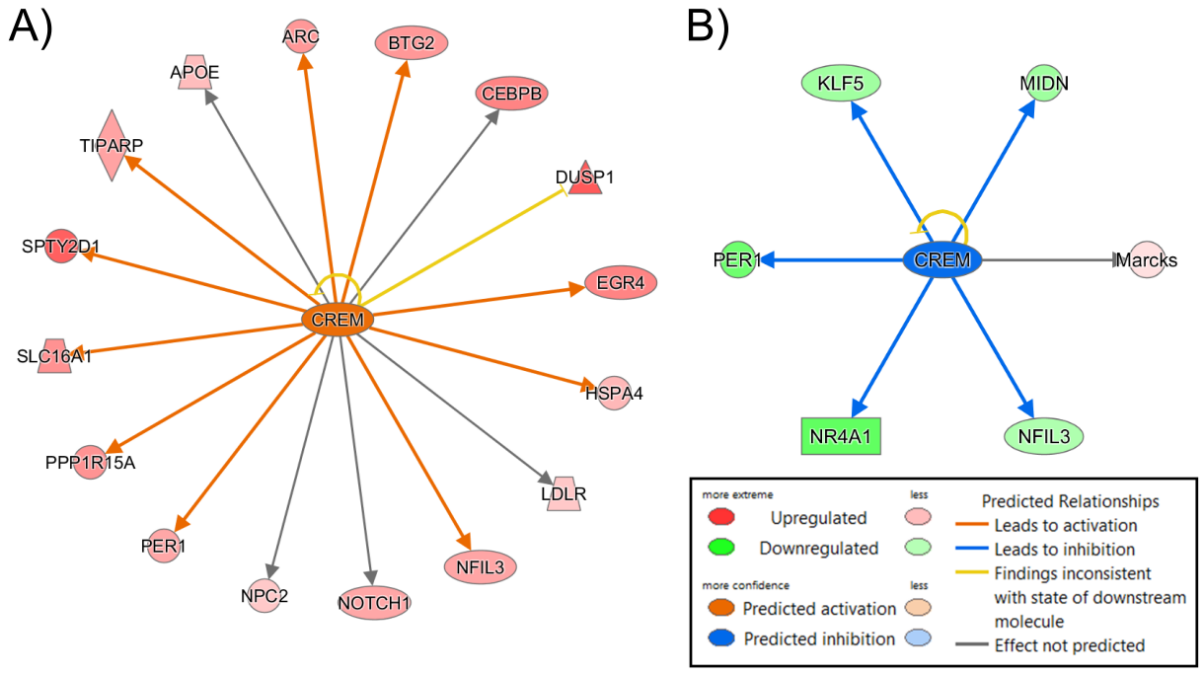


Figure 39: Network of genes regulated by Crem in A) genes exclusively regulated in wild-type and not in Cpeb1 knockout processes upon injury and B) injured processes upon Cpeb1 knockout

# 4. Discussion

## 4.1 Widespread uncoupling between transcription and translation in axonal regeneration and its functional relevance

Neurons are highly polarized cells with axons stretching up to several metres, thus the tip of an axon could be far removed from the cell soma. In such conditions, post-transcriptional regulation in the axoplasm provides a way for better spatial and temporal control over for protein expression (Holt and Schuman, 2013; Jung et al., 2012). This includes regulation of mRNA stability, transport of mRNAs to their target locations, translation silencing and activation, and protein degradation. Several studies have already demonstrated the relevance of localized translation in injured axons (Hanz et al., 2003; Perry et al., 2012; Yan et al., 2009). While these studies point to the behaviour of individual candidate genes, others have revealed that this phenomenon is widespread. For example, it has been discovered that the axonal repertoire of mRNAs changes substantially in response to injury in cortical neuron cultures (Taylor et al., 2009). In DRG neurons, injury-conditioned axons have increased levels of ribosomal protein P0 and phosphorylated eIF4E than non-conditioned ones (Verma et al., 2005). Mirroring these findings, growth cone-associated mRNAs Actb, Gap43 and Nrn1 have increased abundance in regenerating sciatic axons than in naïve ones, and the same goes for ribosomal components S6 and 5.8S rRNA and activated forms of the translation factors eIF2α and 4EBP (Kalinski et al., 2015). Findings from the simultaneous profiling of mRNA abundance and ribosome loading in the current study are in line with this notion, revealing extensive uncoupling between transcription and translation in the injured spinal cord (Fig. 8). Confirming that regenerating axons do have increased levels of protein synthesis, conditioned DRG axons have increased incorporation of radioactively labelled amino acids, and selective treatment of axons with cycloheximide severely hinders regeneration (Verma et al., 2005). Interestingly, the levels of ribosome components, translation factors and growth cone-associated mRNAs in transected spinal cord axons regenerating through a peripheral nerve graft are comparable to those of regenerating sciatic axons, suggesting that the capability to regenerate might be determined by the ability to synthesize certain mRNAs in the axon (Kalinski et al., 2015). Additionally, deletion of Pten, a negative regulator of mTOR signalling and protein synthesis, enhances axon regeneration in

RGCs (Park et al., 2008). Interestingly, in our data, although the time point taken for performing the spinal cord microarray is within the regenerative phase after SCI (Cajal, 1928; Kerschensteiner et al., 2005), a general decrease in ribosomal loading is observed (Fig. 8).

On closer inspection by GO functional clustering of differentially regulated genes in total and polysome-bound RNA fractions, it was found that CNS development genes have reduced mRNA abundance after SCI, being some of the most under-enriched GO categories. On the other hand, their ribosomal loading remained similar (Fig. 9). Down-regulation of mRNAs of neuron development genes could also be seen in injured cortical neurons (Fig. 24E). This suggests that although CNS development genes have their numbers of transcripts decreased after SCI, the remainder are translated more efficiently, possibly supporting the transient regeneration. We thus hypothesise that at this transient regenerative phase, axonal growth comes from translation of pre-existing pro-regeneration mRNAs, and is forced to stop when these mRNAs reach the end of their lifespan and are not replaced.

This is supported by the outgrowth screening in Drosophila, which shows that a considerable number of uncoupled genes that are effectors of axonal outgrowth show uncoupled behaviour after SCI, with reduced mRNA abundance but similar ribosomal loading (Fig. 21, Table 6). The neuron-specific aspect of the screening is important, as it shows that these genes are part of the intrinsic neuronal regenerative programme.

The use of the uncoupled response as a screening criterion in searching for factors influencing axonal growth also proved to be more efficient than based on prior knowledge on their role in neural and neurite development (Bassem Hassan, personal communication), indicating that genes governing regeneration are often subject to a tight post-transcriptional regulation. Interestingly, overexpression of these mRNAs was enough to increase axon outgrowth, hinting that the regulation comes from RNA degradation.

## 4.2 Increase in mRNA abundance of Jun and Fos family of transcription factors upon injury

If regulation of RNA degradation is the main mechanism governing the capability for regeneration, then it could be delineated by analyzing the transcriptome alone. In analyzing

the repertoire of mRNAs in naïve and injured wild-type neuronal processes using RNAseq, neuron-specific responses to injury could be elucidated, and with a much higher resolution than by microarray analysis. With that it was discovered that there is an up-regulation of mRNAs for the Jun and Fos family of transcription factors (Fig. 30).

The AP-1 transcription factor consists of a variety of dimers formed by different combinations of proteins from the Jun and Fos families. Members of the Jun and Fos families are considered to be early response genes that are expressed rapidly following axotomy as well as a number of other cellular insults (Herdegen et al., 1997; Leah et al., 1991). Specifically, c-Jun and c-Fos mRNAs were up-regulated within hours after lesion of sciatic nerve, subsequently inducing expression of nerve growth factor (NGF) (Hengerer et al., 1990). In line with this, c-Jun, Junb, c-Fos and Fosb were all highly up-regulated upon axotomy in wild-type axons. Most interestingly, this increase is much attenuated in Cpeb1 KO axons (Fig. 30), strongly suggesting the involvement of Cpeb1 in their expression regulation. In addition, these genes all contain CPEs in their transcripts. In particular, Cpeb1 has been shown to bind to the 3'UTR of c-Jun mRNA, and Cpeb1 knockout reduces c-Jun protein levels and subsequent activation of c-Jun target genes (Zearfoss et al., 2008).

There is strong evidence linking c-Jun to axonal injury response, with its expression persisting long after axon damage (Jenkins and Hunt, 1991). In addition, c-Jun expression is associated with the intensity of cell body reaction to injury. For example, rat rubrospinal neurons proximally axotomised by a C3 spinal cord transection, which elicits cell death and regeneration responses, expresses c-Jun robustly. On the other hand, those that were distally axotomised by a T10 spinal cord transection, which induces little reaction in the cell body, have minimal c-Jun expression (Jenkins et al., 1993; Richardson and Issa, 1984). The same association was observed upon transection of optic nerve (Hüll and Bähr, 1994; Robinson, 1995). The pro-regenerative effect of c-Jun has been demonstrated in many studies. Strong c-Jun expression correlated with regeneration of RGC axons through a peripheral nerve graft (Robinson, 1995). In another study, using axotomy of rat facial nerve as a model, deletion of c-Jun inhibited target muscle reinnervation, but rendered the motor neurons resistant to axotomy-induced cell death (Raivich et al., 2004). On the other hand, c-Jun is also associated with neuronal cell death, when neutralization of c-Jun protects sympathetic neurons against cell death induced by NGF withdrawal and overexpression of wild-type c-Jun induces apoptosis (Estus et al., 1994; Ham et al., 1995). The apparent ambivalent function of c-Jun

has been proposed to be a result of context-dependent interaction with other AP-1 proteins. Junb, c-Fos and Fosb show fluctuating or no increased expression following sciatic nerve crush injury, in contrast to c-Jun which showed prolonged increased expression for more than 2 months (Herdegen et al., 1992; Molander et al., 1992). In addition, purification of AP-1 consensus sequence binding proteins from axotomised and regenerating DRG neurons contains c-Jun but not c-Fos (De León et al., 1995). These data suggest a role for c-Jun in a signalling crossroad downstream of JNK following axonal injury, with the response determined in conjunction with other AP-1 factors such as c-Fos and ATF2 (Herdegen et al., 1997).

## 4.3 Association of RBPs with changes in mRNA abundance upon injury to spinal cords and cortical neurons

### 4.3.1 Cpeb1 influences changes in mRNA abundance in injured spinal cords and cortical neurons

Through this study, it was confirmed that CPE is a modulator of transcript behaviour in SCI. It is surprising that the influence is in the total and not the polysome-bound RNA fraction (Fig. 11), as Cpeb1 is a well known regulator of cytoplasmic polyadenylation. However, various groups have demonstrated that Cpeb1 has additional functions, such as RNA transport and storage. Cpeb1 transports its target mRNAs into dendrites in ribonucleoprotein (RNP) in rat hippocampal neurons, in a microtubule-dependent manner (Huang et al., 2003). Map2 is one of such targets, and overexpression of Cpeb1 increases dendritic localization of Map2 mRNA (Huang et al., 2003). Also, Cpeb1 has been found to be a component of stress granules and dcp1 bodies, which are involved in mRNA storage and degradation (Wilczynska et al., 2005). Overexpression of Cpeb1 increases the assembly of these structures, and this process is dependent on its RNA binding domain but not the phosphorylation site used by the kinase Aurora A to activate Cpeb1 for polyadenylation (Wilczynska et al., 2005). Similarly, deletion of the phosphorylation site does not alter the distribution of Cpeb1-containing foci within dendrites and synapses of Xenopus optic tectal neurons, suggesting that the function of Cpeb1 to transport and target mRNAs to RNP complexes is independent of its role in

polyadenylation (Bestman and Cline, 2009). Foci of inactive mutant Cpeb1 located near synapses do, however, show higher intensities than those of wild-type Cpeb1, suggesting that inability to activate translation may trap Cpeb1 and its target mRNA within the RNP complex (Bestman and Cline, 2009). A possible scenario linking these observations is that inactive Cpeb1 assembles its binding mRNA into RNP complexes, simultaneously repressing its translation and protecting it from degradation, while guiding it to its final location. This would agree with the observation that CPE-containing mRNAs are less decreased following SCI (Fig. 11A). Cpeb1 could preserve the transcripts and allow rapid reinitiation of translation at later time points. Further details related to Cpeb1 regulation of RNA degradation and transport are discussed in the following sections.

In the RNAseq of neuronal processes, another phenomenon was observed. Knockout of Cpeb1 has a large attenuating effect on the amplitude of the transcriptional injury response, with wild-type processes exhibiting a much larger fold change and in more genes than in Cpeb1 knockout ones (Fig. 24B and C). However, we did not observe an enrichment of the CPE motif among the differentially regulated mRNAs (Fig. 25A and B). One likely reason is that the time point chosen (24 hours post injury) is late, and by then the gene expression response is already dominated by late response genes and indirect downstream targets of CPE-containing transcripts. It would therefore be useful to repeat the experiment at earlier time points to investigate whether the CPE motif is enriched in upstream regulators of the injury response. Although earlier time points might not be easily feasible, as with less time after injury, the processes would have undergone less regrowth, which further reduces the already limited amount of collected RNA.

*In silico* upstream analysis has identified Crem to be a regulator of the injury response, which changes in wild-type processes upon injury but not in their CPEB1-deficient counterparts (Table 7 and Fig. 39). Crem transcripts increase upon injury, and at least some of its isoforms contain CPE. Crem is a part of the cAMP-mediated signal transduction and binds the cAMP responsive element (CRE) in promoters. Together with the closely related CRE binding proteins (Creb), it mediates response to many neurotrophin signalling pathways (Lonze and Ginty, 2002) and confers protective effects against neuronal cell death in the CNS in homeostasis and after injury (Mantamadiotis et al., 2002; Wu et al., 2012) and promotes axon outgrowth both in vivo and in vitro (Lonze et al., 2002). Crem possesses a large number of transcript isoforms that translates into both activators and repressors of transcription,

contributing to spatial and temporal regulation of gene expression (Lonze and Ginty, 2002). Although the repressor forms are driven from a 3' intronic promoter, leading to a truncated 5' end which separates them form the activator forms, the different forms also differ in their 3'UTRs (Sassone-Corsi, 1998). It is thus possible that Cpeb1 could exert its control based on different possession and arrangement of CPEs on the activator and repressor forms of Crem. Targets of Crem found to be up-regulated in our dataset include Btg2 and Cebpb, both of them being enhancers of axonal growth (Miyata et al., 2008; Yan et al., 2009) (Fig. 34).

On scrutinizing by further sub-dividing differentially regulated mRNAs in the RNAseq according to the number of CPEs they possess, a general association could be observed where the proportion of down-regulated transcripts decrease with increasing number of CPEs, whereas the up-regulated ones remains similar (Fig. 25C). This hints at some form of additive effect or interplay between the CPEs. CPE can exist in multiple copies in the 3'UTR of the same transcript, although there are less transcripts possessing higher number of CPEs (Fig. 25C), probably due to limitation from the length of the 3'UTR.

Indeed, it has been shown that the number of CPEs affects the way that Cpeb1 regulates RNA dynamics. In Xenopus meiotic progression, mRNAs of "early" genes, such as Mos and cyclin A1, have only one CPE, and they are polyadenylated once Cpeb1 is activated by phosphorylation. On the other hand, "late" genes such as cyclin B1 have more than one CPE. Dimerisation of the multiple Cpeb1 bound to these mRNAs precludes their interaction with CPSF, and prevents immediate polyadenylation. Subsequent degradation of Cpeb1 mediated by the meiotic programme reduces the Cpeb1:CPE ratio, rendering some of the CPEs empty, allowing the remaining Cpeb1 to interact with CPSF and induce polyadenylation in "late" genes (Méndez et al., 2002). This phenomenon has been discovered later also to occur in mammalian cell cycle progression, with destruction of Cpeb1 mediated by the isomerase Pin1 via ubiquitination (Nechama et al., 2012). This complex step-wise activation allows a single master regulator to control the fate of multiple target mRNAs, even if they are to be translated at different times. In addition, CPE interacts with other cis-acting elements, namely PBE and Hex, and the number, arrangement and distance between these elements on the 3'UTR forms a combinatorial code that will determine the polyadenylation outcome of the mRNAs harbouring them (Piqué et al., 2008). Although the aforementioned studies are concerned with polyadenylation and translation, nevertheless it illustrates the complex

regulation by Cpeb1 and other cis-acting elements on the 3'UTR, implying that perhaps the same is true for regulation of RNA stability.

### 4.3.2 AREs increase mRNA abundance in injured spinal cords

While the direct effect Cpeb1 exerts on its target mRNA upon neuronal injury would require more work to be elucidated, a link was found between CPE and AREs. Most transcripts containing CPE also possess AREs, and transcripts containing both motifs have higher mRNA abundance and ribosomal loading than those that do not after SCI (Fig. 14D). ARE promotes RNA stability when bound by the HuR family of proteins (Peng et al., 1998; Schoenberg and Maquat, 2012). In particular, the neuron specific HuD increases the half-life of the pro-regenerative mRNA Gap43 (Beckel-Mitchener et al., 2002; Mobarak et al., 2000) and is crucial to its localization to axons, where Gap43 induces axon elongation (Yoo et al., 2013). In a study using superior cervical ganglion axons, the mRNA levels of acetylcholinesterase (AChE), an enzyme responsible for neurotransmission that also plays a role in neurite elongation (Koenigsberger et al., 1997), is reduced following axotomy (Deschênes-Furry et al., 2007). This was induced by a decrease in mRNA stability, and coincides with a reduction of HuD binding to the ARE region found on the 3'UTR of AChE mRNA. Exogenous expression of HuD was found to maintain the mRNA levels of AChE as well as Gap43 after SCG axotomy (Deschênes-Furry et al., 2007). Hence, Cpeb1 might work together with HuD in protecting target mRNAs from degradation and enhance axon regrowth upon axonal injury.

On polyadenylation, ARE was found to act opposite to CPE, promoting deadenylation by recruiting the CCR4 deadenylase to the mRNA. This delays polyadenylation of these mRNAs to a "third" wave (after the "early" and "late" genes mentioned previously), which occurs during interkinesis in Xenopus oocyte meiosis (Belloc and Méndez, 2008). However, within our TSAA, no association was observed on ribosome-loading with the possession of both CPE and ARE (Fig. 14D).

## 4.4 Regulation of RNA metabolism on axon growth and regeneration and the involvement of Cpeb1

### 4.4.1 RNA degradation, transport and the role of miRNA and RNPs

One intriguing point coming from this study is that upon the tested target genes, Cpeb1 does not seem to impart any influence on mRNA stability (Fig. 29, 31, 33), but the stability of most targets were increased upon injury (Fig. 33). Therefore there appears to be separate mechanisms in play increasing the stability of RNAs upon injury.

The miRNA pathway, being a common regulator of RNA dynamics, is naturally a prime target for investigation. Indeed, there is extensive differential regulation of miRNAs upon injury to DRG and the spinal cord (Liu et al., 1997; Zhou et al., 2012). Some identified miRNAs had a transient up-regulation within a few hours after SCI followed by long term down-regulation, indicating the temporal control of gene expression in different phases following SCI (Liu et al., 2009). Another study reported that the repertoire of axonal miRNAs changes substantially upon injury to the sciatic nerve. Predicted targets of these miRNAs are related to microtubule dynamics, neurite outgrowth, and degeneration of spinal cord, indicating there is an important functional role played by miRNAs in injury response (Phay et al., 2015). Protein mediators of RNAi such as Ago3, Ago4 and Dicer were also found to localise to DRG growth cones and distal axons (Hengst et al., 2006). Selective application of siRNA against RhoA in distal axons reduces RhoA mRNA levels only in distal axons and prevented Sema3A-induced growth cone collapse, demonstrating the functionality of the axonal RNAi machinery (Hengst et al., 2006). Among the miRNAs that are down-regulated upon SCI, many are predicted to target apoptosis related genes such as caspase-3 and Bcl2 (Liu et al., 2009). The loosening of repression on anti-apoptosis genes agrees with the observation in our data, that they are up-regulated after injury (Fig. 24). In addition, miR-222, which is differentially regulated upon injury in DRG neurons, directly targets Pten mRNA and increases neurite outgrowth in DRG neurons (Zhou et al., 2012). Interestingly, microRNAs are involved in activities of Cpeb1. Cpeb1 and its activating kinase Aurora A are targeted by miR-122 and let-7 respectively (Burns et al., 2011; Schnepp et al., 2015).

miRNA-directed RNA silencing was shown to have a heavy connection to p-bodies and other RNPs, which are RNA-protein complexes for storage and degradation of RNAs. Many proteins associated with RNA-induced silencing complex (RISC) were found in p-bodies, including the argonaute proteins (Kulkarni et al., 2010). In addition, the decapping enzyme Dcp1 and the 5' to 3' riboexonuclease Xrn1p, both components of p-bodies, as well as Ago2 and Upf1 (mediators of nonsense mediated decay), are concentrated in Staufen- and FMRP-containing RNPs in Drosophila CNS neuron cultures, linking miRNA and p-bodies to these RNPs in a neuronal context (Barbee et al., 2006). These RNPs do appear to be associated to injury response, as expression of FMRP, Ago2 and Dcp1 are induced upon injury to sciatic nerve and DRG neurons, and Dcp1 localisation to DRG axons increases after a conditioning injury (Wu et al., 2011).

Of particular note, LSm1, another factor for RNA degradation, forms RNPs together with Dcp1 and Xrn1p (Ingelfinger et al., 2002), and transports RNAs such as β-actin, Map1b and eEF1α to dendrites, with stimulation of glutamatergic receptors inducing localisation of LSm1 into dendritic spines of cultured hippocampal neurons (di Penta et al., 2009). The fact that these RNPs contains RNA degradation enzymes but also transports mRNAs suggests that the transport and degradation of mRNAs are tightly connected. LSm1 RNPs also contains CBP80, a cap binding protein that associates with pre-mRNAs, indicating that the complex is formed inside the nucleus (di Penta et al., 2009).

Interestingly, Cpeb1 is also found within the LSm1 containing p-bodies in the hippocampus (di Penta et al., 2009) and in p-bodies as well as stress granules in HeLa cells (Wilczynska et al., 2005), which are structures for RNA storage during cell stress. It is thus speculated that Cpeb1 could shuffle its target RNAs into p-bodies, which then undergo transport or degradation. Supporting this notion, Cpeb1 mutants lacking its RRM is unable to be incorporated into p-bodies and stress granules (Wilczynska et al., 2005). In addition, stress granules induced by Cpeb1 overexpression but not by arsenite treatment, was shown to recruit components of p-bodies, and it was proposed that Cpeb1 is responsible for linking stress granules and p-bodies, shuffling RNAs stored in stress granules down the path to degradation by p-bodies (Wilczynska et al., 2005).

Within our data, Cpeb1 knockout induces a change in axonal levels of a number of CPE containing mRNAs upon injury (Fig. 32). However the lack of association between Cpeb1

and the stability of tested CPE containing mRNAs (Fig. 33) suggests that Cpeb1 probably plays a bigger role in the transport rather than the degradation or RNA storage aspect of RNPs. Indeed, Cpeb1 do serves a role in neuronal mRNA transport. Cpeb1 is able to transport mRNAs of Bdnf, CamKII and Map2 into dendrites of hippocampal neurons (Huang et al., 2003; Oe and Yoneda, 2010). It was demonstrated that CPE alone is sufficient to target mRNA to dendrites, when Gfp reporter with a polylinker containing a triplicate CPE has increased transport into dendrites over one without CPE (Huang et al., 2003). Cpeb1 RNPs contain the motor proteins dynein and kinesin, and a Cpeb1 mutant that could not interact with these motor proteins causes hindered transport of Map2 mRNA. Proving that the transport mechanism is dependent on microtubules, dendritic localisation of Cpeb1 particles is abolished when the microtubule is disrupted by vincristine treatment (Huang et al., 2003). In addition, activity-dependent transport of Bdnf mRNA into hippocampal neuron dendrites is Cpeb1 dependent, with depolarisation enhancing the binding of Cpeb1 to the 3'UTR (Oe and Yoneda, 2010), demonstrating it is part of the temporal control of localised gene expression.

Together, these findings points to the direction that Cpeb1 organises its target mRNAs into RNPs for degradation or storage and transport. One important point that remains unclear, is whether this is mediated actively by Cpeb1 itself via modifications or dimerisation of the Cpeb1 protein; or if Cpeb1 is bound to these RNAs merely due to its role in repressing translation, and the fate of the repressed mRNAs are decided by other factors.

### 4.4.2 Alternative polyadenylation

Among the many means to regulate protein expression, alternative polyadenylation (APA) is one of them. APA determines where polyadenylation begins in the 3'UTR, thus generating heterogeneous 3'UTRs, similar to what alternative splicing does to coding exons (Di Giammartino et al., 2011). This affects the presence of motifs on the 3'UTR such as binding motifs for RBPs and miRNAs, and may have an effect on the stability, intracellular localization and translation of the transcript.

Polyadenylation signals consists of the canonical AAUAAA and AUUAAA sequences, but 10 single base variants have been discovered (Beaudoing, 2000). Up to 54% and 32% of

genes were found to contain multiple polyadenylation sites for their transcripts in the human and mouse genomes respectively (Tian et al., 2005). Within transcripts containing multiple polyadenylation sites, the 3'-most site tends to use canonical signals and the 5' sites tend to use variant signals, suggesting that proximal sites are used less efficiently and requires auxiliary factors (Beaudoing, 2000). A shorter 3'UTR leads to higher mRNA stability and protein expression, due to loss of miRNA binding sites and other cis regulatory elements (Mayr and Bartel, 2009). APA has been found to affect ubiquitiously transcribed genes during transformation and differentiation and creates different 3'UTR ratios, with genes involved in tissue-specific processes having their shorter 3'UTR isoforms being predominantly expressed (Lianoglou et al., 2013). APA was found to feature extensively in cancer cells where the mRNA isoforms of shorter 3'UTR is preferentially expressed (Mayr and Bartel, 2009). The shorter isoforms of the proto-oncogene IGF2BP1/IMP-1 has a higher transformation potential than the full length mRNA, leading to the hypothesis that APA is the reason that oncogenes are overexpressed in some cases where there is no genetic alteration (Mayr and Bartel, 2009).

In our data, with the DaPars algorithm, genes were analyzed for the occurrence of APA. In wild-type processes, a considerable number of genes underwent 3'UTR lengthening upon injury, with the corresponding expected down-regulation in expression, likely due to the presence of more miRNA binding sites in the longer 3'UTR (Fig. 34C). However this expected correlation between 3'UTR lengthening and expression is not observed for other comparisons. Regardless, APA events were also detected in naïve and injured processes upon Cpeb1 knockout (Fig. 34A and B), suggesting a role for Cpeb1. Indeed, of the many functions discovered for Cpeb1, regulation of APA is one of them. Cpeb1 was found to shuttle into the nucleus and recruit splicing factors to different polyadenylation sites and mediates the 3'UTR shortening of a cohort of transcripts, and this correlates with increased cell proliferation and tumourigenesis in tumour cells (Bava et al., 2013). In our dataset, Map2k7 is among the genes identified by DaPars to have undergone APA upon Cpeb1 knockout. Map2k7 poses as an interesting target, as Map2k7 promotes elongation of neurites via organisation of microtubules (Yamasaki et al., 2011), and is thus a candidate gene for Cpeb1 to promote regeneration via activation of the JNK pathway in our system. Importantly, the long 3'UTR isoform increases the effectiveness of Map2k7, by increasing localisation to neurites and enhances phosphorylation and activation of the protein. Importantly, Cpeb1

knockout shifts the bias towards the short 3'UTR in our data (Fig. 35A), and the long 3'UTR contains CPEs whereas the short one contains none. This highly suggests that Cpeb1 promotes usage of the longer 3'UTR via binding to CPEs. On validation, the long to short 3'UTR ratio is indeed lower upon Cpeb1 knockout, but only in whole neuron samples (Fig. 35B). Perhaps the amount of RNA extracted from processes is too low, reducing sensitivity. A good alternative experiment would be to transfect cells with a reporter mRNA like Gfp fused to the 3'UTR of Map2k7, and check for differences in APA events as well as reporter expression and localisation upon Cpeb1 knockout or overexpression.

### 4.4.3 Polyadenylation and translation

Localised translation in axonal regeneration has been demonstrated in various studies (Kalinski et al., 2015; Verma et al., 2005). Interestingly, in one study, inhibition of translation by systemic treatment with cycloheximide immediately after SCI reduced neuronal apoptosis and long term functional recovery (Liu et al., 1997), though perhaps this is mediated via reduction in inflammation as the aforementioned treatment is not neuron specific. As cytoplasmic polyadenylation is a precursor to reactivation of translation of repressed mRNAs, it is thought that this is perhaps the way through which regulation of translation in SCI is executed. Indeed, in a neuronal context, blocking polyadenylation reduces growth cone collapse in response to Sema3A treatment in Xenopus retinal axons (Lin et al., 2009). In addition, Cpeb1 mediates dendrite morphogenesis of hippocampal neurons via cytoplasmic polyadenylation of NDUFV2, a component of the electron transport chain complex I (Oruganty-Das et al., 2012). Knockout of Cpeb1 reduces translation of Ndufv2, activity of electron transport chain complex I and cellular ATP levels, ultimately decreasing dendrite length and branching in the dentate gyrus (Oruganty-Das et al., 2012). However, we were able to detect little definitive changes in poly(A) tail lengths upon Cpeb1 knockout among our tested targets (Fig. 37). This could be attributed to the complex regulation of polyadenylation, with the number and arrangement of CPE and other RBP binding motifs all exerting an influence on the timing and sequence of polyadenylation events (Méndez et al., 2002; Nechama et al., 2012; Piqué et al., 2008).

In this case a screening approach would be helpful. For example, a column based approach with poly(U) sepharose column to capture RNAs with poly(A) tails longer than 50 bases (Udagawa et al., 2013). With recent advances in RNAseq and the many modifications developed for specific purposes, this can be applied to perform genome-wide measurements of poly(A) tail lengths. One such method is TAIL-seq, which via ligating an adapter at the end of the poly(A) tail, generates libraries only from the 3'UTR and poly(A) tail, allowing much higher resolution in this region than would be provided by standard RNAseq protocols (Chang et al., 2014). Surprisingly, the study revealed that poly(A) tail length does not correlate with translation efficiency in terms of ribosome density and translation rate reported in other studies, but a mild correlation is found with mRNA half-lives, where mRNAs with a longer poly(A) tail generally have longer half-lives (Aviner et al., 2013; Chang et al., 2014; Schwanhäusser et al., 2011). This agrees with the notion that poly(A) tail length and deadenylation drives mRNAs into decay pathways.

### 4.4.4 Retrograde transport of locally translated proteins

One important question arising from the RNAseq data is: What are the mRNAs of transcription factors doing in the axon? One hypothesis is retrograde signalling, where factors that elicit a cell body response for injury is translated in the axon tip and retrogradely transported back to the cell nucleus. For example, retrograde transport of Importin β1, part of a protein complex that binds nuclear localisation signals (NLS) and is transported in a retrograde manner towards the cell body, is translated locally in axons (Hanz et al., 2003). Saturating retrograde transport with NLS peptides abolishes the regenerative effect of a conditioning lesion in sciatic nerve and axon specific depletion of Importin β1 mRNA reduces the transcriptional response to nerve injury in DRGs and delays functional recovery (Hanz et al., 2003; Perry et al., 2012). Knockout of Cpeb1 in injured processes down-regulates genes related to nuclear import (Fig. 26E), suggesting that the retrograde transport in injury response is Cpeb1-dependent. Similar to Cpeb1 knockout in our data (Fig. 26C), axonal depletion of Importin β1 has little effect in uninjured neurons, in line with its role as a mediator of injury response. Importin β1 mRNA is localised to axons via its 3'UTR (Perry et al., 2012), affirming the role of 3'UTR in harbouring targeting elements for mRNAs and making it a potential Cpeb1 target. However, despite CPEs being present on the 3'UTR of

Importin β1, Cpeb1 knockout did not alter the polyadenylation status of the mRNA (Fig. 37). It would be of interest to perform mRNA stability assay and deletion of the CPE motif on Importin β1 mRNA, to ascertain if Cpeb1 has any effect on its degradation and transport.

Retrograde transport were also discovered for signalling molecules upstream of the JNK pathway such as Mekk1, Map2k7, Map2k4 and Mlk3, following sciatic nerve axotomy, with increasing nuclear phosphorylation of c-Jun (Lindwall and Kanje, 2005). While this agrees with the model of the injured axons signalling the cell body to initiate a response, it casts doubt over why is there up-regulation of c-Jun mRNA in injured processes (Fig. 30). However, another study observed c-Jun proteins in dendrites, lending support to the notion of localised translation of c-Jun. Additionally, Cpeb1 was found to bind the 3'UTR of c-Jun mRNA in hippocampal neurons, and knockout of Cpeb1 reduces c-Jun protein levels and growth hormone (GH) mRNA, a target gene of c-Jun (Zearfoss et al., 2008). Therefore it is hypothesised that Cpeb1 induces axonal localisation or translation of c-Jun, which is subsequently transported back into the nucleus where it induces transcription of GH. The lack of change in c-Jun mRNA stability after Cpeb1 knockout confirms that it does not work via protecting the mRNA from degradation (Fig. 31 and 33). Similar behaviour of Junb, c-Fos and Fosb mRNAs suggests they are regulated in the same way. More experiments are needed to prove if this is indeed the case. If true, then there would be a redundancy of having two mechanisms to get c-Jun into the nucleus, perhaps as a way to amplify the injury response.

## 4.5 Conclusion

In summary, starting from TSAA using SCI as a model, we discovered that uncoupling of transcription and translation is a widespread phenomenon in the injury response. Translation of mRNAs related to CNS development appears to be prioritised in the acute phase after injury, and limitations in their mRNA abundance likely lead to the eventual failure in regeneration. Many uncoupled genes were found to be regulators of axonal growth, demonstrating that uncoupling behaviour could be used for screening for regulators of regeneration. In addition, Cpeb1 was identified to be a regulator of mRNA abundance after neuronal injury, as well as being a positive regulator of neuronal regeneration in both mice and Drosophila, with highly conserved functions across the two species. Knockout of Cpeb1

greatly attenuated the transcriptome response of injured processes in cortical neurons. It was also discovered that there is substantial APA and increase in RNA stability upon injury in cortical neurons. The direct targets and exact mechanism through which Cpeb1 exerts its function remains elusive, however, as the experiments in this study could not identify targets for Cpeb1-mediated mRNA stability or polyadenylation.

# 5. References


Alexandrov, I.M., Ivshina, M., Jung, D.Y., Friedline, R., Ko, H.J., Xu, M., O'Sullivan-Murphy, B., Bortell, R., Huang, Y.-T., Urano, F., et al. (2012). Cytoplasmic Polyadenylation Element Binding Protein Deficiency Stimulates PTEN and Stat3 mRNA Translation and Induces Hepatic Insulin Resistance. PLoS Genet. *8*, e1002457.

Amrute-Nayak, M., and Bullock, S.L. (2012). Single-molecule assays reveal that RNA localization signals regulate dynein-dynactin copy number on individual transcript cargoes. Nat. Cell Biol. *14*, 416–423.

Anders, S., Pyl, P.T., and Huber, W. (2014). HTSeq - A Python framework to work with high-throughput sequencing data. Bioinformatics *31*, 166–169.

Ashburner, M., Ball, C.A., Blake, J.A., Botstein, D., Butler, H., Cherry, J.M., Davis, A.P., Dolinski, K., Dwight, S.S., Eppig, J.T., et al. (2011). The Gene Ontology Consortium. Gene ontology: tool for the unification of biology. Nat. Genet. *25*, 25–29.

Aviner, R., Geiger, T., and Elroy-Stein, O. (2013). Novel proteomic approach (PUNCH-P) reveals cell cycle-specific fluctuations in mRNA translation. Genes Dev. *27*, 1834–1844.

Ayaz, D., Leyssen, M., Koch, M., Yan, J., Srahna, M., Sheeba, V., Fogle, K.J., Holmes, T.C., and Hassan, B. a (2008). Axonal injury and regeneration in the adult brain of Drosophila. J. Neurosci. *28*, 6010–6021.

Baker, K.E., and Coller, J. (2006). The many routes to regulating mRNA translation. Genome Biol. *7*, 332.

Baker, B.J., Akhtar, L.N., and Benveniste, E.N. (2009). SOCS1 and SOCS3 in the control of CNS immunity. Trends Immunol. *30*, 392–400.

Barbee, S.A., Estes, P.S., Cziko, A.-M., Hillebrand, J., Luedeman, R.A., Coller, J.M., Johnson, N., Howlett, I.C., Geng, C., Ueda, R., et al. (2006). Staufen- and FMRP-containing neuronal RNPs are structurally and functionally related to somatic P bodies. Neuron *52*, 997–1009.

Bareyre, F.M., Garzorz, N., Lang, C., Misgeld, T., Büning, H., and Kerschensteiner, M.

(2011). In vivo imaging reveals a phase-specific role of STAT3 during central and peripheral nervous system axon regeneration. Proc. Natl. Acad. Sci. *108*, 6282–6287.

Barnard, D.C., Ryan, K., Manley, J.L., and Richter, J.D. (2004). Symplekin and xGLD-2 are required for CPEB-mediated cytoplasmic polyadenylation. Cell *119*, 641–651.

Barreau, C., Paillard, L., and Osborne, H.B. (2005). AU-rich elements and associated factors: are there unifying principles? Nucleic Acids Res. *33*, 7138–7150.

Bava, F.-A., Eliscovich, C., Ferreira, P.G., Miñana, B., Ben-Dov, C., Guigó, R., Valcárcel, J., and Méndez, R. (2013). CPEB1 coordinates alternative 3′-UTR formation with translational regulation. Nature 1–7.

Beaudoing, E. (2000). Patterns of Variant Polyadenylation Signal Usage in Human Genes. Genome Res. *10*, 1001–1010.

Beckel-Mitchener, A.C., Miera, A., Keller, R., and Perrone-Bizzozero, N.I. (2002). Poly(A) tail length-dependent stabilization of GAP-43 mRNA by the RNA-binding protein HuD. J. Biol. Chem. *277*, 27996–28002.

Beelman, C.A., and Parker, R. (1995). Degradation of mRNA in eukaryotes. Cell *81*, 179–183.

Behr, R. (2000). CREM activator and repressor isoforms in human testis: sequence variations and inaccurate splicing during impaired spermatogenesis. Mol. Hum. Reprod. *6*, 967–972.

Belloc, E., and Méndez, R. (2008). A deadenylation negative feedback mechanism governs meiotic metaphase arrest. Nature *452*, 1017–1021.

Bernstein, D.R., and Stelzner, D.J. (1983). Plasticity of the corticospinal tract following midthoracic spinal injury in the postnatal rat. J. Comp. Neurol. *221*, 382–400.

Bestman, J.E., and Cline, H.T. (2009). The Relationship between Dendritic Branch Dynamics and CPEB-Labeled RNP Granules Captured in Vivo. Front. Neural Circuits *3*, 1–14.

Blichenberg, a, Schwanke, B., Rehbein, M., Garner, C.C., Richter, D., and Kindler, S. (1999). Identification of a cis-acting dendritic targeting element in MAP2 mRNAs. J. Neurosci. *19*, 8818–8829.

Bradke, F., Fawcett, J.W., and Spira, M.E. (2012). Assembly of a new growth cone after axotomy: the precursor to axon regeneration. Nat. Rev. Neurosci. *13*, 183–193.

Bramham, C.R., and Wells, D.G. (2007). Dendritic mRNA: transport, translation and function. Nat. Rev. Neurosci. *8*, 776–789.

Brand, A.H., and Perrimon, N. (1993). Targeted gene expression as a means of altering cell fates and generating dominant phenotypes. Development *118*, 401–415.

Brittis, P. a, Lu, Q., and Flanagan, J.G. (2002). Axonal protein synthesis provides a mechanism for localized regulation at an intermediate target. Cell *110*, 223–235.

Bullock, S.L., Nicol, A., Gross, S.P., and Zicha, D. (2006). Guidance of bidirectional motor complexes by mRNA cargoes through control of dynein number and activity. Curr. Biol. *16*, 1447–1452.

Burns, D.M., D'Ambrogio, A., Nottrott, S., and Richter, J.D. (2011). CPEB and two poly(A) polymerases control miR-122 stability and p53 mRNA translation. Nature *473*, 105–108.

Cajal, S.R. y (1928). Degeneration and regeneration of the nervous system. Oxford Press 799–802.

Cajal, S.R., DeFelipe, J., and Jones, E.G. (1991). Cajal's Degeneration and Regeneration of the Nervous System (Oxford University Press).

Campbell, D.S., and Holt, C.E. (2001). Chemotropic Responses of Retinal Growth Cones Mediated by Rapid Local Protein Synthesis and Degradation. Neuron *32*, 1013–1026.

Cargnin, F., Nechiporuk, T., Müllendorff, K., Stumpo, D.J., Blackshear, P.J., Ballas, N., and Mandel, G. (2014). An RNA binding protein promotes axonal integrity in peripheral neurons by destabilizing REST. J. Neurosci. *34*, 16650–16661.

Chang, H., Lim, J., Ha, M., and Kim, V.N. (2014). TAIL-seq: Genome-wide Determination of Poly(A) Tail Length and 3' End Modifications. Mol. Cell *53*, 1044–1052.

Chang, Y.-F., Imam, J.S., and Wilkinson, M.F. (2007). The nonsense-mediated decay RNA surveillance pathway. Annu. Rev. Biochem. *76*, 51–74.

Charlesworth, A., Meijer, H.A., and de Moor, C.H. (2013). Specificity factors in cytoplasmic

polyadenylation. Wiley Interdiscip. Rev. RNA *4*, 437–461.

Cho, Y., and Cavalli, V. (2012). HDAC5 is a novel injury-regulated tubulin deacetylase controlling axon regeneration. EMBO J. *31*, 3063–3078.

Cho, K.-S., Yang, L., Lu, B., Feng Ma, H., Huang, X., Pekny, M., and Chen, D.F. (2005). Re-establishing the regenerative potential of central nervous system axons in postnatal mice. J. Cell Sci. *118*, 863–872.

Cho, Y., Sloutsky, R., Naegle, K.M., and Cavalli, V. (2013). Injury-Induced HDAC5 Nuclear Export Is Essential for Axon Regeneration. Cell *155*, 894–908.

Côté, M.-P., Amin, A.A., Tom, V.J., and Houle, J.D. (2011). Peripheral nerve grafts support regeneration after spinal cord injury. Neurotherapeutics *8*, 294–303.

Couttet, P., Fromont-Racine, M., Steel, D., Pictet, R., and Grange, T. (1997). Messenger RNA deadenylylation precedes decapping in mammalian cells. Proc. Natl. Acad. Sci. U. S. A. *94*, 5628–5633.

David, S., and Aguayo, A.J. (1981). Axonal elongation into peripheral nervous system "bridges" after central nervous system injury in adult rats. Science *214*, 931–933.

Davidovic, L., Jaglin, X.H., Lepagnol-Bestel, A.-M., Tremblay, S., Simonneau, M., Bardoni, B., and Khandjian, E.W. (2007). The fragile X mental retardation protein is a molecular adaptor between the neurospecific KIF3C kinesin and dendritic RNA granules. Hum. Mol. Genet. *16*, 3047–3058.

Decker, C.J., and Parker, R. (2012). P-bodies and stress granules: possible roles in the control of translation and mRNA degradation. Cold Spring Harb. Perspect. Biol. *4*, a012286.

Deschênes-Furry, J., Mousavi, K., Bolognani, F., Neve, R.L., Parks, R.J., Perrone-Bizzozero, N.I., and Jasmin, B.J. (2007). The RNA-binding protein HuD binds acetylcholinesterase mRNA in neurons and regulates its expression after axotomy. J. Neurosci. *27*, 665–675.

Di Giammartino, D.C., Nishida, K., and Manley, J.L. (2011). Mechanisms and Consequences of Alternative Polyadenylation. Mol. Cell *43*, 853–866.

Dionne, M.S., Brunet, L.J., Eimon, P.M., and Harland, R.M. (2002). Noggin Is Required for

Correct Guidance of Dorsal Root Ganglion Axons. Dev. Biol. *251*, 283–293.

Dobin, A., Davis, C.A., Schlesinger, F., Drenkow, J., Zaleski, C., Jha, S., Batut, P., Chaisson, M., and Gingeras, T.R. (2013). STAR: ultrafast universal RNA-seq aligner. Bioinformatics *29*, 15–21.

Donnelly, C.J., Willis, D.E., Xu, M., Tep, C., Jiang, C., Yoo, S., Schanen, N.C., Kirn-Safran, C.B., van Minnen, J., English, A., et al. (2011). Limited availability of ZBP1 restricts axonal mRNA localization and nerve regeneration capacity. EMBO J. *30*, 4665–4677.

Donnelly, C.J., Park, M., Spillane, M., Yoo, S., Pacheco, a., Gomes, C., Vuppalanchi, D., McDonald, M., Kim, H.K., Merianda, T.T., et al. (2013). Axonally Synthesized -Actin and GAP-43 Proteins Support Distinct Modes of Axonal Growth. J. Neurosci. *33*, 3311–3322.

Dumont, R.J., Okonkwo, D.O., Verma, S., Hurlbert, R.J., Boulos, P.T., Ellegala, D.B., and Dumont, A.S. Acute spinal cord injury, part I: pathophysiologic mechanisms. Clin. Neuropharmacol. *24*, 254–264.

Elsaeidi, F., Bemben, M. a, Zhao, X.-F., and Goldman, D. (2014). Jak/STAT signaling stimulates zebrafish optic nerve regeneration and overcomes the inhibitory actions of socs3 and sfpq. J. Neurosci. *34*, 2632–2644.

Ertürk, A., Hellal, F., Enes, J., and Bradke, F. (2007). Disorganized microtubules underlie the formation of retraction bulbs and the failure of axonal regeneration. J. Neurosci. *27*, 9169–9180.

Estus, S., Zaks, W.J., Freeman, R.S., Gruda, M., Bravo, R., and Johnson, E.M. (1994). Altered gene expression in neurons during programmed cell death: identification of c-jun as necessary for neuronal apoptosis. J. Cell Biol. *127*, 1717–1727.

Falcon, S., and Gentleman, R. (2007). Using GOstats to test gene lists for GO term association. Bioinformatics *23*, 257–258.

Feltrin, D., Fusco, L., Witte, H., Moretti, F., Martin, K., Letzelter, M., Fluri, E., Scheiffele, P., and Pertz, O. (2012). Growth cone MKK7 mRNA targeting regulates MAP1b-dependent microtubule bundling to control neurite elongation. PLoS Biol. *10*, e1001439.

Ford, L.P., Bagga, P.S., and Wilusz, J. (1997). The poly(A) tail inhibits the assembly of a 3'-

to-5' exonuclease in an in vitro RNA stability system. Mol. Cell. Biol. *17*, 398–406.

Ford, L.P., Watson, J., Keene, J.D., and Wilusz, J. (1999). ELAV proteins stabilize deadenylated intermediates in a novel in vitro mRNA deadenylation/degradation system. Genes Dev. *13*, 188–201.

Foulkes, N.S., Mellström, B., Benusiglio, E., and Sassone-Corsi, P. (1992). Developmental switch of CREM function during spermatogenesis: from antagonist to activator. Nature *355*, 80–84.

Gadani, S.P., Walsh, J.T., Lukens, J.R., and Kipnis, J. (2015). Dealing with Danger in the CNS: The Response of the Immune System to Injury. Neuron *87*, 47–62.

Gebauer, F., and Hentze, M.W. (2004). Molecular mechanisms of translational control. Nat. Rev. Mol. Cell Biol. *5*, 827–835.

Goldberg, J.L., Espinosa, J.S., Xu, Y., Davidson, N., Kovacs, G.T. a, and Barres, B. a (2002). Retinal ganglion cells do not extend axons by default: promotion by neurotrophic signaling and electrical activity. Neuron *33*, 689–702.

Görlach, M., Burd, C.G., and Dreyfuss, G. (1994). The mRNA poly(A)-binding protein: localization, abundance, and RNA-binding specificity. Exp. Cell Res. *211*, 400–407.

Grafi, G., Sela, I., and Galili, G. (1993). Translational regulation of human beta interferon mRNA: association of the 3' AU-rich sequence with the poly(A) tail reduces translation efficiency in vitro. Mol. Cell. Biol. *13*, 3487–3493.

Grosset, C., Boniface, R., Duchez, P., Solanilla, A., Cosson, B., and Ripoche, J. (2004). In vivo studies of translational repression mediated by the granulocyte-macrophage colony-stimulating factor AU-rich element. J. Biol. Chem. *279*, 13354–13362.

Guertin, D.A., and Sabatini, D.M. (2007). Defining the role of mTOR in cancer. Cancer Cell *12*, 9–22.

Gumy, L.F., Yeo, G.S.H., Tung, Y.-C.L., Zivraj, K.H., Willis, D., Coppola, G., Lam, B.Y.H., Twiss, J.L., Holt, C.E., and Fawcett, J.W. (2011). Transcriptome analysis of embryonic and adult sensory axons reveals changes in mRNA repertoire localization. RNA *17*, 85–98.

Gumy, L.F., Katrukha, E. a, Kapitein, L.C., and Hoogenraad, C.C. (2013). New insights into mRNA trafficking in axons. Dev. Neurobiol. *74*, 233–244.

Hake, L.E., and Richter, J.D. (1994). CPEB is a specificity factor that mediates cytoplasmic polyadenylation during Xenopus oocyte maturation. Cell *79*, 617–627.

Ham, J., Babij, C., Whitfield, J., Pfarr, C.M., Lallemand, D., Yaniv, M., and Rubin, L.L. (1995). A c-Jun dominant negative mutant protects sympathetic neurons against programmed cell death. Neuron *14*, 927–939.

Hanz, S., Perlson, E., Willis, D., Zheng, J.Q., Massarwa, R., Huerta, J.J., Koltzenburg, M., Kohler, M., Van-Minnen, J., Twiss, J.L., et al. (2003). Axoplasmic importins enable retrograde injury signaling in lesioned nerve. Neuron *40*, 1095–1104.

Hanz, S., Perlson, E., Willis, D., Zheng, J.-Q., Massarwa, R., Huerta, J.J., Koltzenburg, M., Kohler, M., Van-Minnen, J., Twiss, J.L., et al. (2007). Retrograde injury signaling in lesioned nerve. J. … *40*, 1095–1104.

Harris, W.A., Holt, C.E., and Bonhoeffer, F. (1987). Retinal axons with and without their somata, growing to and arborizing in the tectum of Xenopus embryos: a time-lapse video study of single fibres in vivo. Development *101*, 123–133.

Hausmann, O.N. (2003). Post-traumatic inflammation following spinal cord injury. Spinal Cord *41*, 369–378.

Hengerer, B., Lindholm, D., Heumann, R., Ruther, U., Wagner, E.F., and Thoenen, H. (1990). Lesion-induced increase in nerve growth factor mRNA is mediated by c-fos. Proc. Natl. Acad. Sci. *87*, 3899–3903.

Hengst, U., Cox, L.J., Macosko, E.Z., and Jaffrey, S.R. (2006). Functional and selective RNA interference in developing axons and growth cones. J. Neurosci. *26*, 5727–5732.

Herdegen, T., Fiallos-Estrada, C.E., Schmid, W., Bravo, R., and Zimmermann, M. (1992). The transcription factors c-JUN, JUN D and CREB, but not FOS and KROX-24, are differentially regulated in axotomized neurons following transection of rat sciatic nerve. Brain Res. Mol. Brain Res. *14*, 155–165.

Herdegen, T., Skene, P., and Bahr, M. (1997). The c-Jun transcription factor--bipotential

mediator of neuronal death, survival and regeneration. Trends Neurosci *20*, 227–231.

Hill, C.E., Beattie, M.S., and Bresnahan, J.C. (2001). Degeneration and sprouting of identified descending supraspinal axons after contusive spinal cord injury in the rat. Exp. Neurol. *171*, 153–169.

Holt, C.E., and Schuman, E.M. (2013). The Central Dogma Decentralized: New Perspectives on RNA Function and Local Translation in Neurons. Neuron *80*, 648–657.

Horner, P.J., and Gage, F.H. (2000). Regenerating the damaged central nervous system. October 963–970.

Huang, Y.-S., Carson, J.H., Barbarese, E., and Richter, J.D. (2003). Facilitation of dendritic mRNA transport by CPEB. Genes Dev. *17*, 638–653.

Huber, K.M. (2000). Role for Rapid Dendritic Protein Synthesis in Hippocampal mGluR-Dependent Long-Term Depression. Science (80-. ). *288*, 1254–1256.

Huber, W., von Heydebreck, A., Sültmann, H., Poustka, A., and Vingron, M. (2002). Variance stabilization applied to microarray data calibration and to the quantification of differential expression. Bioinformatics *18*, S96–S104.

Huebner, E.A., and Strittmatter, S.M. (2009). Axon regeneration in the peripheral and central nervous systems. Results Probl. Cell Differ. *48*, 339–351.

Hüll, M., and Bähr, M. (1994). Differential regulation of c-JUN expression in rat retinal ganglion cells after proximal and distal optic nerve transection. Neurosci. Lett. *178*, 39–42.

Hur, E.-M., Saijilafu, and Zhou, F.-Q. (2012). Growing the growth cone: remodeling the cytoskeleton to promote axon regeneration. Trends Neurosci. *35*, 164–174.

Hüttelmaier, S., Zenklusen, D., Lederer, M., Dictenberg, J., Lorenz, M., Meng, X., Bassell, G.J., Condeelis, J., and Singer, R.H. (2005). Spatial regulation of beta-actin translation by Src-dependent phosphorylation of ZBP1. Nature *438*, 512–515.

Igea, A., and Méndez, R. (2010). Meiosis requires a translational positive loop where CPEB1 ensues its replacement by CPEB4. EMBO J. *29*, 2182–2193.

Ince-Dunn, G., Hall, B.J., Hu, S.-C., Ripley, B., Huganir, R.L., Olson, J.M., Tapscott, S.J.,

and Ghosh, A. (2006). Regulation of thalamocortical patterning and synaptic maturation by NeuroD2. Neuron *49*, 683–695.

Ingelfinger, D., Arndt-Jovin, D.J., Lührmann, R., and Achsel, T. (2002). The human LSm1-7 proteins colocalize with the mRNA-degrading enzymes Dcp1/2 and Xrnl in distinct cytoplasmic foci. RNA *8*, 1489–1501.

Jackson, R.J., Hellen, C.U.T., and Pestova, T. V (2010). The mechanism of eukaryotic translation initiation and principles of its regulation. Nat. Rev. Mol. Cell Biol. *11*, 113–127.

Jain, R.G., Andrews, L.G., McGowan, K.M., Pekala, P.H., and Keene, J.D. (1997). Ectopic expression of Hel-N1, an RNA-binding protein, increases glucose transporter (GLUT1) expression in 3T3-L1 adipocytes. Mol. Cell. Biol. *17*, 954–962.

Jansen, R.P. (2001). mRNA localization: message on the move. Nat. Rev. Mol. Cell Biol. *2*, 247–256.

Jenkins, R., and Hunt, S.P. (1991). Long-term increase in the levels of c-jun mRNA and jun protein-like immunoreactivity in motor and sensory neurons following axon damage. Neurosci. Lett. *129*, 107–110.

Jenkins, R., Tetzlaff, W., and Hunt, S.P. (1993). Differential Expression of Immediate Early Genes in Rubrospinal Neurons Following Axotomy in Rat. Eur. J. Neurosci. *5*, 203–209.

Ji, S.-J., and Jaffrey, S.R. (2012). Intra-axonal Translation of SMAD1/5/8 Mediates Retrograde Regulation of Trigeminal Ganglia Subtype Specification. Neuron *74*, 95–107.

Jung, H., Yoon, B.C., and Holt, C.E. (2012). Axonal mRNA localization and local protein synthesis in nervous system assembly, maintenance and repair. Nat. Rev. Neurosci. *13*, 308–324.

Kaech, S., and Banker, G. (2006). Culturing hippocampal neurons. Nat. Protoc.

Kalinski, A.L., Sachdeva, R., Gomes, C., Lee, S.J., Shah, Z., Houle, J.D., and Twiss, J.L. (2015). mRNAs and Protein Synthetic Machinery Localize into Regenerating Spinal Cord Axons When They Are Provided a Substrate That Supports Growth. J. Neurosci. *35*, 10357–10370.

Kang, H., and Schuman, E.M. (1996). A requirement for local protein synthesis in neurotrophin-induced hippocampal synaptic plasticity. Science *273*, 1402–1406.

Kedersha, N., and Anderson, P. (2007). Mammalian stress granules and processing bodies. Methods Enzymol. *431*, 61–81.

Kedersha, N., Cho, M.R., Li, W., Yacono, P.W., Chen, S., Gilks, N., Golan, D.E., and Anderson, P. (2000). Dynamic Shuttling of Tia-1 Accompanies the Recruitment of mRNA to Mammalian Stress Granules. J. Cell Biol. *151*, 1257–1268.

Kedersha, N., Stoecklin, G., Ayodele, M., Yacono, P., Lykke-Andersen, J., Fritzler, M.J., Scheuner, D., Kaufman, R.J., Golan, D.E., and Anderson, P. (2005). Stress granules and processing bodies are dynamically linked sites of mRNP remodeling. J. Cell Biol. *169*, 871–884.

Kedersha, N.L., Gupta, M., Li, W., Miller, I., and Anderson, P. (1999). RNA-Binding Proteins Tia-1 and Tiar Link the Phosphorylation of Eif-2α to the Assembly of Mammalian Stress Granules. J. Cell Biol. *147*, 1431–1442.

Kerschensteiner, M., Schwab, M.E., Lichtman, J.W., and Misgeld, T. (2005). In vivo imaging of axonal degeneration and regeneration in the injured spinal cord. Nat. Med. *11*, 572–577.

Kim, J.H., and Richter, J.D. (2006). Opposing polymerase-deadenylase activities regulate cytoplasmic polyadenylation. Mol. Cell *24*, 173–183.

Koch, M.H., and Hassan, B.A. (2012). Out with the Brain: Drosophila Whole-Brain Explant Culture. In The Making and Un-Making of Neuronal Circuits in Drosophila, B. a Hassan, ed. (Humana Press),.

Koenigsberger, C., Chiappa, S., and Brimijoin, S. (1997). Neurite differentiation is modulated in neuroblastoma cells engineered for altered acetylcholinesterase expression. J. Neurochem. *69*, 1389–1397.

Kojima, S., Sher-Chen, E.L., and Green, C.B. (2012). Circadian control of mRNA polyadenylation dynamics regulates rhythmic protein expression. Genes Dev. *26*, 2724–2736.

Kong, Y. (2011). Btrim: a fast, lightweight adapter and quality trimming program for next-generation sequencing technologies. Genomics *98*, 152–153.

Kruys, V., Marinx, O., Shaw, G., Deschamps, J., and Huez, G. (1989). Translational blockade imposed by cytokine-derived UA-rich sequences. Science *245*, 852–855.

Kulkarni, M., Ozgur, S., and Stoecklin, G. (2010). On track with P-bodies. Biochem. Soc. Trans. *38*, 242–251.

Lamphear, B.J., Kirchweger, R., Skern, T., and Rhoads, R.E. (1995). Mapping of Functional Domains in Eukaryotic Protein Synthesis Initiation Factor 4G (eIF4G) with Picornaviral Proteases: IMPLICATIONS FOR CAP-DEPENDENT AND CAP-INDEPENDENT TRANSLATIONAL INITIATION. J. Biol. Chem. *270*, 21975–21983.

Lang, C., Bradley, P.M., Jacobi, A., Kerschensteiner, M., and Bareyre, F.M. (2013). STAT3 promotes corticospinal remodelling and functional recovery after spinal cord injury. EMBO Rep. *14*, 931–937.

Laroia, G., Cuesta, R., Brewer, G., and Schneider, R.J. (1999). Control of mRNA decay by heat shock-ubiquitin-proteasome pathway. Science *284*, 499–502.

Lau, A.G., Irier, H. a, Gu, J., Tian, D., Ku, L., Liu, G., Xia, M., Fritsch, B., Zheng, J.Q., Dingledine, R., et al. (2010). Distinct 3'UTRs differentially regulate activity-dependent translation of brain-derived neurotrophic factor (BDNF). Proc. Natl. Acad. Sci. U. S. A. *107*, 15945–15950.

Leah, J.D., Herdegen, T., and Bravo, R. (1991). Selective expression of Jun proteins following axotomy and axonal transport block in peripheral nerves in the rat: evidence for a role in the regeneration process. Brain Res. *566*, 198–207.

Lejeune, F., Li, X., and Maquat, L.E. (2003). Nonsense-Mediated mRNA Decay in Mammalian Cells Involves Decapping, Deadenylating, and Exonucleolytic Activities. Mol. Cell *12*, 675–687.

De León, M., Nahin, R.L., Molina, C.A., De Léon, D.D., and Ruda, M.A. (1995). Comparison of c-jun, junB, and junD mRNA expression and protein in the rat dorsal root ganglia following sciatic nerve transection. J. Neurosci. Res. *42*, 391–401.

Levy, N.S., Chung, S., Furneaux, H., and Levy, A.P. (1998). Hypoxic stabilization of vascular endothelial growth factor mRNA by the RNA-binding protein HuR. J. Biol. Chem.

*273*, 6417–6423.

Li, B., and Dewey, C.N. (2011). RSEM: accurate transcript quantification from RNA-Seq data with or without a reference genome. BMC Bioinformatics *12*, 323.

Li, Y., and Raisman, G. (1995). Sprouts from cut corticospinal axons persist in the presence of astrocytic scarring in long-term lesions of the adult rat spinal cord. Exp. Neurol. *134*, 102–111.

Li, Y., Field, P.M., and Raisman, G. (1997). Repair of adult rat corticospinal tract by transplants of olfactory ensheathing cells. Science *277*, 2000–2002.

Lianoglou, S., Garg, V., Yang, J.L., Leslie, C.S., and Mayr, C. (2013). Ubiquitously transcribed genes use alternative polyadenylation to achieve tissue-specific expression. Genes Dev. *27*, 2380–2396.

Lieberman, A.R. (1971). The Axon Reaction: A Review of the Principal Features of Perikaryal Responses to Axon Injury. Int. Rev. Neurobiol. *14*, 49–124.

Lin, A.C., Tan, C.L., Lin, C.-L., Strochlic, L., Huang, Y.-S., Richter, J.D., and Holt, C.E. (2009). Cytoplasmic polyadenylation and cytoplasmic polyadenylation element-dependent mRNA regulation are involved in Xenopus retinal axon development. Neural Dev. *4*, 1–20.

Lin, C.-L., Evans, V., Shen, S., Xing, Y., and Richter, J.D. (2010). The nuclear experience of CPEB: implications for RNA processing and translational control. RNA *16*, 338–348.

Lindwall, C., and Kanje, M. (2005). Retrograde axonal transport of JNK signaling molecules influence injury induced nuclear changes in p-c-Jun and ATF3 in adult rat sensory neurons. Mol. Cell. Neurosci. *29*, 269–282.

Liu, K., Lu, Y., Lee, J., Samara, R., and Willenberg, R. (2010). PTEN deletion enhances the regenerative ability of adult corticospinal neurons. Nature *13*, 1075–1081.

Liu, K., Tedeschi, A., Park, K.K., and He, Z. (2011). Neuronal intrinsic mechanisms of axon regeneration. Annu. Rev. Neurosci. *34*, 131–152.

Liu, N.-K., Wang, X.-F., Lu, Q.-B., and Xu, X.-M. (2009). Altered microRNA expression following traumatic spinal cord injury. Exp. Neurol. *219*, 424–429.

Liu, X.Z., Xu, X.M., Hu, R., Du, C., Zhang, S.X., McDonald, J.W., Dong, H.X., Wu, Y.J., Fan, G.S., Jacquin, M.F., et al. (1997). Neuronal and glial apoptosis after traumatic spinal cord injury. J. Neurosci. *17*, 5395–5406.

Lodish, H., Berk, A., Zipursky, S.L., Matsudaira, P., Baltimore, D., and Darnell, J. (2000). Overview of Neuron Structure and Function.

Lonze, B.E., and Ginty, D.D. (2002). Function and regulation of CREB family transcription factors in the nervous system. Neuron *35*, 605–623.

Lonze, B.E., Riccio, A., Cohen, S., and Ginty, D.D. (2002). Apoptosis, Axonal Growth Defects, and Degeneration of Peripheral Neurons in Mice Lacking CREB. Neuron *34*, 371–385.

Lou, W.P.-K., Baser, A., Klußmann, S., and Martin-Villalba, A. (2014). In vivo interrogation of central nervous system translatome by polyribosome fractionation. J. Vis. Exp.

Mandel, C.R., Kaneko, S., Zhang, H., Gebauer, D., Vethantham, V., Manley, J.L., and Tong, L. (2006). Polyadenylation factor CPSF-73 is the pre-mRNA 3'-end-processing endonuclease. Nature *444*, 953–956.

Mantamadiotis, T., Lemberger, T., Bleckmann, S.C., Kern, H., Kretz, O., Martin Villalba, A., Tronche, F., Kellendonk, C., Gau, D., Kapfhammer, J., et al. (2002). Disruption of CREB function in brain leads to neurodegeneration. Nat. Genet. *31*, 47–54.

Mayr, C., and Bartel, D.P. (2009). Widespread shortening of 3'UTRs by alternative cleavage and polyadenylation activates oncogenes in cancer cells. Cell *138*, 673–684.

Mazumder, B., Seshadri, V., and Fox, P.L. (2003). Translational control by the 3'-UTR: the ends specify the means. Trends Biochem. Sci. *28*, 91–98.

Méndez, R., Barnard, D., and Richter, J.D. (2002). Differential mRNA translation and meiotic progression require Cdc2-mediated CPEB destruction. EMBO J. *21*, 1833–1844.

Merianda, T.T., Coleman, J., Kim, H.H., Kumar Sahoo, P., Gomes, C., Brito-Vargas, P., Rauvala, H., Blesch, a., Yoo, S., and Twiss, J.L. (2015). Axonal Amphoterin mRNA Is Regulated by Translational Control and Enhances Axon Outgrowth. J. Neurosci. *35*, 5693–5706.

Merrick, W.C. (2004). Cap-dependent and cap-independent translation in eukaryotic systems. Gene *332*, 1–11.

Mi, S., Lee, X., Shao, Z., Thill, G., Ji, B., Relton, J., Levesque, M., Allaire, N., Perrin, S., Sands, B., et al. (2004). LINGO-1 is a component of the Nogo-66 receptor/p75 signaling complex. Nat. Neurosci. *7*, 221–228.

Mikl, M., Vendra, G., and Kiebler, M.A. (2011). Independent localization of MAP2, CaMKIIα and β-actin RNAs in low copy numbers. EMBO Rep. *12*, 1077–1084.

Miller, S., Yasuda, M., Coats, J.K., Jones, Y., Martone, M.E., and Mayford, M. (2002). Disruption of Dendritic Translation of CaMKIIα Impairs Stabilization of Synaptic Plasticity and Memory Consolidation. Neuron *36*, 507–519.

Mingorance, A., Soriano, E., and Río, J.A. (2004). Nogo, myelin and axonal regeneration. Contrib. to Sci. *2*, 499–512.

Miyata, S., Mori, Y., and Tohyama, M. (2008). PRMT1 and Btg2 regulates neurite outgrowth of Neuro2a cells. Neurosci. Lett. *445*, 162–165.

Mobarak, C.D., Anderson, K.D., Morin, M., Beckel-Mitchener, A., Rogers, S.L., Furneaux, H., King, P., and Perrone-Bizzozero, N.I. (2000). The RNA-binding protein HuD is required for GAP-43 mRNA stability, GAP-43 gene expression, and PKC-dependent neurite outgrowth in PC12 cells. Mol. Biol. Cell *11*, 3191–3203.

Molander, C., Hongpaisan, J., and Grant, G. (1992). Changing pattern Of C-FOS expression in spinal cord neurons after electrical stimulation of the chronically injured sciatic nerve in the rat. Neuroscience *50*, 223–236.

Moore, M.J. (2005). From birth to death: the complex lives of eukaryotic mRNAs. Science *309*, 1514–1518.

Moore, D.L., Blackmore, M.G., Hu, Y., Kaestner, K.H., Bixby, J.L., Lemmon, V.P., and Goldberg, J.L. (2009). KLF family members regulate intrinsic axon regeneration ability. Science *326*, 298–301.

Morell, P., and Quarles, R.H. (1999). The Myelin Sheath.

Muramatsu, R., and Yamashita, T. (2014). Concept and molecular basis of axonal regeneration after central nervous system injury. Neurosci. Res. *78*, 45–49.

Nakahata, S., Katsu, Y., Mita, K., Inoue, K., Nagahama, Y., and Yamashita, M. (2001). Biochemical identification of Xenopus Pumilio as a sequence-specific cyclin B1 mRNA-binding protein that physically interacts with a Nanos homolog, Xcat-2, and a cytoplasmic polyadenylation element-binding protein. J. Biol. Chem. *276*, 20945–20953.

Nakahata, S., Kotani, T., Mita, K., Kawasaki, T., Katsu, Y., Nagahama, Y., and Yamashita, M. (2003). Involvement of Xenopus Pumilio in the translational regulation that is specific to cyclin B1 mRNA during oocyte maturation. Mech. Dev. *120*, 865–880.

National Spinal Cord Injury Statistical Centre (2014). Annual Statistical Report.

Nechama, M., Lin, C.-L., and Richter, J.D. (2012). An Unusual Two Step Control of CPEB Destruction by Pin1. Mol. Cell. Biol. *33*.

Neumann, S., and Woolf, C.J. (1999). Regeneration of Dorsal Column Fibers into and beyond the Lesion Site following Adult Spinal Cord Injury. Neuron *23*, 83–91.

Oe, S., and Yoneda, Y. (2010). Cytoplasmic polyadenylation element-like sequences are involved in dendritic targeting of BDNF mRNA in hippocampal neurons. FEBS Lett. *584*, 3424–3430.

Oruganty-Das, A., Ng, T., Udagawa, T., Goh, E.L.K., and Richter, J.D. (2012). Translational control of mitochondrial energy production mediates neuron morphogenesis. Cell Metab. *16*, 789–800.

Park, J.W., Vahidi, B., Taylor, A.M., Rhee, S.W., and Jeon, N.L. (2006). Microfluidic culture platform for neuroscience research. Nat. Protoc. *1*, 2128–2136.

Park, K., Liu, K., Hu, Y., and Smith, P. (2008). Promoting axon regeneration in the adult CNS by modulation of the PTEN/mTOR pathway. Science (80-. ). *322*, 963–966.

Parker, R., and Sheth, U. (2007). P bodies and the control of mRNA translation and degradation. Mol. Cell *25*, 635–646.

Peltz, S.W., Brewer, G., Bernstein, P., Hart, P.A., and Ross, J. (1991). Regulation of mRNA

turnover in eukaryotic cells. Crit. Rev. Eukaryot. Gene Expr. *1*, 99–126.

Peng, S.S.Y., Chen, C.Y. a, Xu, N., and Shyu, A. Bin (1998). RNA stabilization by the AU-rich element binding protein, HuR, an ELAV protein. EMBO J. *17*, 3461–3470.

di Penta, A., Mercaldo, V., Florenzano, F., Munck, S., Ciotti, M.T., Zalfa, F., Mercanti, D., Molinari, M., Bagni, C., and Achsel, T. (2009). Dendritic LSm1/CBP80-mRNPs mark the early steps of transport commitment and translational control. J. Cell Biol. *184*, 423–435.

Perry, R.B.-T., Doron-Mandel, E., Iavnilovitch, E., Rishal, I., Dagan, S.Y., Tsoory, M., Coppola, G., McDonald, M.K., Gomes, C., Geschwind, D.H., et al. (2012). Subcellular knockout of importin β1 perturbs axonal retrograde signaling. Neuron *75*, 294–305.

Pesole, G. (2002). UTRdb and UTRsite: specialized databases of sequences and functional elements of 5' and 3' untranslated regions of eukaryotic mRNAs. Update 2002. Nucleic Acids Res. *30*, 335–340.

Pestova, T. V, Borukhov, S.I., and Hellen, C.U. (1998). Eukaryotic ribosomes require initiation factors 1 and 1A to locate initiation codons. Nature *394*, 854–859.

Phay, M., Kim, H.H., and Yoo, S. (2015). Dynamic Change and Target Prediction of Axon-Specific MicroRNAs in Regenerating Sciatic Nerve. PLoS One *10*, e0137461.

Picelli, S., Faridani, O.R., Björklund, A.K., Winberg, G., Sagasser, S., and Sandberg, R. (2014). Full-length RNA-seq from single cells using Smart-seq2. Nat. Protoc. *9*, 171–181.

Piqué, M., López, J.M., Foissac, S., Guigó, R., and Méndez, R. (2008). A combinatorial code for CPE-mediated translational control. Cell *132*, 434–448.

Poulin, F., and Sonenberg, N. (2013). Mechanism of Translation Initiation in Eukaryotes.

Raineri, I., Wegmueller, D., Gross, B., Certa, U., and Moroni, C. (2004). Roles of AUF1 isoforms, HuR and BRF1 in ARE-dependent mRNA turnover studied by RNA interference. Nucleic Acids Res. *32*, 1279–1288.

Raivich, G., Bohatschek, M., Da Costa, C., Iwata, O., Galiano, M., Hristova, M., Nateri, A.S., Makwana, M., Riera-Sans, L., Wolfer, D.P., et al. (2004). The AP-1 transcription factor c-Jun is required for efficient axonal regeneration. Neuron *43*, 57–67.

Richardson, P.M., and Issa, V.M. (1984). Peripheral injury enhances central regeneration of primary sensory neurones. Nature *309*, 791–793.

Richardson, P.M., and Verge, V.M. (1986). The induction of a regenerative propensity in sensory neurons following peripheral axonal injury. J. Neurocytol. *15*, 585–594.

Richter, J.D. (2007). CPEB: a life in translation. Trends Biochem. Sci. *32*, 279–285.

Robinson, G.A. (1995). Axotomy-induced regulation of c-Jun expression in regenerating rat retinal ganglion cells. Mol. Brain Res. *30*, 61–69.

Sachs, A., and Wahle, E. (1993). Poly(A) tail metabolism and function in eucaryotes. J. Biol. Chem. *268*, 22955–22958.

Sarkissian, M., Méndez, R., and Richter, J.D. (2004). Progesterone and insulin stimulation of CPEB-dependent polyadenylation is regulated by Aurora A and glycogen synthase kinase-3. 48–61.

Sassone-Corsi, P. (1998). Coupling gene expression to cAMP signalling: role of CREB and CREM. Int. J. Biochem. Cell Biol. *30*, 27–38.

Schnepp, R.W., Khurana, P., Attiyeh, E.F., Raman, P., Chodosh, S.E., Oldridge, D.A., Gagliardi, M.E., Conkrite, K.L., Asgharzadeh, S., Seeger, R.C., et al. (2015). A LIN28B-RAN-AURKA Signaling Network Promotes Neuroblastoma Tumorigenesis. Cancer Cell *28*, 599–609.

Schoenberg, D.R., and Maquat, L.E. (2012). Regulation of cytoplasmic mRNA decay. Nat. Rev. Genet. *13*, 448–448.

Schwanhäusser, B., Busse, D., Li, N., Dittmar, G., Schuchhardt, J., Wolf, J., Chen, W., and Selbach, M. (2011). Global quantification of mammalian gene expression control. Nature *473*, 337–342.

Setou, M., Hayasaka, T., and Yao, I. (2004). Axonal transport versus dendritic transport. J. Neurobiol. *58*, 201–206.

Shalek, A.K., Satija, R., Adiconis, X., Gertner, R.S., Gaublomme, J.T., Raychowdhury, R., Schwartz, S., Yosef, N., Malboeuf, C., Lu, D., et al. (2013). Single-cell transcriptomics

reveals bimodality in expression and splicing in immune cells. Nature *498*, 236–240.

Shannon, P., Markiel, A., Ozier, O., Baliga, N.S., Wang, J.T., Ramage, D., Amin, N., Schwikowski, B., and Ideker, T. (2003). Cytoscape: a software environment for integrated models of biomolecular interaction networks. Genome Res. *13*, 2498–2504.

Short, S. (2000). Structural Determinants for Post-transcriptional Stabilization of Lactate Dehydrogenase A mRNA by the Protein Kinase C Signal Pathway. J. Biol. Chem. *275*, 12963–12969.

Silva, N. a, Sousa, N., Reis, R.L., and Salgado, A.J. (2014). From basics to clinical: a comprehensive review on spinal cord injury. Prog. Neurobiol. *114*, 25–57.

Smith, P.D., Sun, F., Park, K.K., Cai, B., Wang, C., Kuwako, K., Martinez-Carrasco, I., Connolly, L., and He, Z. (2009). SOCS3 deletion promotes optic nerve regeneration in vivo. Neuron *64*, 617–623.

Smyth, G.K. (2004). Linear Models and Empirical Bayes Methods for Assessing Differential Expression in Microarray Experiments. Stat. Appl. Genet. Mol. Biol. *3*, 1–25.

Sonenberg, N. (1994). mRNA translation: influence of the 5’ and 3' untranslated regions. Curr. Opin. Genet. Dev. *4*, 310–315.

Song, Y., Sretavan, D., Salegio, E. a, Berg, J., Huang, X., Cheng, T., Xiong, X., Meltzer, S., Han, C., Nguyen, T.-T., et al. (2015). Regulation of axon regeneration by the RNA repair and splicing pathway. Nat. Neurosci. *18*, 817–825.

Subtelny, A.O., Eichhorn, S.W., Chen, G.R., Sive, H., and Bartel, D.P. (2014). Poly(A)-tail profiling reveals an embryonic switch in translational control. Nature.

Sun, F., Park, K.K.K., Belin, S., Wang, D., Lu, T., Chen, G., Zhang, K., Yeung, C., Feng, G., Yankner, B. a, et al. (2011). Sustained axon regeneration induced by co-deletion of PTEN and SOCS3. Nature *480*, 372–375.

Szostak, E., and Gebauer, F. (2013). Translational control by 3’-UTR-binding proteins. Brief. Funct. Genomics *12*, 58–65.

Taylor, A.M., Berchtold, N.C., Perreau, V.M., Tu, C.H., Li Jeon, N., and Cotman, C.W.

(2009). Axonal mRNA in uninjured and regenerating cortical mammalian axons. J. Neurosci. *29*, 4697–4707.

Tian, B., Hu, J., Zhang, H., and Lutz, C.S. (2005). A large-scale analysis of mRNA polyadenylation of human and mouse genes. Nucleic Acids Res. *33*, 201–212.

Udagawa, T., Farny, N.G., Jakovcevski, M., Kaphzan, H., Alarcon, J.M., Anilkumar, S., Ivshina, M., Hurt, J. a, Nagaoka, K., Nalavadi, V.C., et al. (2013). Genetic and acute CPEB1 depletion ameliorate fragile X pathophysiology. Nat. Med. *19*, 1473–1477.

Veldman, M.B., Bemben, M.A., Thompson, R.C., and Goldman, D. (2007). Gene expression analysis of zebrafish retinal ganglion cells during optic nerve regeneration identifies KLF6a and KLF7a as important regulators of axon regeneration. Dev. Biol. *312*, 596–612.

Veldman, M.B., Bemben, M.A., and Goldman, D. (2010). Tuba1a gene expression is regulated by KLF6/7 and is necessary for CNS development and regeneration in zebrafish. Mol. Cell. Neurosci. *43*, 370–383.

Verma, P., Chierzi, S., Codd, A.M., Campbell, D.S., Meyer, R.L., Holt, C.E., and Fawcett, J.W. (2005). Axonal protein synthesis and degradation are necessary for efficient growth cone regeneration. J. Neurosci. *25*, 331–342.

Villalba, A., Coll, O., and Gebauer, F. (2011). Cytoplasmic polyadenylation and translational control. Curr. Opin. Genet. Dev. *21*, 452–457.

Wang, K.C., Kim, J.A., Sivasankaran, R., Segal, R., and He, Z. (2002). P75 interacts with the Nogo receptor as a co-receptor for Nogo, MAG and OMgp. Nature *420*, 74–78.

Wells, S.E., Hillner, P.E., Vale, R.D., and Sachs, A.B. (1998). Circularization of mRNA by Eukaryotic Translation Initiation Factors. Mol. Cell *2*, 135–140.

Wilczynska, A., Aigueperse, C., Kress, M., Dautry, F., and Weil, D. (2005). The translational regulator CPEB1 provides a link between dcp1 bodies and stress granules. J. Cell Sci. *118*, 981–992.

Willis, D.E., Xu, M., Donnelly, C.J., Tep, C., Kendall, M., Erenstheyn, M., English, A.W., Schanen, N.C., Kirn-Safran, C.B., Yoon, S.O., et al. (2011). Axonal Localization of transgene mRNA in mature PNS and CNS neurons. J. Neurosci. *31*, 14481–14487.

Wilson, T., and Treisman, R. (1988). Removal of poly(A) and consequent degradation of c-fos mRNA facilitated by 3' AU-rich sequences. Nature *336*, 396–399.

Wu, D., Raafat, M., Pak, E., Hammond, S., and Murashov, A.K. (2011). MicroRNA machinery responds to peripheral nerve lesion in an injury-regulated pattern. Neuroscience *190*, 386–397.

Wu, K.Y., Hengst, U., Cox, L.J., Macosko, E.Z., Jeromin, A., Urquhart, E.R., and Jaffrey, S.R. (2005). Local translation of RhoA regulates growth cone collapse. Nature *436*, 1020–1024.

Wu, L., Wells, D., Tay, J., Mendis, D., Abbott, M. a, Barnitt, A., Quinlan, E., Heynen, A., Fallon, J.R., and Richter, J.D. (1998). CPEB-mediated cytoplasmic polyadenylation and the regulation of experience-dependent translation of alpha-CaMKII mRNA at synapses. Neuron *21*, 1129–1139.

Wu, X., Jin, W., Liu, X., Fu, H., Gong, P., Xu, J., Cui, G., Ni, Y., Ke, K., Gao, Z., et al. (2012). Cyclic AMP response element modulator-1 (CREM-1) involves in neuronal apoptosis after traumatic brain injury. J. Mol. Neurosci. *47*, 357–367.

Wunderlich, C.M., Hövelmeyer, N., and Wunderlich, F.T. (2013). Mechanisms of chronic JAK-STAT3-SOCS3 signaling in obesity. JAK-STAT *2*, e23878.

Xia, Z., Donehower, L.A., Cooper, T.A., Neilson, J.R., Wheeler, D.A., Wagner, E.J., and Li, W. (2014). Dynamic analyses of alternative polyadenylation from RNA-seq reveal a 3'-UTR landscape across seven tumour types. Nat. Commun. *5*, 5274.

Xu, N., Chen, C.Y., and Shyu, A.B. (2001). Versatile role for hnRNP D isoforms in the differential regulation of cytoplasmic mRNA turnover. Mol. Cell. Biol. *21*, 6960–6971.

Yamasaki, S., and Anderson, P. (2008). Reprogramming mRNA translation during stress. Curr. Opin. Cell Biol. *20*, 222–226.

Yamasaki, T., Kawasaki, H., Arakawa, S., Shimizu, K., Shimizu, S., Reiner, O., Okano, H., Nishina, S., Azuma, N., Penninger, J.M., et al. (2011). Stress-Activated Protein Kinase MKK7 Regulates Axon Elongation in the Developing Cerebral Cortex. J. Neurosci. *31*, 16872–16883.

Yan, D., Wu, Z., Chisholm, A.D., and Jin, Y. (2009). The DLK-1 kinase promotes mRNA stability and local translation in C. elegans synapses and axon regeneration. Cell *138*, 1005–1018.

Yoo, S., Kim, H.H., Kim, P., Donnelly, C.J., Kalinski, A.L., Vuppalanchi, D., Park, M., Lee, S.J., Merianda, T.T., Perrone-Bizzozero, N.I., et al. (2013). A HuD-ZBP1 ribonucleoprotein complex localizes GAP-43 mRNA into axons through its 3′ untranslated region AU-rich regulatory element. J. Neurochem. *126*, 792–804.

Zearfoss, N.R., Alarcon, J.M., Trifilieff, P., Kandel, E., and Richter, J.D. (2008). A molecular circuit composed of CPEB-1 and c-Jun controls growth hormone-mediated synaptic plasticity in the mouse hippocampus. J. Neurosci. *28*, 8502–8509.

Zhang, H.L., Eom, T., Oleynikov, Y., Shenoy, S.M., Liebelt, D.A., Dictenberg, J.B., Singer, R.H., and Bassell, G.J. (2001). Neurotrophin-induced transport of a beta-actin mRNP complex increases beta-actin levels and stimulates growth cone motility. Neuron *31*, 261–275.

Zhang, N., Yin, Y., Xu, S.-J., Wu, Y.-P., and Chen, W.-S. (2012). Inflammation & apoptosis in spinal cord injury. Indian J. Med. Res. *135*, 287–296.

Zheng, S., Gray, E.E., Chawla, G., Porse, B.T., O'Dell, T.J., and Black, D.L. (2012). PSD-95 is post-transcriptionally repressed during early neural development by PTBP1 and PTBP2. Nat. Neurosci. *15*, 381–388, S1.

Zhou, S., Shen, D., Wang, Y., Gong, L., Tang, X., Yu, B., Gu, X., and Ding, F. (2012). microRNA-222 targeting PTEN promotes neurite outgrowth from adult dorsal root ganglion neurons following sciatic nerve transection. PLoS One *7*, e44768.

Zivraj, K.H., Tung, Y.C.L., Piper, M., Gumy, L., Fawcett, J.W., Yeo, G.S.H., and Holt, C.E. (2010). Subcellular profiling reveals distinct and developmentally regulated repertoire of growth cone mRNAs. J. Neurosci. *30*, 15464–15478.